

A Simulation Model of Infant - Incubator - Feedback System with Humidification and Temperature Control

A Thesis

Presented to

The Faculty of Engineering and Science of Auckland University of Technology, AUT

In Partial Fulfilment

of the Requirements for the Degree

Master of Engineering

Yasser Amer Al-Taweel

August, 2006

Abstract

A comprehensive simulation model for the infant-incubator-feedback system was developed in a Matlab/Simulink[®] environment to investigate all heat exchange relationships, variables and factors that have an influence on the overall thermo-neutrality of the environment. The model was also used to determine the benefits and limitations of using a convectively heated single-walled incubator in nursing preterm infants with very low birth weight < 1000 grams and low gestational age 28 weeks.

The infant was modelled as one-lump with two layers; core and skin. The infant shape was approximated to a cylinder. The model incorporated all compartments of the infant-incubator system including core, skin, incubator air space, mattress, incubator walls, air-circulating fan, heating element, added oxygen (for resuscitation purposes), and humidification chamber, which has not previously been considered.

The results of the simulation were in terms of the temperature variation over time, of the following parts of the system: core and skin temperatures and incubator air space temperature. Results of the simulation with added humidity showed that the body temperature of a 900 gram infant, with an initial body temperature of 35.5 °C, did not reach the thermo-neutral range between 36.5-37.5 °C in two hours, on air mode. Whereas, on skin mode, both core and skin temperature reached to 36.87 °C and 36.5 °C in two hours, and thus a thermo-neutral environment was achieved. These outcomes are consistent with clinical empirical reports.

The simulation model is a closed-loop system with a PID controller for each mode; air servo controlled and skin servo controlled. The controller parameters were virtually estimated by the Zeigler-Nichols Method as real values were not available. Nevertheless, the overall stability of the whole system has been achieved by applying a step input which was verified by the Root Locus Method.

Acknowledgments

In the beginning, I wish to thank all the people, friends and colleagues who have helped and supported me in so many different ways during the past two years. There are too many to name here, yet there are those that should be acknowledged for the considerable help they have provided.

I am most grateful to my supervisor, Professor Ahmed Al-Jumaily, for his guidance and limitless encouragement and invaluable advice during this work, without which this project could not have been completed.

I also wish to thank Jon Church, Industrial Mentor for this project, Neil Prime, Neonatal Group Manager and other staff in the Neonatal Department especially, Dr. Geoff Bold, Mr. Nick Dibley, and Mr. Ben Caldwell at Fisher and Paykel Healthcare Ltd.(Auckland) for their assistance and technical expertise. I also wish to acknowledge the skill of Mr. Chris Hutchinson, Fisher and Paykel Healthcare Ltd.(USA) with his vast experience in infant warming devices.

Special thanks to AUT senior lecturers especially, Mr. Mike Protheroe, Department of Mechanical and Production Engineering for his expertise and advice, Dr. Mike Meyer, Neonatal Consultant in NICU at Middlemore Hospital (Auckland) for his cooperation and support in providing clinical data, and the DCRC staff and students especially, Dr. Max Ramos, Dr. Robert Paxton, Mr. Joe El-Aklouk, Mr. Youhua (Alex) Du, Mrs. Prasika Reddy and Ms. Marijke Mulder, for their assistance and cooperation.

This work is dedicated to all parents who have lost their children due to premature birth; to my parents and siblings who have given me so many things I could not even begin to list them all, they are the motivation that I continued my study; and last but not least, my brother Ali Al-Taweel who have been a very great support in most difficult times.

Declaration

I hereby declare that this submission is my own work and that, to the best knowledge and belief, it contains no material previously published or written by another person nor material which to a substantial extent has been accepted for the qualification of any other degree or diploma of a university or other institution of higher learning, except where due acknowledgment is made in the acknowledgments.

Signature _____

Table of Contents

List of Tables	ix
List of Figures	x
Nomenclature	xiii
Chapter 1 Introduction.....	1
1.1 Review of Literature.....	1
1.1.1 Background.....	1
1.1.2 Thermoregulation (Environmental Temperature Control) and Determinants.....	2
1.1.3 Heat Loss and Production Mechanisms and Assessments	5
1.1.4 Comparison between Radiant Warmers and Incubators.....	7
1.1.4.1 Temperature Control Set-up.....	7
1.1.4.2 Heat Shields	7
1.1.4.3 Accessibility for Care Giving.....	8
1.1.4.4 Humidity and Insensible Water Losses:.....	8
1.2 Objectives	10
Chapter 2 Model Development.....	11
2.1 Introduction	11
2.2 Infant-Incubator System	11
2.3 Infant Modelling.....	14
2.3.1 Core layer	17
2.3.1.1 Heat production of infant core, Q_{met}	17
2.3.1.2 Heat losses of infant core	18
2.3.2 Skin layer	21
2.4 Incubator Modelling	25
2.4.1 Air Space Modelling.....	25
2.4.2 Wall (hood) Modelling.....	28
2.4.3 Mattress Modelling.....	31
2.5 Heating Element Modelling.....	32
2.6 Humidification System Modelling	37

Chapter 3	Development of SIMULINK Model	47
3.1	Introduction	47
3.2	Infant-Incubator System Compartments (PLANT)	50
3.2.1	The Infant Core Compartment	51
3.2.1.1	Heat Production of the Infant Core	53
3.2.1.2	Core-Skin Conduction	53
3.2.1.3	Core-Skin Blood Convection	54
3.2.1.4	Sensible Heat Losses	54
3.2.1.5	Latent Heat Losses	55
3.2.1.6	Mass of the Infant Core	55
3.2.2	The Infant Skin Compartment	56
3.2.2.1	Skin-Incubator Air Space Convection	58
3.2.2.2	Skin-Mattress Conduction Subsystem	59
3.2.2.3	Evaporative Loss from the Skin	60
3.2.2.4	Skin-Wall Radiation	60
3.2.2.5	Mass of the Infant Skin	61
3.2.3	The Incubator Air Space Compartment	62
3.2.3.1	Heat Supply Sub-System	64
3.2.3.2	Incubator Air-Walls Convection Heat Transfer Sub-System	65
3.2.3.3	Incubator Air-Mattress Convection Heat Transfer Sub-System	65
3.2.3.4	Mass of the Incubator Air Space Sub-System	66
3.2.4	The Incubator Wall Compartment	67
3.2.4.1	Incubator Walls-Room Environment Free-Convection Sub-Systems	69
3.2.4.1.1	The hood top surface free convection subsystem	69
3.2.4.1.2	The hood vertical surfaces free convection subsystem	70
3.2.4.2	Incubator Walls- Room Environment Radiation Sub-System	72
3.2.5	The Incubator Mattress Compartment	72
3.2.6	The Circulated - Air Fan Compartment (Mixed Air Compartment)	74
3.2.6.1	The Nitrogen Density Sub-System	74
3.2.6.2	The Oxygen Density Sub-System	75
3.2.7	The Heated Air Compartment (Heater Element Compartment)	75
3.2.8	The Humidification System Compartment	76
3.2.8.1	The Air Space Inside the Water Chamber Compartment	77
3.2.8.2	The Water Mass in the Water Chamber Compartment	79

3.2.8.3	The Aluminium Block the Water Chamber Compartment	80
3.2.9	The Supplied Air Temperature Compartment.....	81
3.2.9.1	The Wet Air Mass Flow Rate Subsystem	82
3.2.9.2	The dry air mass flow rate subsystem	83
3.3	Feedback System and Temperature Control.....	85
3.4	Overall System Stability and Transfer Function	86
Chapter 4 Results and Validation		95
4.1	Introduction	95
4.2	Initial Conditions	96
4.3	Results	97
4.3.1	Air Mode Results.....	97
4.3.1.1	Incubator Air Temperature, T_a	97
4.3.1.2	Infant Core and Skin Temperatures, T_c , T_s	99
4.3.2	Skin Mode Results.....	101
4.3.2.1	Infant Core and Skin Temperatures, T_c and T_s	101
4.3.2.2	Incubator Air Temperature, T_a	104
4.3.3	Other Outcomes	105
Chapter 5 Discussion		106
5.1	Introduction	106
5.2	Infant Modelling.....	106
5.3	Incubator Modelling	107
5.4	Feedback System and Overall Stability Performance	107
5.5	Air Mode.....	108
5.6	Skin Mode.....	109
5.7	Model Limitations	109
5.8	The Significance of the Model	110
5.9	Conclusions	110

Appendices	111
Appendix 1	112
1.1	Initial Conditions for the infant-Incubator Simulink Model, M-File ...	112
1.2	State-Space Code for Skin Mode.....	114
1.3	State-Space Code for Air Mode.....	115
Appendix 2	116
2.1	Air Mode Figures.....	116
2.1.1	Temperature Figures.....	116
2.1.2	Heat Energy Relationships Figures.....	117
2.1.3	Feedback system Related Figures.....	119
Appendix 3	120
3.1	Skin Mode Figures.....	120
3.1.1	Temperature Figures.....	120
3.1.2	Heat Energy Relationships Figures.....	121
3.1.3	Feedback System Related Figures.....	123
References	124

List of Tables

Table 2-1 Oxygen flow rates and concentrations.....	33
Table 3-1 Number of components of the simulation model	50
Table 3-2 Sub-systems of the infant core compartment.....	53
Table 3-3 Sub-systems of the infant skin compartment.....	58
Table 3-4 Sub-systems of the incubator air space.....	64
Table 3-5 Sub-systems of the incubator walls compartment	68
Table 3-6 Sub-systems of the incubator mattress compartment	73

List of Figures

Figure 1-1 The neutral thermal zone at rest [1].....	2
Figure 1-2 Neutral thermal environment (Courtesy Fisher and Paykel Healthcare Ltd., Auckland).....	3
Figure 1-3 Neutral temperature from [9], compared with the recommendations of <i>Hey and Katz</i> [12].....	4
Figure 1-4 Temperature control factors [5].....	4
Figure 1-5 Functional chart for warming devices [1-20, 22-24].....	5
Figure 1-6 Heat exchange mechanism [1-20, 22-24].....	6
Figure 2-1 Interaction between compartments of infant-incubator system	12
Figure 2-2 Incubator/ATOM V-850 (Courtesy Atom Medical Corporation, Tokyo)	13
Figure 2-3 Heat flow diagram.....	13
Figure 2-4 Infant Model (A)/Segments-Layers (B)	15
Figure 2-5 (A) / (B) - Heat exchange block diagram.....	15
Figure 2-6 Pressure-temperature curve [35]	19
Figure 2-7 Infant shape approximation.....	22
Figure 2-8 Block diagram for heat exchange within the air space.....	25
Figure 2-9 Temperature difference across the wall.....	28
Figure 2-10 Heat transfer diagram.....	28
Figure 2-11 Block diagram for heat exchange across the wall.....	29
Figure 2-12 Block diagram for the mattress	32
Figure 2-13 Schematic diagram for Fan/Heater compartment.....	33
Figure 2-14 Block diagram for the Fan.....	34
Figure 2-15 Block diagram for the heater.....	36
Figure 2-16 Humidification system diagram	38
Figure 2-17 Water chamber-Heat exchange/Cross-sectional diagram.....	38
Figure 2-18 Air space above water surface (a)	40
Figure 2-19 Water surface (b).....	42
Figure 2-20 Finned-aluminium block/exposed and immersed parts (c)	44
Figure 2-21 Slider/Air outlets assembly	44
Figure 2-22 Area m ² vs. RH%.....	45
Figure 3-1 Feedback block diagram.....	47
Figure 3-3 Combined system compartments	51

Figure 3-5 Heat production sub-system	53
Figure 3-6 Core-skin conduction subsystem.....	54
Figure 3-7 Core-skin blood convection subsystem.....	54
Figure 3-8 Sensible heat losses subsystem	54
Figure 3-9 Latent heat losses subsystem.....	55
Figure 3-10 The mass of the infant core subsystem.....	56
Figure 3-12 Skin–air convective heat exchange	59
Figure 3-13 Skin-mattress conduction	59
Figure 3-14 Evaporative loss from the skin	60
Figure 3-15 Skin-wall radiation	61
Figure 3-16 Mass of the infant skin	61
Figure 3-18 Heat supply sub-system.....	64
Figure 3-19 Incubator air-walls convection sub-system	65
Figure 3-20 Incubator air-mattress convection sub-system	66
Figure 3-21 Mass of the incubator air space sub-system.....	66
Figure 3-22 The incubator wall compartment.....	67
Figure 3-23 Incubator walls-environment free convection sub-systems	69
Figure 3-24 Incubator horizontal surface-free convection subsystem	70
Figure 3-25 Incubator vertical surface free convection-Long side	71
Figure 3-26 Incubator vertical surface free convection-Short side.....	71
Figure 3-27 Incubator walls-room environment radiation.....	72
Figure 3-28 The incubator mattress compartment	73
Figure 3-29 The circulated-air fan compartment	74
Figure 3-30 The nitrogen density sub-system.....	75
Figure 3-31 The oxygen density sub-system	75
Figure 3-32 The heater element compartment	76
Figure 3-33 Humidification process-air space simulink model	77
Figure 3-34 Air density variation at heated air temperature	78
Figure 3-35 Air density variation at wet air temperature.....	78
Figure 3-36 Water-vapour partial pressure at T_{ha}	79
Figure 3-37 Water-vapour partial pressure at T_{wet}	79
Figure 3-38 Humidification process-water mass simulink model	80
Figure 3-39 Humidification process-aluminium block simulink model.....	81
Figure 3-40 Supplied air temperature compartment	82
Figure 3-41 Wet air mass flow rate subsystem	83

Figure 3-42 Dry air mass flow rate subsystem	84
Figure 3-43 Open-Loop sub-system	84
Figure 3-44 Sisotool Simulink Model-Skin Mode.....	87
Figure 3-45 Sisotool Simulink Model-Air Mode.....	87
Figure 3-46 SISO Window- Skin Mode/open-loop	88
Figure 3-47 SISO Window-Air Mode/open-loop	88
Figure 3-48 Simulink Model-LTI Blocks-Skin Mode	90
Figure 3-49 Step Response-Skin Temperature/closed-loop.....	90
Figure 3-50 Step Response - Heater Power/Skin Mode/closed-loop.....	91
Figure 3-51 System Stability-Skin Mode/closed-loop.....	92
Figure 3-52 Simulink Model-LTI Blocks-Air Mode	92
Figure 3-53 Step Response-Incubator Air Temperature/closed-loop	93
Figure 3-54 Step Response - Heater Power/Air Mode/closed-loop.....	93
Figure 3-55 System Stability-Air Mode/closed-loop.....	94
Figure 4-1 Incubator air temperature variation vs. time	98
Figure 4-2 Operative temperature of Air Shields C-100 under air servo control (33.8 ± 0.1 °C), A 2-minute incubator opening (*) was performed after 3 hours of recordings [17].....	98
Figure 4-3 Infant core temperature variation vs. time.....	99
Figure 4-4 Mean core temperature of normal infants during the first 8 hours of postnatal life [11].....	100
Figure 4-5 Infant skin temperature variation vs. time.....	100
Figure 4-6 Comparison of mean core and abdominal skin temperatures after birth [11]	101
Figure 4-7 Infant core temperature variation vs. time.....	102
Figure 4-8 Infant skin temperature variation vs. time.....	103
Figure 4-9 Incubator air temperature variation vs. time	104

Nomenclature

Q_{met} : Rate of metabolic heat production of the core, watt.

Q_{sen} : Rate of sensible heat energy due to breathing, watt.

Q_{lat} : Rate of latent heat energy due to breathing, watt.

Q_{bc} : Rate of convection heat transfer between core and skin via blood, watt.

Q_{cd} : Rate of conductive heat transfer between core and skin, watt.

Q_{scv} : Rate of convective heat transfer between skin and incubator air, watt.

Q_{mc} : Rate of conductive heat transfer between skin and mattress, watt.

Q_{se} : Rate of evaporative heat transfer between skin and incubator air, watt.

Q_{sr} : Rate of radiation heat transfer between skin and incubator wall, watt.

Q_{acv} : Rate of convective heat transfer between incubator air and incubator wall, watt.

Q_{cvo} : Rate of convective heat transfer between incubator walls and environment, watt.

Q_{ro} : Rate of radiation heat transfer between incubator walls and environment, watt.

Q_{mat} : Rate of convective heat transfer between incubator air and mattress, watt.

Q_{ht} : Rate of convective heat energy supplied to hood, watt.

Q_{ic} : Rate of conductive heat transfer between mattress and incubator body, watt.

Q_{heater} : Heater rated power given by the manufacturer, 0-260 watt.

S_a : Surface area of the local body segment, m².

M_{rst} : Resting metabolic rate at the thermo neutral zone for the 1st week of life, W/m².

mr_i : Percentage of the total heat production for each segment of the infant.

rr : Respiratory rate, sec^{-1} .

T_c : Core temperature, $^{\circ}\text{C}$.

T_{ex} : Exhaled air temperature, $^{\circ}\text{C}$.

T_a : Air temperature/inhaled air temperature, $^{\circ}\text{C}$.

T_w : Wall temperature, $^{\circ}\text{C}$.

T_e : Ambient (room) temperature, $^{\circ}\text{C}$.

T_m : Mattress temperature, $^{\circ}\text{C}$.

T_s : Skin temperature, $^{\circ}\text{C}$.

T_{ha} : Heated air temperature, $^{\circ}\text{C}$.

T_{mx} : Mixed air temperature, $^{\circ}\text{C}$.

T_{wet} : Wetted air temperature, $^{\circ}\text{C}$.

T_{wa} : Water air temperature inside humidification chamber, $^{\circ}\text{C}$.

T_{al} : Aluminium block temperature inside humidification chamber, $^{\circ}\text{C}$.

T_{sply} : Supplied air temperature, $^{\circ}\text{C}$.

v_t : Tidal volume, mL.

W_{ex} : Humidity ration of the exhaled air, kg of water vapour / kg of dry air.

W_a : Humidity ratio of the inhaled air, kg of water vapour / kg of dry air.

C_{p_a} : Specific heat of air, $\text{J.kg}^{-1} \cdot ^{\circ}\text{C}^{-1}$.

C_{p_c} : Specific heat of the core, $\text{J.kg}^{-1} \cdot ^{\circ}\text{C}^{-1}$.

C_{P_s} : Specific heat of the skin, $J.kg^{-1} . ^\circ C^{-1}$.

C_{P_b} : Specific heat of the blood, $J.kg^{-1} . ^\circ C^{-1}$.

C_{P_w} : Specific heat of the wall, $J.kg^{-1} . ^\circ C^{-1}$.

$C_{P_{O_2}}$: Specific heat of oxygen, $J.kg^{-1} . ^\circ C^{-1}$.

$C_{P_{N_2}}$: Specific heat of nitrogen, $J.kg^{-1} . ^\circ C^{-1}$.

C_{P_m} : Specific heat of mattress, $J.kg^{-1} . ^\circ C^{-1}$.

$C_{P_{wa}}$: Specific heat of water, $J.kg^{-1} . ^\circ C^{-1}$.

$C_{P_{al}}$: Specific heat of aluminium, $J.kg^{-1} . ^\circ C^{-1}$.

C_P : Specific heat of air, $J.kg^{-1} . ^\circ C^{-1}$.

C_{P_m} : Specific heat of moist air, $J.kg^{-1} . ^\circ C^{-1}$.

C_{ps} : Specific heat of vapour, $J.kg^{-1} . ^\circ C^{-1}$.

hfg : Latent heat of the water @ 35 °C, $J.kg^{-1}$.

hfg_1 : Latent heat of the water @ 50 °C, $J.kg^{-1}$.

IV : Inspired second volume, $mL.kg^{-1}$ mass of infat. sec^{-1} .

P_t : Atmospheric pressure, torr.

P_{H_2O} : Partial pressure of water-vapour @ T_a & T_{ex} , torr.

P_{sat} : Saturation pressure @ T_a & T_{ex} , torr.

RH : Relative humidity inside incubator, %.

th_s : Skin thickness, m.

th_m : Mattress thickness, m.

th_w : Wall thickness, m.

ρ_s : Skin density, kg.m^{-3} .

ρ_c : Core density, kg.m^{-3} .

ρ_a : Air density, kg/mL .

ρ_{H_2O} : Water density, kg/mL .

ρ_{bl} : Blood density, kg/mL .

ρ_w : Wall density, kg/m^3 .

ρ_{h_2O} : Water density, kg/mL .

ρ_{ha} : Heated air density, kg/m^3 .

ρ_{wet} : Wetted air density, kg/m^3 .

m_s : Mass of the skin, kg.

m : Mass of the infant, kg.

m_c : Mass of the core, kg.

M_w : Mass of the wall, kg.

M_a : Mass of the incubator air, kg.

M_m : Mass of mattress, kg.

M_{al} : Mass of the aluminium block, kg.

K_c : Thermal conductivity of the core, $\text{W.m}^{-1}.\text{°C}^{-1}$.

K_{mat} : Thermal conductivity of the mattress, $\text{W.m}^{-1}.\text{°C}^{-1}$.

k_a : Thermal conductivity of the air $\text{W.m}^{-1}.\text{°C}^{-1}$.

V_{cb} : Blood volume, mL.

bf : Blood flow rate parameter, sec^{-1} .

Nu : Nusselt number, dimensionless.

Re : Reynolds number, dimensionless.

h_{scv} : Heat transfer coefficient for infant skin, $\text{W.m}^{-2}.\text{°C}^{-1}$.

h_{acv} : Heat transfer coefficient for forced convection, $\text{W.m}^{-2}.\text{°C}^{-1}$.

h_{wa} : Heat transfer coefficient for water, $\text{W.m}^{-2}.\text{°C}^{-1}$.

h_{al_1} : Heat transfer coefficient for the exposed parts of aluminium block, $\text{W.m}^{-2}.\text{°C}^{-1}$.

h_{al_2} : Heat transfer coefficient for the submerged parts of aluminium block, $\text{W.m}^{-2}.\text{°C}^{-1}$.

V_a : Air velocity, m.sec^{-1} .

D_{sph} : Approximated infant diameter, m.

μ_a : Dynamic (absolute) viscosity of air, $\text{kg.m}^{-1}.\text{sec}^{-1}$.

ν : Kinematic viscosity of the air, m^2/sec .

GA : Gestational age, weeks.

age : Postnatal age, days.

σ : Stefan-Boltzmann constant, $5.64 \times 10^{-8} \text{ W/m}^2.\text{K}^4$.

ε_s : Radiant emissivity of the skin, assumed to be 1.0

ε_w : Radiant emissivity of the wall, assumed to be 0.86

A_{wi} : Surface area of the incubator walls, m^2 .

A_w : Normal surface area of the incubator, m^2 .

A_{net} : Area of the mattress not covered by the infant, m².

A_{mat} : Total area of the mattress, m² (measured).

A_r : Surface area of the neonate's local segment normal to the incubator walls, m².

A_s : Surface area of skin in contact with the mattress, m².

A_{cv} : Surface area of skin exposed to the air, m².

A_c : Incubator area based on the direction of the air flow, m².

A_{al_1} : Total surface area of the exposed parts of the finned-aluminium block, m².

A_{al_2} : Total surface area of the submerged parts of the finned-aluminium block, m².

p : Incubator perimeter based on the direction of the air flow, m.

W_{con} : Width of the water container, m.

L_{con} : Length of the water container, m.

N_f : Number of fins of the aluminium block.

th_f : Fin thickness, m.

l_f : Fin length, m.

w_t : Height of the fin above water surface, m.

w_{hw} : Height of the fin inside water, m.

W_g : Width of the gap between the fins of the aluminium block, m.

n_g : Number of the gaps between the fins of the aluminium block.

Table of Contents

List of Tables	ix
List of Figures	x
Nomenclature	xiii
Chapter 1 Introduction.....	1
1.1 Review of Literature.....	1
1.1.1 Background.....	1
1.1.2 Thermoregulation (Environmental Temperature Control) and Determinants.....	2
1.1.3 Heat Loss and Production Mechanisms and Assessments	5
1.1.4 Comparison between Radiant Warmers and Incubators.....	7
1.1.4.1 Temperature Control Set-up.....	7
1.1.4.2 Heat Shields	7
1.1.4.3 Accessibility for Care Giving.....	8
1.1.4.4 Humidity and Insensible Water Losses:.....	8
1.2 Objectives	10
Chapter 2 Model Development.....	11
2.1 Introduction	11
2.2 Infant-Incubator System	11
2.3 Infant Modelling.....	14
2.3.1 Core layer	17
2.3.1.1 Heat production of infant core, Q_{met}	17
2.3.1.2 Heat losses of infant core	18
2.3.2 Skin layer	21
2.4 Incubator Modelling	25
2.4.1 Air Space Modelling.....	25
2.4.2 Wall (hood) Modelling.....	28
2.4.3 Mattress Modelling.....	31
2.5 Heating Element Modelling.....	32
2.6 Humidification System Modelling	37

Chapter 3	Development of SIMULINK Model	47
3.1	Introduction	47
3.2	Infant-Incubator System Compartments (PLANT)	50
3.2.1	The Infant Core Compartment.....	51
3.2.1.1	Heat Production of the Infant Core	53
3.2.1.2	Core-Skin Conduction.....	53
3.2.1.3	Core-Skin Blood Convection	54
3.2.1.4	Sensible Heat Losses.....	54
3.2.1.5	Latent Heat Losses	55
3.2.1.6	Mass of the Infant Core.....	55
3.2.2	The Infant Skin Compartment	56
3.2.2.1	Skin-Incubator Air Space Convection	58
3.2.2.2	Skin-Mattress Conduction Subsystem	59
3.2.2.3	Evaporative Loss from the Skin.....	60
3.2.2.4	Skin-Wall Radiation.....	60
3.2.2.5	Mass of the Infant Skin	61
3.2.3	The Incubator Air Space Compartment.....	62
3.2.3.1	Heat Supply Sub-System	64
3.2.3.2	Incubator Air-Walls Convection Heat Transfer Sub-System.....	65
3.2.3.3	Incubator Air-Mattress Convection Heat Transfer Sub-System	65
3.2.3.4	Mass of the Incubator Air Space Sub-System.....	66
3.2.4	The Incubator Wall Compartment.....	67
3.2.4.1	Incubator Walls-Room Environment Free-Convection Sub-Systems	69
3.2.4.1.1	The hood top surface free convection subsystem	69
3.2.4.1.2	The hood vertical surfaces free convection subsystem.....	70
3.2.4.2	Incubator Walls- Room Environment Radiation Sub-System	72
3.2.5	The Incubator Mattress Compartment.....	72
3.2.6	The Circulated - Air Fan Compartment (Mixed Air Compartment) ..	74
3.2.6.1	The Nitrogen Density Sub-System	74
3.2.6.2	The Oxygen Density Sub-System	75
3.2.7	The Heated Air Compartment (Heater Element Compartment).....	75
3.2.8	The Humidification System Compartment.....	76
3.2.8.1	The Air Space Inside the Water Chamber Compartment	77
3.2.8.2	The Water Mass in the Water Chamber Compartment.....	79

3.2.8.3	The Aluminium Block the Water Chamber Compartment	80
3.2.9	The Supplied Air Temperature Compartment.....	81
3.2.9.1	The Wet Air Mass Flow Rate Subsystem	82
3.2.9.2	The dry air mass flow rate subsystem	83
3.3	Feedback System and Temperature Control.....	85
3.4	Overall System Stability and Transfer Function	86
Chapter 4	Results and Validation	95
4.1	Introduction	95
4.2	Initial Conditions	96
4.3	Results	97
4.3.1	Air Mode Results.....	97
4.3.1.1	Incubator Air Temperature, T_a	97
4.3.1.2	Infant Core and Skin Temperatures, T_c , T_s	99
4.3.2	Skin Mode Results.....	101
4.3.2.1	Infant Core and Skin Temperatures, T_c and T_s	101
4.3.2.2	Incubator Air Temperature, T_a	104
4.3.3	Other Outcomes	105
Chapter 5	Discussion	106
5.1	Introduction	106
5.2	Infant Modelling.....	106
5.3	Incubator Modelling	107
5.4	Feedback System and Overall Stability Performance	107
5.5	Air Mode.....	108
5.6	Skin Mode.....	109
5.7	Model Limitations	109
5.8	The Significance of the Model	110
5.9	Conclusions	110

Appendices	111
Appendix 1	112
1.1	Initial Conditions for the infant-Incubator Simulink Model, M-File ...	112
1.2	State-Space Code for Skin Mode.....	114
1.3	State-Space Code for Air Mode.....	115
Appendix 2	116
2.1	Air Mode Figures.....	116
2.1.1	Temperature Figures.....	116
2.1.2	Heat Energy Relationships Figures.....	117
2.1.3	Feedback system Related Figures.....	119
Appendix 3	120
3.1	Skin Mode Figures.....	120
3.1.1	Temperature Figures.....	120
3.1.2	Heat Energy Relationships Figures.....	121
3.1.3	Feedback System Related Figures.....	123
References	124

List of Tables

Table 2-1 Oxygen flow rates and concentrations.....	33
Table 3-1 Number of components of the simulation model	50
Table 3-2 Sub-systems of the infant core compartment.....	53
Table 3-3 Sub-systems of the infant skin compartment.....	58
Table 3-4 Sub-systems of the incubator air space.....	64
Table 3-5 Sub-systems of the incubator walls compartment	68
Table 3-6 Sub-systems of the incubator mattress compartment	73

List of Figures

Figure 1-1 The neutral thermal zone at rest [1].....	2
Figure 1-2 Neutral thermal environment (Courtesy Fisher and Paykel Healthcare Ltd., Auckland).....	3
Figure 1-3 Neutral temperature from [9], compared with the recommendations of <i>Hey and Katz</i> [12].....	4
Figure 1-4 Temperature control factors [5].....	4
Figure 1-5 Functional chart for warming devices [1-20, 22-24].....	5
Figure 1-6 Heat exchange mechanism [1-20, 22-24].....	6
Figure 2-1 Interaction between compartments of infant-incubator system	12
Figure 2-2 Incubator/ATOM V-850 (Courtesy Atom Medical Corporation, Tokyo)	13
Figure 2-3 Heat flow diagram.....	13
Figure 2-4 Infant Model (A)/Segments-Layers (B)	15
Figure 2-5 (A) / (B) - Heat exchange block diagram.....	15
Figure 2-6 Pressure-temperature curve [35]	19
Figure 2-7 Infant shape approximation.....	22
Figure 2-8 Block diagram for heat exchange within the air space.....	25
Figure 2-9 Temperature difference across the wall.....	28
Figure 2-10 Heat transfer diagram.....	28
Figure 2-11 Block diagram for heat exchange across the wall.....	29
Figure 2-12 Block diagram for the mattress	32
Figure 2-13 Schematic diagram for Fan/Heater compartment.....	33
Figure 2-14 Block diagram for the Fan.....	34
Figure 2-15 Block diagram for the heater.....	36
Figure 2-16 Humidification system diagram	38
Figure 2-17 Water chamber-Heat exchange/Cross-sectional diagram.....	38
Figure 2-18 Air space above water surface (a)	40
Figure 2-19 Water surface (b).....	42
Figure 2-20 Finned-aluminium block/exposed and immersed parts (c)	44
Figure 2-21 Slider/Air outlets assembly	44
Figure 2-22 Area m ² vs. RH%.....	45
Figure 3-1 Feedback block diagram.....	47
Figure 3-3 Combined system compartments	51

Figure 3-5 Heat production sub-system	53
Figure 3-6 Core-skin conduction subsystem.....	54
Figure 3-7 Core-skin blood convection subsystem.....	54
Figure 3-8 Sensible heat losses subsystem	54
Figure 3-9 Latent heat losses subsystem.....	55
Figure 3-10 The mass of the infant core subsystem.....	56
Figure 3-12 Skin–air convective heat exchange	59
Figure 3-13 Skin-mattress conduction	59
Figure 3-14 Evaporative loss from the skin	60
Figure 3-15 Skin-wall radiation	61
Figure 3-16 Mass of the infant skin	61
Figure 3-18 Heat supply sub-system.....	64
Figure 3-19 Incubator air-walls convection sub-system	65
Figure 3-20 Incubator air-mattress convection sub-system	66
Figure 3-21 Mass of the incubator air space sub-system	66
Figure 3-22 The incubator wall compartment.....	67
Figure 3-23 Incubator walls-environment free convection sub-systems	69
Figure 3-24 Incubator horizontal surface-free convection subsystem	70
Figure 3-25 Incubator vertical surface free convection-Long side	71
Figure 3-26 Incubator vertical surface free convection-Short side.....	71
Figure 3-27 Incubator walls-room environment radiation.....	72
Figure 3-28 The incubator mattress compartment	73
Figure 3-29 The circulated-air fan compartment	74
Figure 3-30 The nitrogen density sub-system.....	75
Figure 3-31 The oxygen density sub-system	75
Figure 3-32 The heater element compartment	76
Figure 3-33 Humidification process-air space simulink model	77
Figure 3-34 Air density variation at heated air temperature	78
Figure 3-35 Air density variation at wet air temperature.....	78
Figure 3-36 Water-vapour partial pressure at T_{ha}	79
Figure 3-37 Water-vapour partial pressure at T_{wet}	79
Figure 3-38 Humidification process-water mass simulink model	80
Figure 3-39 Humidification process-aluminium block simulink model.....	81
Figure 3-40 Supplied air temperature compartment	82
Figure 3-41 Wet air mass flow rate subsystem	83

Figure 3-42 Dry air mass flow rate subsystem	84
Figure 3-43 Open-Loop sub-system	84
Figure 3-44 Sisotool Simulink Model-Skin Mode.....	87
Figure 3-45 Sisotool Simulink Model-Air Mode.....	87
Figure 3-46 SISO Window- Skin Mode/open-loop	88
Figure 3-47 SISO Window-Air Mode/open-loop	88
Figure 3-48 Simulink Model-LTI Blocks-Skin Mode	90
Figure 3-49 Step Response-Skin Temperature/closed-loop.....	90
Figure 3-50 Step Response - Heater Power/Skin Mode/closed-loop.....	91
Figure 3-51 System Stability-Skin Mode/closed-loop.....	92
Figure 3-52 Simulink Model-LTI Blocks-Air Mode	92
Figure 3-53 Step Response-Incubator Air Temperature/closed-loop	93
Figure 3-54 Step Response - Heater Power/Air Mode/closed-loop.....	93
Figure 3-55 System Stability-Air Mode/closed-loop.....	94
Figure 4-1 Incubator air temperature variation vs. time	98
Figure 4-2 Operative temperature of Air Shields C-100 under air servo control (33.8 ± 0.1 °C), A 2-minute incubator opening (*) was performed after 3 hours of recordings [17].....	98
Figure 4-3 Infant core temperature variation vs. time.....	99
Figure 4-4 Mean core temperature of normal infants during the first 8 hours of postnatal life [11].....	100
Figure 4-5 Infant skin temperature variation vs. time.....	100
Figure 4-6 Comparison of mean core and abdominal skin temperatures after birth [11]	101
Figure 4-7 Infant core temperature variation vs. time.....	102
Figure 4-8 Infant skin temperature variation vs. time.....	103
Figure 4-9 Incubator air temperature variation vs. time	104

Chapter 1 Introduction

Generally, preterm infants are not capable of maintaining their body temperature because they have immature thermal regulation systems. This means that their mechanisms for heat production are under developed and they have insufficient energy reserves. Therefore, some form of external thermoregulatory support is vital.

There are two main types of heating devices used to help infants maintain their temperature; incubators and radiant warmers. These are often used immediately after delivery and for the first few months of life.

Radiant warmers use infrared radiation to control the temperature of infants, while incubators use the convection of warm, humidified air. Both these warming devices are a feedback system. The radiant warmer uses only the skin servo control, while the incubator has two modes: skin and air servo control.

The use of these two devices has considerably reduced the rate of infant mortality and morbidity. While both have advantages, they also have shortcomings and improvements to both are possible.

1.1 Review of Literature

The literature survey will provide a background on radiant warmers and incubators as well as a comparison between these two thermo regulation devices. Various factors and heat exchange relationships involved with the use of each type of thermoregulation devices, will be discussed in the following sections

1.1.1 Background

The first use of incubators for the care of premature infants was in 1722. Trainer (Parisian obstetrician) [1] adapted the idea of using chicken incubators for the care of premature infants. Since that time, the incubator industry witnessed a great development and by 1896 the basic configuration of incubator design was completed and still forms the basis of today's incubators. Radiant warmers however are quite new, and have been only used for nursing ill infants with very low birth weight since 1969 [2].

Initially, a radiantly heated skin servo controlled incubator was used, but the glass top was badly affected by radiated heat. This defect ended the use of this type of heating systems and convectively heated incubators emerged [1].

1.1.2 Thermoregulation (Environmental Temperature Control) and Determinants

Many studies have demonstrated that the survival rate of low birth weight infants cared for in incubators or under radiant warmers increases when warmer environment conditions are provided. This is particularly vital during the first week of life. Although providing a neutral thermal environment is essential for premature babies during the first month of life, primarily due to very high evaporative losses resulted by large skin surface area, this could only be achieved at a very small range of temperatures usually in a margin of $+1\text{ }^{\circ}\text{C}$ when the admission temperature to the incubator $> 36\text{ }^{\circ}\text{C}$ [1, 3-13].

The actual environmental temperature required to achieve thermo-neutrality for a premature infant with very low birth weight during the first day of life is around $39\text{ }^{\circ}\text{C}$ [1]. This temperature is significantly influenced by the insensible water losses of premature infants. Also it is worth noting that babies under radiant warmer have a higher metabolic rate than those are cared for in incubators. This may be attributed to the inconsistency of radiated energy distributed over the exposed surface area of the baby's body in which some parts of the body receive more heat than other parts while the vertical parts might remain cold (no heat received) [5, 8, 14-16].

The performance trends of the physiologic thermoregulation factors such as, core and skin temperatures, metabolic rate, evaporative heat loss and blood flow convection, for infants in the neutral thermal zone (NTZ) at rest are illustrated in Figure 1-1, as a function of environmental temperature [1].

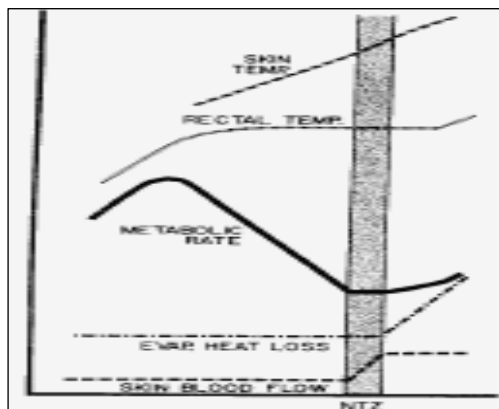


Figure 1-1 The neutral thermal zone at rest [1]

Generally, optimal thermal conditions are achieved when baby's temperature remains in the range between 36.8 - 37.2 °C [11, 17] and both oxygen consumption (heat production) and insensible water losses (heat loss) are at minimum levels . In the real world however, there is no pure thermo-neutrality zone. This is reflected on incubators, and thus convective incubator tend to provide a greater approximation of ideal thermo-neutrality than radiant warmer. This may be attributed to the variation of physiological conditions of premature infants; which also vary from one infant to another. In addition, the determinants of thermo neutrality are gestational age and body weight [5].

Figure 1-2 illustrates the normal range of infant body temperature at which thermo neutrality is achieved [9]. This temperature range is very narrow and lies between 36.5 - 37.5 °C. Thus, the environmental (ambient) temperature at which the infant regulates his/her body temperature can be considered as the neutral (operative) temperature.

The operative environmental temperature (or environment neutral temperature) can be defined as the temperature of an enclosed environment (i.e. such an incubator) in which an infant would exchange the same amount of heat by radiation and convection as in an open (ambient) environment [18]. It can be determined as the weighted average of wall and air temperatures [5, 9, 19].

In addition, for different postnatal ages and birth weights there are different operative (neutral) temperatures [9, 12], as shown in Figure 1-3:

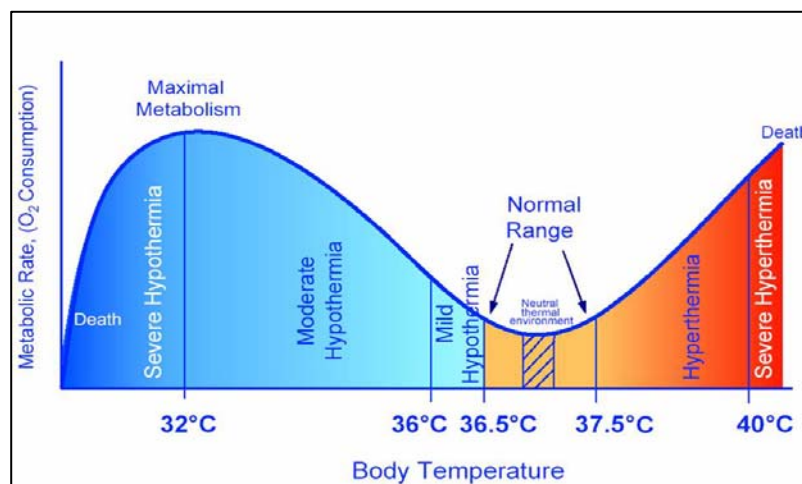


Figure 1-2 Neutral thermal environment (Courtesy Fisher and Paykel Healthcare Ltd., Auckland)

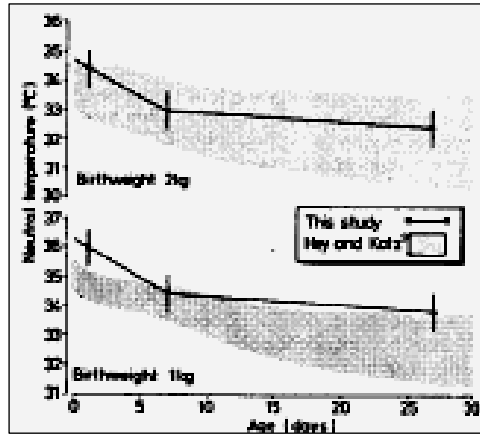


Figure 1-3 Neutral temperature from [9], compared with the recommendations of *Hey and Katz* [12]

The significance of the operative (neutral) temperature is that, it can hypothetically be used to estimate the setting temperature in a single-walled incubator (i.e. incubator air temperature measured by a thermometer inside the incubator) if the room temperature is known, usually $< 27\text{ }^{\circ}\text{C}$ [12]. This assumption is based on fact that the incubator wall temperature is usually less than incubator air temperature, and thus the operative temperature within the incubator fell one degree below incubator air temperature for every seven degrees by which incubator air temperature exceeds room temperature [12, 20].

The neutral conditions can be described by a single variable such as temperature $T_{control}$ [5]. The factors that control this temperature are defined in Figure 1-4, however temperature control differs for infants of different body weights and ages.

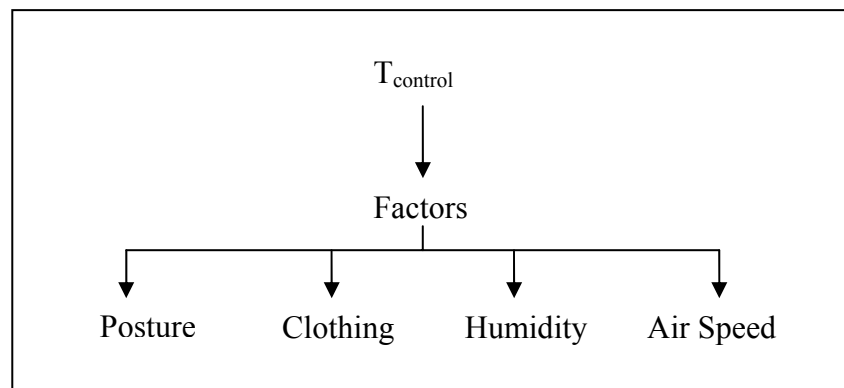


Figure 1-4 Temperature control factors [5]

A foetus's temperature is approximately $0.5\text{ }^{\circ}\text{C}$ above its mother's temperature [21], and soon after birth the newborn's temperature starts to drop due to the differences in environmental conditions. This causes an imbalance in the thermo-neutrality (in other words, heat production does not match heat losses). This usually occurs during the first few minutes of newborn's life. For those infants born with very low birth weight, which

normally accompanied with illnesses, their body's temperature is vulnerable to fall significantly at birth. Therefore maintaining the infant's body temperature is crucial in the first day of life which may reduce the mortality rate of preterm infants.

Figure 1-5 illustrates the functional chart of both an infant warming devices, convectively heated incubator (C.H.I) and an infra radiant warmer (RW) in terms of the factors involved with use of each device.

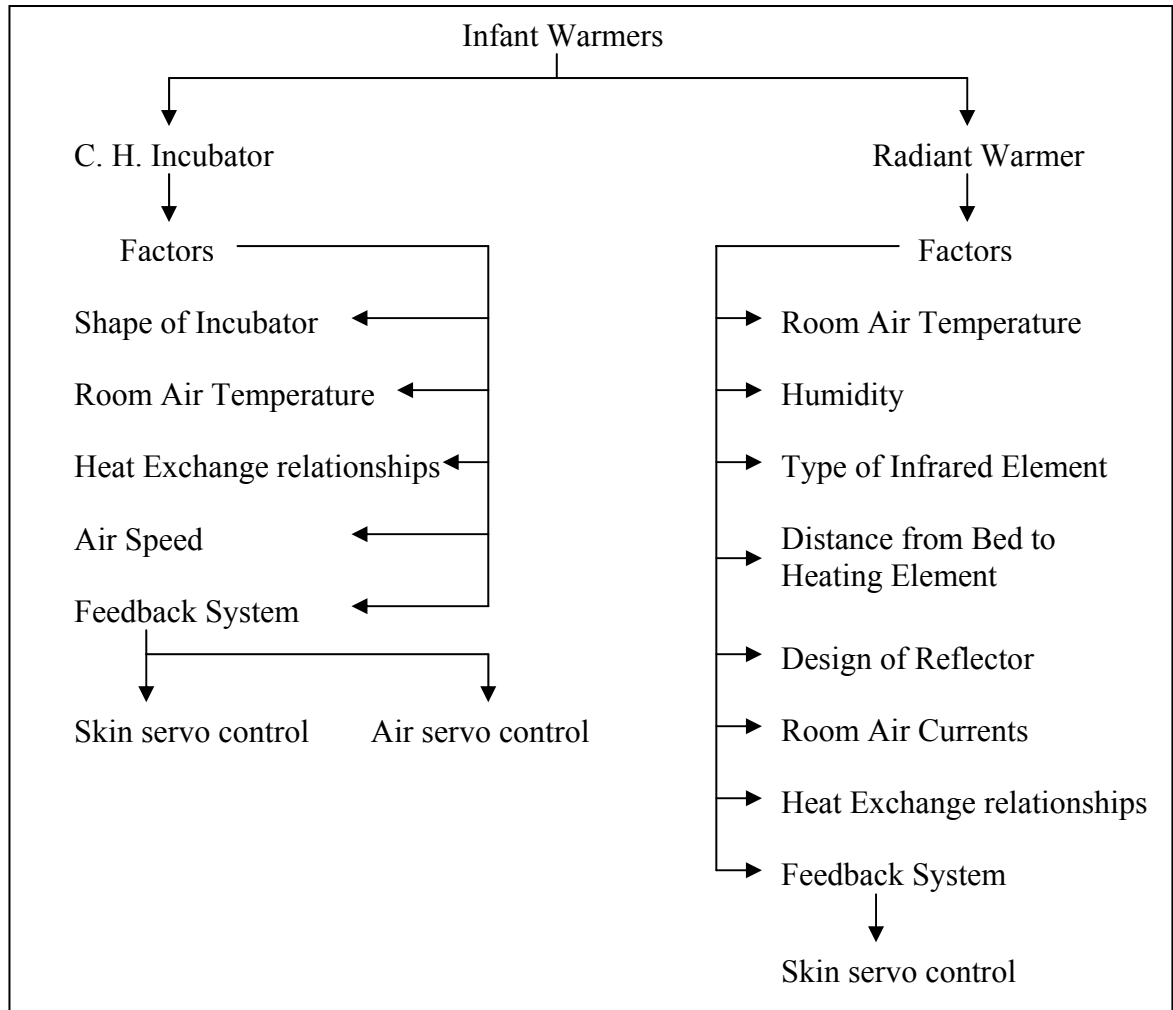


Figure 1-5 Functional chart for warming devices [1-20, 22-24]

1.1.3 Heat Loss and Production Mechanisms and Assessments

The heat production is represented by the amount of the oxygen consumption. Whereas the heat losses are come from evaporative heat losses (i.e. insensible water losses) and non-evaporative heat losses (including both the convective and radiative heat loss). The conductive heat loss is considered negligible since the mattress is made of a low thermal conductivity material such as foam [1]. Figure 1-6 demonstrates thermal gain and loss relationships for the incubator and radiant warmer warming devices.

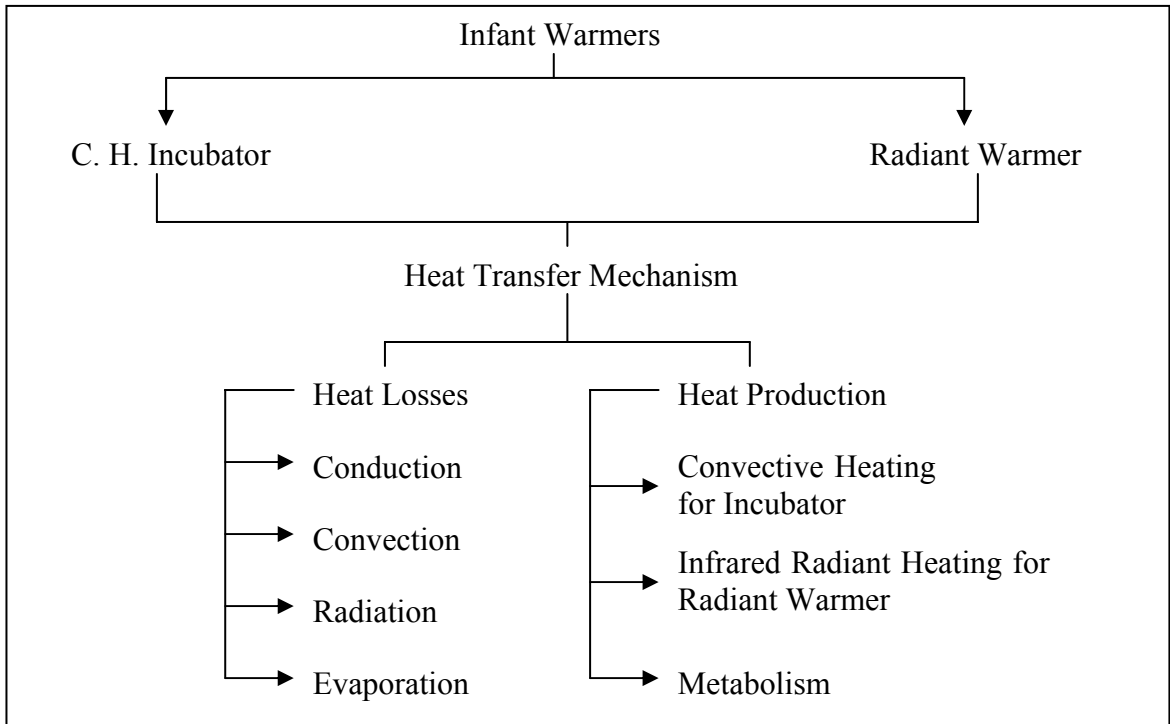


Figure 1-6 Heat exchange mechanism [1-20, 22-24]

Thus, it can be said that the “evaporative heat loss is an inverse exponential function of both postnatal age and gestational age” [1]. From this perspective, evaporative heat loss from the skin is a major problem facing premature infants with low birth weight and small gestational age, particularly when they are nursed under radiant warmer. In fact, those who nursed in conventional convective incubator are not vulnerable to dehydration because the relative humidity inside the incubator and/or the ambient (room) is maintained at $\geq 50\%$ [1, 3, 5, 7, 12-16, 22-24].

The environmental conditions of the incubators are controlled by the incubator’s inside and outside temperatures as well as the heat losses through conduction, convection, radiation and evaporation. These heating losses have been assessed using an experimental metabolism chamber which it is expected to be similar to commercial incubator [12].

The relationship between the evaporative and convective heat losses is that the air currents near the baby’s body works as a transmission medium in which the evaporative heat losses (insensible water loss) transmit into incubator air space via convection processes. Thus, a reduction in the air current velocity would cause a reduction in the convective heat and evaporation losses accordingly [1, 5, 8, 14, 16, 23, 24].

1.1.4 Comparison between Radiant Warmers and Incubators

1.1.4.1 Temperature Control Set-up

The temperature control systems in incubators can be implemented using either a skin servo control or air servo control. Consecutive studies [1, 3, 5, 17], showed the advantage of using air servo control is to reduce the fluctuation in regulating incubator air temperature. Radiant warmers use only skin servo control due to the fact that it is difficult to measure the environmental temperature of an opened area [1].

Other investigations however [5, 17], have reported that the fluctuation in environmental temperatures is only manipulated by the temperature set up regardless the design of the incubators (i.e. whether it is single or double-walled).

The maximum range of temperatures that one can set commercial incubators in which naked babies are nursed safely is between 30-35 °C [12]. At this range, the optimum thermo-neutral environment can be created.

According to British Standard 3061 (1965) [12], the incubator's air design temperature should not exceed 35 °C. At this temperature, babies are safe from hyperthermia or hypothermia. However, for those born with low birth weight and need to be nursed in a radiant warmer where the setting temperature exceeds 35 °C, they are more likely to receive much more fluid intake to prevent dehydration. On the other hand, in case of using an incubator, the room temperature should be kept at high levels ≥ 25 °C, this can create an uncomfortable environment for the caregivers [1, 3].

1.1.4.2 Heat Shields

In order to reduce the evaporative heat losses from the infant skin, Baumgart et al [13] suggested "a thin plastic blanket as an effective shield to reduce evaporative loss under radiant warmers". Leblanc [13] has shown that the occlusive wrap of neonates must be made of polyethylene rather than polystyrene because only polyethylene transmits the long wavelength energy of radiant heat. Thus, polyethylene became the material of choice for infant blankets construction.

Wrapping newborns of very low birth weight soon after birth without drying has been shown to significantly reduce oxygen consumption (heat production) and insensible water losses (heat losses). Accordingly, there is a significant decrease in the amount of

the radiated energy required to maintain the baby's body temperature. Eventually, this stabilises the environmental temperature and achieves thermo-neutrality [1, 5, 13, 16, 23, 24]. The polyethylene blanket also reduces the velocity of the air currents above the baby and consequently the convective heat losses [8, 13].

The other way of providing heat shield under radiant warmer is by placing plastic walls around the cot (walled chamber). This reduces evaporative and convective heat losses, but not to the level achieved with a blanket. In addition, no change occurs in the radiated power density [1, 5, 7, 8, 14-16, 23].

For infants nursed in convective incubators, the use of plastic blanket reduces the insensible water loss which is inversely proportional to the body weight. Apparently there is no significance change in oxygen consumption for infants of this group [1, 3, 5, 7, 8, 14, 23].

1.1.4.3 Accessibility for Care Giving

Although convective incubators can provide a certain level of water vapour pressure to reduce insensible water losses through the skin, its environmental temperature varies each time the incubator portholes are opened for nursing purposes. Whereas a radiant warmer gives more accessibility for nursing (as it is an opened environment), it does not maintain the required level of relative humidity. Moreover, the number of times infants are handled when nursed under radiant warmers may increase the oxygen consumption compared to those cared for in incubators [3, 5, 7].

1.1.4.4 Humidity and Insensible Water Losses:

Low relative humidity of a servo controlled incubator increases the temperature of the incubator itself and the oxygen consumption of premature infants accordingly. This causes an increase in the insensible water losses. In addition, premature infants with small weight or illnesses are susceptible to unfavourable incidents such as apneic spells¹ [10]. However, insensible water losses under radiant warmers are higher than conventional incubators [3, 7, 23-26].

¹ Periods of cessation of spontaneous breathing, characteristic of prematurity and newborn brain-damage.

Minimal oxygen consumption has also been achieved under radiant warmer regardless of the insensible water loss. These losses via evaporation can be balanced by decreasing the heat losses through other routes (non-evaporative heat losses), or by increasing the amount of radiated heat from the warmer over heat losses via radiation. This causes an increase in a net heat gain from the warmer without increasing the total consumed energy, Thus thermo-neutrality can be created under a radiant warmer [23-25].

Apparently, small variations in relative humidity inside incubators with skin servo control do not influence the insensible water loss; however significant fluctuations in relative humidity would vary the amount of insensible water losses [27]. Few investigations [15, 27] have shown that the body weight and insensible water loss is inversely proportional to the water loss.

Basically, non-ionising radiant energy converts into heat inside the baby's body via photochemical reactions and interactions with the bio-system [27]. High insensible water losses have been obtained under radiant heat warmers with infrared lamps in comparison with other radiant energy sources (for example nichrome wire and carbon heat shield) [27].

When ill infants with low birth weight receive phototherapy² in incubators, their insensible water losses are significantly doubled or tripled [27]. This is attributed to the heat source placed inside the incubator for the purpose of phototherapy. It may also be attributed to the delay in time until the effectiveness of phototherapeutic processes is reached.

Furthermore, when premature infants are nursed under radiant warmer and receive phototherapy at same time, their insensible water losses are increased to a minimum of 44% [22]. In a radiant heat warmer, the exposure to non-ionizing radiant energy causes several changes in infants who required phototherapy (such as, changes in body temperature, higher insensible water loss and fluid intakes) [28]. Although it can be necessary to use radiant heat warmer to nurse premature infants with low birth weight instead of incubators, this causes an increase of insensible water losses. Thus, the smaller the infant (small body weight) the higher the insensible water losses and the fluid intakes accordingly.

² Phototherapy is used for the treatment of neonatal jaundice (when newborns skin goes "Yellow").

Moreover, the ratio of skin surface area to body weight for an infant is four times greater than an adult [21], this means the ratio of skin surface area to body weight is increasing when body weight decreases. Therefore, the radiant energy required to maintain body's temperature increases with decreasing weight. The body's surface area-weight ratio of small infants could be one of the reasons for the increase of the insensible water losses under radiant warmer. This may be attributed to resuscitation methods. The working conditions of these methods in ventilating airways may increase the insensible water losses instead of decreasing. One can conclude however, that both radiant energy and insensible water losses depend on body area-weight ratio.

1.2 Objectives

This research aims to employ physics, mathematics and biological data to:

1. Develop a comprehensive simulation model for an infant-incubator system to investigate the relationship of heat exchange variables and factors that influence the overall thermal environment of the infant.
2. Model the performance of a convectively-heated single-walled incubator used to nurse preterm infants with very low birth weight and low gestational age.
3. use available data to validate the above model.

Chapter 2 Model Development

2.1 Introduction

One of the major concerns in nursing newborn infants particularly preterm infants soon after birth, is providing them with appropriate thermo neutral environments. This can maintain their body's temperature at the normal level of 36.5-37.5 °C (Figure 1-2). This can only be implemented by placing the newborn infants inside thermoregulation devices, which are also called 'infants warmers'.

To provide the necessary heat and humidity for the preterm infants immediately after delivery, there are two types of heating warmers used in infant incubators, namely, radiant and convective.

In this chapter, a mathematical model for a 'convective incubator' will be developed. The modelling is primarily based on heat and mass conservation laws.

2.2 Infant-Incubator System

An incubator system comprises of an infant and incubator. The proposed model is intended to develop and study the heat exchange relationships between the infant, incubator compartments and the environment.

In this chapter, a mathematical model of the infant-incubator system will be developed with all heat exchange routes incorporated. These include conduction, convection, evaporation, radiation, and heat generation from the infant in terms of metabolic rates. For this research, the model targets preterm infants, as they are more susceptible to illnesses than full-term infants.

Appropriate assumptions are made wherever needed to simplify the modelling. Also, some empirical relationships (such as an estimation of the surface area of the infant in terms of infant weight [18]) are used in the modelling to further simplify the equations.

Although other simplified models are available in this regard [29-31], the present model provides better accuracy and is more comprehensiveness. It also considers the fan-heater/humidification system which is not available in other models. Figure 2-1 illustrates all interactions within the infant-incubator system including the baby's core

and skin layers, mattress, incubator air space, incubator's walls, and the fan-heater/humidification section. All of these interactions are considered in the present development.

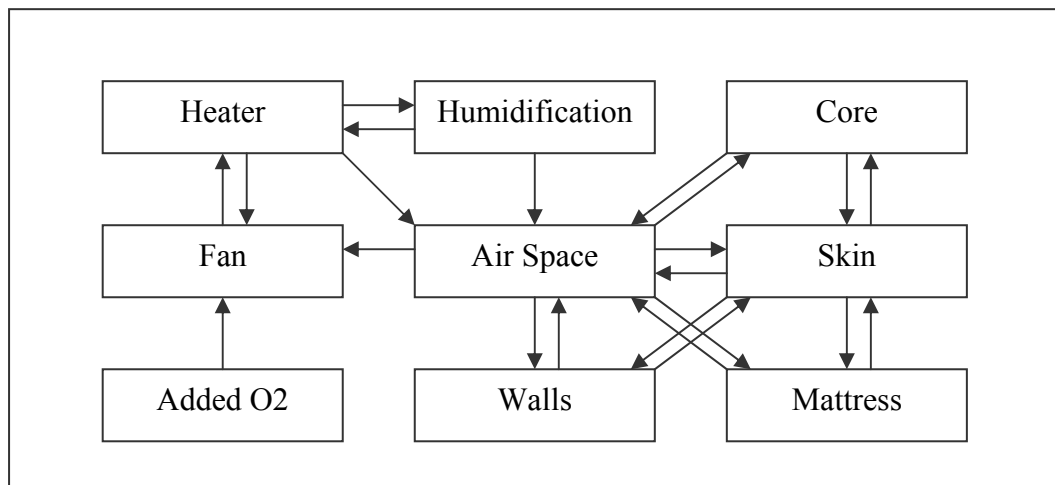


Figure 2-1 Interaction between compartments of infant-incubator system

The incubator used for modelling is an ATOM V-850 manufactured in Japan in 1985 by ATOM Medical and is provided by Fisher and Paykel Healthcare Ltd. The incubator is single-walled with a slanted front and is convectively heated using a fan and a heating element. It also has a humidification system that maintains the required humidity level inside the incubator at all times.

Figure 2-2 shows all the compartments of the incubator. The hood is equipped with 6 port doors plus a front door panel for care giving purposes and is made from transparent plexiglass. The mattress with the bed is placed inside the hood on 2 rails, the lower part of the incubator is right underneath the hood and is called heating/humidification compartment. This includes a fan section/housing, electric heater and a water chamber. The fan continuously blows air over the heater, which passes into the water chamber through an air duct to increase the amount of absorbed water depending on the required humidity. Finally, the moist air enters the incubator air space. (see Figure 2-3 for illustration).

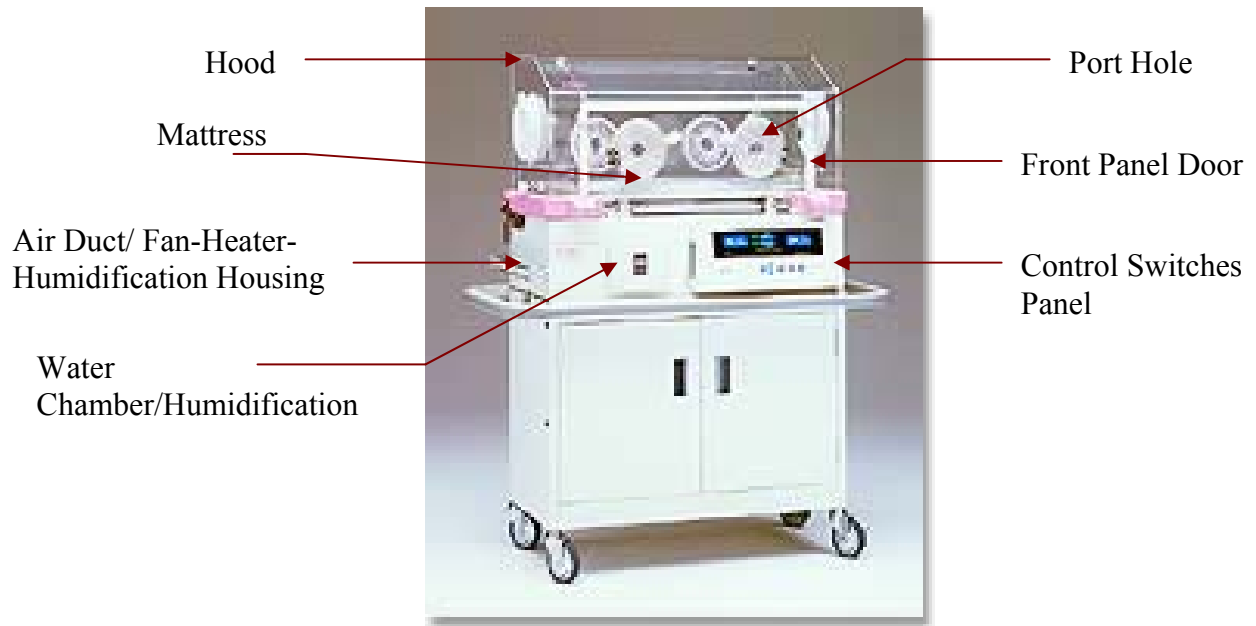


Figure 2-2 Incubator/ATOM V-850 (Courtesy Atom Medical Corporation, Tokyo)

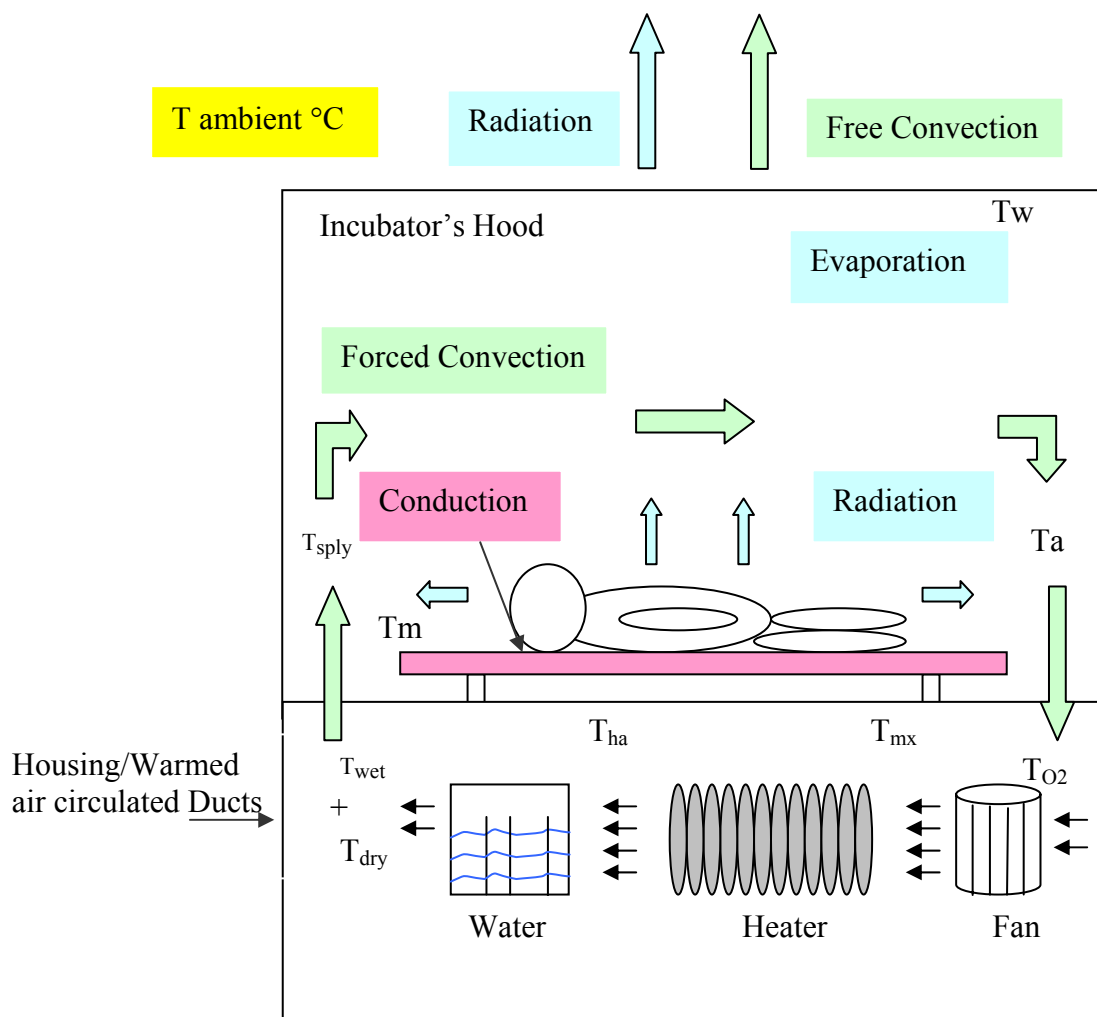


Figure 2-3 Heat flow diagram

Pure oxygen (100% O_2) is supplied to the incubator for resuscitation purposes via a bottle connected to a throttle valve placed at the back of the incubator. This valve regulates the oxygen flow rate to the system based upon the required concentration of oxygen (O_2 %) and dependent on the condition of the infant. The concentration level is determined by a medical doctor (staff). However, the current practice they do not tend to use this facility and instead rely on other resuscitation devices such as an nCPAP (Nasal Continuous Positive Air Pressure) device to supply oxygen to ill infants.

Therefore the air change mechanism for this incubator can be explained as follows: The size (volume) of the hood with respect to the infant's size (infant's breath volume) is significantly large, for this reason it is assumed the incubator air space doesn't change its percentages of oxygen and nitrogen significantly (i.e. 21% O_2 and 79% N_2). Also, taking in consideration that during care giving the incubator air would change as the incubator's port doors are opened, and that this often happens every 2 hours or less [3].

There are two methods of providing feedback to this incubator: skin servo control and air servo control. The feedback scheme normally operates by having the fan of the incubator maintain the circulation of the heated air inside the incubator at all times regardless of the variation in the setting temperature. Therefore, the whole system undergoes heat exchange in a pattern of forced convection. The heating element however, varies its power from 0-260 watts in a response to the variation in controlled temperature (i.e. skin-controlled temperature or air-controlled temperature). The modelling of the components in Figure 2-3 will be detailed in the following sections.

2.3 Infant Modelling

There are several methods available for modelling infants. An infant can be modelled as a one-lumped mass [29] or as a four-lumped mass representing the head, trunk, upper limbs and lower limbs [30]. The latter model has the advantage in demonstrating that there is a temperature difference between the infant segments, and that this temperature gradient is attributed to the allocation of heat production and heat losses for each segment. Rojas however showed that this temperature difference is usually not significant [30].

Both of the formulated models consider the infant with two layers: core and skin. Thus, in the one-lump model, there are two infant compartments plus a central blood

compartment, while with the four-lump model, there are nine compartments in total. (see Figure 2-4 and Figure 2-5).

Both models use the same technique to describe the heat exchange processes within the infant. Thus, their mathematical equations have similar forms regardless of the direction of the heat flow from one layer to another. Models A and B in Figure 2-5 illustrate the heat exchange between the core and skin within an infant's body as one-lump and four-lumps models respectively.

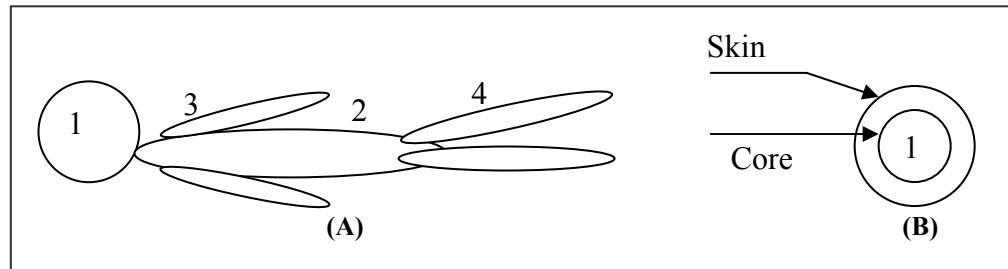


Figure 2-4 Infant Model (A)/Segments-Layers (B)

These two models can be described as follows:

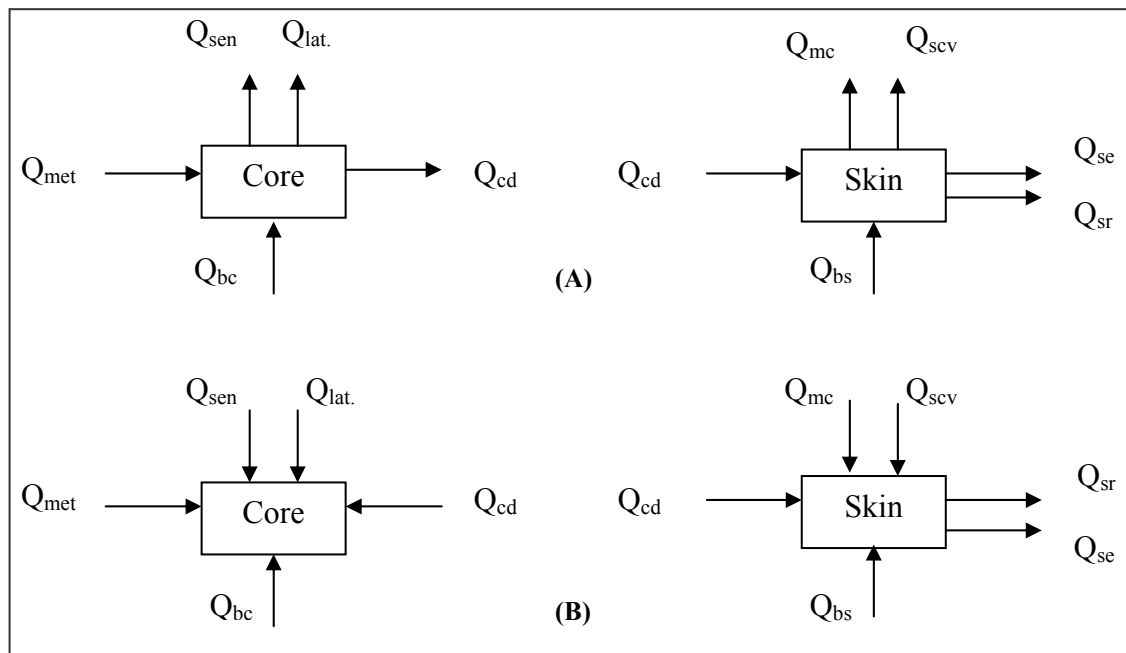


Figure 2-5 (A) / (B) - Heat exchange block diagram

Model A is based on Simon's model [29], and model B is based on Rojas's model [30] (Figure 2-5 A / B). From Figure 2-5, the core gains heat via:

- Metabolic rate, Q_{met} .
- Convection with the blood of the core, Q_{bc} .

while the routes of heat losses are via:

- Respiration (i.e. sensible and latent heat, $Q_{sen} - Q_{lat}$).
- Conduction with the adjacent layer the skin Q_{cd} .

Similarly the skin layer gains heat via conduction with the core, Q_{cd} but loses heat via:

- Conduction with the mattress, Q_{mc} .
- Convection with both incubator air space, Q_{scv} , and with the skin blood, Q_{bc} .
- Radiation losses to the incubator walls, Q_{sr} .
- And finally losses through evaporation from the skin, Q_{se} .

In the Simon [29] and Rojas [30] models, the rate of conductive heat between the mattress and the incubator Q_{ic} is considered to be negligible.

In this work to simplify the model the following assumptions are made:

1. Single-walled rectangular incubator with one slanted front wall, forced convection heating and a humidification system.
2. The material of each compartment has homogenous properties.
3. Uniform airflow throughout the system.
4. Consider the required metabolic rate for self-thermoregulatory of the infant is the resting metabolic rate, M_{rst} [9].
5. For modelling purposes, the infant is considered as a black coloured cylinder.
6. The preterm infant is healthy and no resuscitation devices are used such as CPAP (Continuous Positive Air Pressure) device or fluid intakes are given for dehydration treatment purposes.
7. The self-thermoregulatory systems of the infant are not included in the model (i.e. sweating and shivering).
8. X-ray facility is excluded from the model.
9. The conductive heat between the mattress and the incubator, Q_{ic} , is neglected.
10. The only perturbation occurs to the model via port doors and/or front panel for care giving purposes.
11. The mattress and its pan are considered one lump, also no other linen is added.

12. The infant incubator is placed in a thermo-regulated room, and the velocity of air currents is minimal. Thus, only external free convection is permissible.

Each of the model equations describes the temperature variation of each compartment over time (i.e. instantaneous temperature).

Each compartment of the model is subjected to the 1st law of thermodynamics (law of energy conservation), namely that in a period of dt , heat balance results in:

$$[\text{Heat in} - \text{Heat out}] dt = \text{Heat Storage} \quad (2.1)$$

2.3.1 Core layer

Consider a one-lumped mass model for the infant as shown in Figure 2-5. In a period of time, dt , the heat balance of the core layer can be written as:

$$[Q_{met} - Q_{sen} - Q_{lat} - Q_{cd} - Q_{bc}]dt = M_c C_{p_c} dT_c \quad (2.2)$$

Therefore, the instantaneous temperature of the core can be written as:

$$\frac{dT_c}{dt} = \frac{Q_{met} - Q_{sen} - Q_{lat} - Q_{cd} - Q_{bc}}{m_c C_{p_c}} \quad (2.3)$$

Using the differential operator $D = d/dt$ allows equation (2.3) to be written as:

$$T_c = \frac{Q_{met} - Q_{sen} - Q_{lat} - Q_{cd} - Q_{bc}}{m_c C_{p_c} D} \quad (2.4)$$

Equation (2.4) describes all heat flow rates that manipulate the heat transfer relationships associated with the infant body. Each one of the terms in this equation is defined in the nomenclature and can be determined as follows:

2.3.1.1 Heat production of infant core, Q_{met}

The heat production of the core of the infant body can be written as:

$$Q_{met} = M_{rst} \times S_a \quad (2.5)$$

where M_{rst} is the resting metabolic rate as opposed to the basal metabolic rate and S_a is the surface area of the infant. This is a function of infant weight and can be determined using an empirical formula that will be shown later in this chapter. It is necessary to use the resting metabolic rate because the basal metabolic rate can only be measured after overnight fasting and this is ethically unacceptable for neonates [26, 32]. The estimated value for M_{rst} is 24.80 W/m^2 [9, 26]. This is determined at the thermo-neutral zone during the 1st week of life.

2.3.1.2 Heat losses of infant core

The infant core loses heat during breathing in the form of convective heat which takes the form of Q_{sen} due to warming the inhaled air and Q_{lat} caused by the difference between water-vapour pressure of the inhaled and exhaled air. In terms of respiratory rate and tidal volume, the equations for respiration losses can be determined by [29] :

$$Q_{sen} = rr \times C_{p_a} \times v_t \times \rho_a \times (T_{ex} - T_a) \quad (2.6)$$

$$Q_{lat} = hfg \times rr \times \rho_a \times v_t \times (W_{ex} - W_a) \quad (2.7)$$

Equations (2.6) and (2.7) will be modified in terms of inspired minute volume (IMV) of 200 mL/kg of infant mass [33]. This value represents the total volume of the air inhaled and exhaled in one minute per kilogram mass of infant.

Equations (2.6) and (2.7) may then be re-written as:

$$Q_{sen} = IV \times m \times C_{p_a} \times \rho_a \times (T_{ex} - T_a) \quad (2.8)$$

$$Q_{lat} = IV \times m \times hfg \times \rho_a \times (W_{ex} - W_a) \quad (2.9)$$

where the inspired air volume, IV , equals to 3.333 mL/kg mass of the infant/sec.

Equations (2.8) and (2.9) are written in terms of infant's mass m or mass of the body local segment and inspired air volume (IV). They are more reliable in comparison with Simon's equations [29], particularly since the respiratory rate and tidal volume of infant is not well-documented. In the model proposed in this work, equations (2.8) and (2.9) will be employed. For more precise results, T_{ex} is assumed to be equal to T_c .

The humidity ratio of the exhaled air is determined by [34]:

$$W_{ex} = 0.622 \frac{P_{H_2O}}{P_t - P_{H_2O}} \quad (2.10)$$

and for the inhaled air by:

$$W_a = 0.622 \frac{P_{H_2O}}{P_t - P_{H_2O}} \quad (2.11)$$

The partial pressure of water-vapour P_{H_2O} in the air at T_a & T_{ex} is determined by:

$$P_{H_2O} = P_{sat.} \times RH\% \quad (2.12)$$

where P_t is the atmospheric pressure and P_{sat} is the saturation pressure for air which can be found from tables available in most heat transfer books (example Stoecker [34] or Cengel [35])[34, 35]. P_{sat} is a function of air temperature and for simulation purposes, exponential formula can be developed from Figure 2-6 [35]:

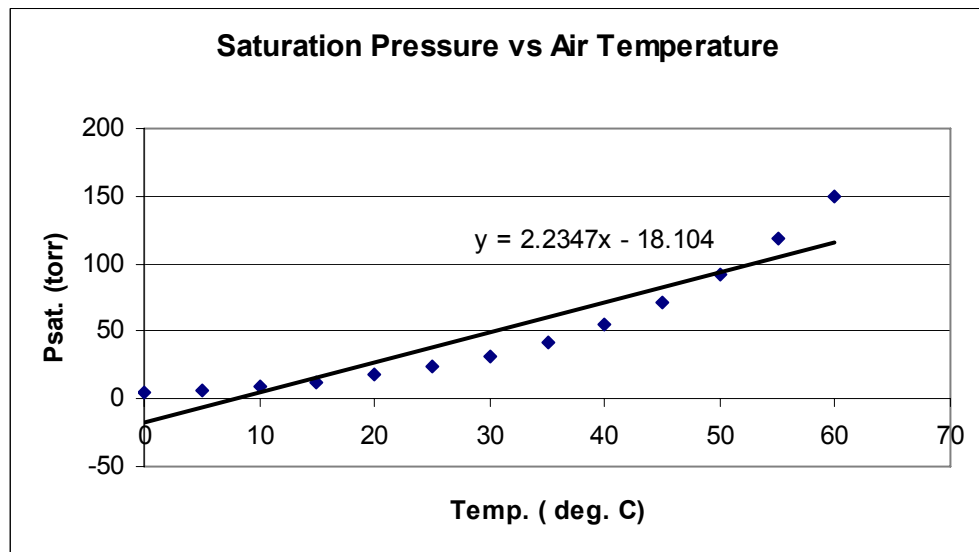


Figure 2-6 Pressure-temperature curve [35]

Thus, the relationship between P_{sat} and T can be written as:

$$P_{sat} = 2.2347T - 18.104 \quad (2.13)$$

This is calculated for a temperature range of 0.01-60 °C and is used to estimate the saturation pressure at any given temperature within that range. The relative humidity of the exhaled air $RH\%$ at 37 °C body core temperature is also assumed to be 100% [36].

The core also loses heat via conduction through the skin layer. Thus, the rate of conduction can be determined by:

$$Q_{cd} = \frac{(T_c - T_s) \times K_c \times S_a}{(m / \rho_c \times S_a)} \quad (2.14)$$

where all the parameters in equation (2.14) are defined in the nomenclature (page xiii). The core blood constitutes a medium for convective heat losses, which can be determined by:

$$Q_{bc} = (T_c - T_s) \times \rho_{bl} \times bf \times C_{p_b} \times V_{cb} \quad (2.15)$$

The blood volume V_{cb} in equation (2.15) is directly determined from the mass of the layer of the infant body using [37]:

$$V_{cb} (mL) = 80 \left(\frac{mL}{kg} \right) \times m (kg) \quad (2.16)$$

The blood flow rate parameter bf in 1/sec for the infant body is derived as follows:

$$bf = \rho_{bl} \times q_b \quad (2.17)$$

where q_c is the cardiac output of the infant (3.333 mL/kg.sec) [38] and ρ_{bl} is 1.06×10^{-3} kg/mL [39]. Using these values in equation (2.17) results in a blood flow parameter of 0.00353 (sec^{-1}).

The mass of the infant core m_c can be determined as follows:

$$m_c = m \times m_s \quad (2.18)$$

where m_s is the mass of the infant skin and is determined using:

$$m_s = th_s \times \rho_s \times S_a \quad (2.19)$$

The total surface area of either the infant body or the local body segment S_a can be calculated using the empirical formula [18].

$$S_a = mass^{0.75}/10.80 \quad (2.20)$$

where S_a is in m^2 and mass is in kilograms.

In equation (2.20), the surface area of the infant is considered to be a function of mass only. Which is consistent with the trend of this model.

2.3.2 Skin layer

Consider the skin layer shown in Figure 2-5. In a period of time, dt , the heat balance equation for the skin layer can be written as follows:

$$[Q_{cd} + Q_{bc} - Q_{scv} - Q_{mc} - Q_{se} - Q_{sr}]dt = m_s C_{p_s} dT_s \quad (2.21)$$

Therefore, the instantaneous temperature of the skin can be written as:

$$\frac{dT_s}{dt} = \frac{Q_{cd} + Q_{bc} - Q_{mc} - Q_{scv} - Q_{se} - Q_{sr}}{m_s C_{p_s}} \quad (2.22)$$

Using the D-operator, the skin temperature of the infant can be written as:

$$T_s = \frac{Q_{cd} - Q_{bc} - Q_{mc} - Q_{scv} - Q_{se} - Q_{sr}}{m_s C_{p_s} D} \quad (2.23)$$

where Q_{cd} , Q_{bc} and m_s are given in equations (2.14), (2.15) and (2.19) respectively, while the rate of conductive heat loss from the skin in contact with the mattress Q_{mc} can be determined by:

$$Q_{mc} = A_s \times K_{mat} \times (T_s - T_m)/th_m \quad (2.24)$$

The average mattress temperature is taken in the middle of the given thickness of the mattress. Thus the mattress thickness, th_m , is halved. The surface area of the skin in contact with the mattress for either infant local segment or infant body A_s is estimated to be 10% of the total infant surface area (m^2) [18] thus:

$$A_s = 0.1 \times S_a \quad (2.25)$$

In addition, the skin undergoes convective heat losses due to the difference in temperature between skin and air space. This can be determined by:

$$Q_{scv} = h_{scv} \times A_{cv} \times (T_s - T_a) \quad (2.26)$$

Since the surface area in contact with the mattress is 10% of the total surface area, the surface area exposed to the air is 90%. A_{cv} can then be written as:

$$A_{cv} = 0.9 \times S_a \quad (2.27)$$

In equation (2.26) the convective heat transfer coefficient for forced convection h_{scv} depends on the geometry of the infant and is a function of the Nusselt and Reynolds numbers. The Nusselt number is defined as:

$$Nu_{sph} = \frac{h_{scv} D_{sph}}{K_a} \quad (2.28)$$

and the Reynolds number as;

$$Re_D = \frac{\rho_a V_a D_{sph}}{\mu_a} \quad (2.29)$$

The shape of the infant body is not uniform and is difficult to model. The direction of the air flow parallel to the infant longitudinal axis creates another complexity in choosing appropriate empirical formulas for Nusselt number. Therefore, in this work the infant body is approximated as a cylinder with air flows parallel to its axis, as shown in Figure 2-7.

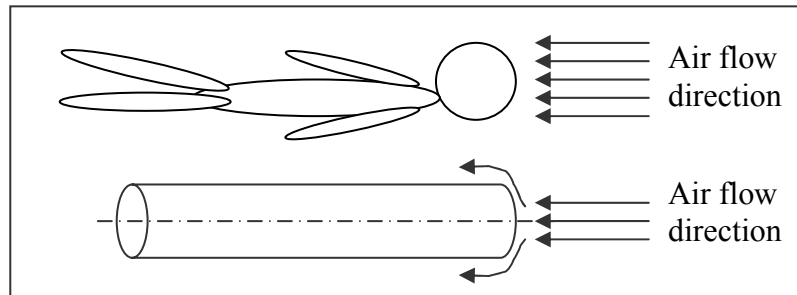


Figure 2-7 Infant shape approximation

Since the cross-section area for the cylinder with regard to the direction of air flow is as for a sphere. Thus, the Nusselt number for this situation can then be approximated as [35]:

$$Nu_{sph} = \frac{h_{scv} D_{sph}}{K_a} = 2 + [0.4 Re^{1/2} + 0.06 Re^{2/3}] Pr^{0.4} \left(\frac{\mu_a}{\mu_s} \right) \quad (2.30)$$

where the Prandtl number is defined by [35]:

$$Pr = \frac{\mu_a C_{p_a}}{K_a} \quad (2.31)$$

The air properties in equations (30-33) are evaluated at T_a , except for μ_s which is evaluated at skin temperature, T_s .

The water loss from the skin to the air space through evaporation is inversely proportional to the ambient partial pressure of water vapour [18]. The evaporation heat rate Q_{se} (in watts) can be determined by:

$$Q_{se} = \frac{hfg \times m \times Evap. \times \rho_{h_2o}}{86400} \quad (2.32)$$

where $Evap.$ is the evaporation loss from the skin of the infant to the environment (in mL/kg/day), which is a function of gestational age (GA) and postnatal age (age), and can be determined from the equation developed by LeBlanc [18] as follows:

$$Evap. = \left[6.5 \exp(168/(age + 11.8)) \times \exp(-5.2GA/(age + 12.2)) + 4.8 \right] * \left[2 - \left(\frac{P_{H_2O}}{23} \right) \right] \quad (2.33)$$

where P_{H_2O} is determined by equation (2.13).

The skin also loses heat to the walls of the incubator by radiation. Thus, the rate of radiant heat losses can be determined by:

$$Q_{sr} = A_r \times \sigma \times \varepsilon_s \times [(T_s + 273.15)^4 - (T_w + 273.15)^4] \quad (2.34)$$

The surface area of the neonate body normal to the walls of the incubator, A_r , is a fraction of the infant surface area exposed to air, A_{cv} , and for various parts of the infant body is defined as [18]:

1. 30% of total surface area is given to the objects directly above a reclining infant.
2. 17% of total surface area is given to the sides.
3. 8.5% of total surface area for above the head or below the feet.

Equations (2.2 – 2.34) describe the heat exchange of the infant model as a one lump. For the four-lump model however, each segment should be dealt with separately similar to the one-lump model. The same set of equations described above can be employed with some considerations as follows:

1. The respirations losses from the core for each of the four body segments are assumed to be percentages of the total heat losses by respiration for the head and trunk, while for the extremities are zero [30]. Equations (2.8) and (2.9) however are still applicable.
2. The heat production of the core for each segment is multiplied by a factor, mr_i , which represents the percentages of the total heat production of the infant core [30]. For instance, heat production for the core of the head makes up 70% of total heat production in the infant [40], the trunk core 24%, the upper limbs core 2% and the lower limbs core 6% [30]. While for the infant model of one lump, mr_i , equals 100% as the core of the infant is considered as one lump.

For the four-lump model, equation (2.5) can be modified as follows:

$$Q_{met} = M_{rst} \times S_{ai} \times mr_i \quad (2.35)$$

The subscript i symbolises the local segment of the infant body and should appear next to all parameters in all equations above.

2.4 Incubator Modelling

The incubator comprises of the following parts:

1. Air space.
2. Walls (hood).
3. Mattress.

2.4.1 Air Space Modelling

The incubator air space exchanges heat with all compartments of the infant-incubator system, mainly by convection, but also by heat and mass transfer via respiration and evaporation. Figure 2-8 illustrates all heat gains and losses within the air space compartment.

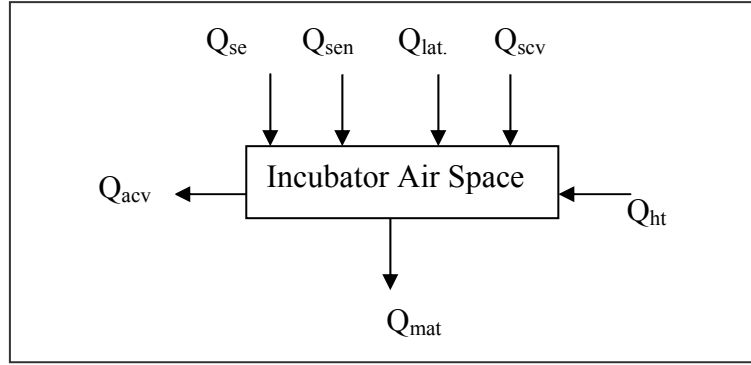


Figure 2-8 Block diagram for heat exchange within the air space

In a period of dt , the heat balance equation for the incubator air space can be written using equation (2.1) as follows:

$$[Q_{scv} + Q_{se} + Q_{ht} + Q_{sen.} + Q_{lat.} - Q_{acv} - Q_{mat}]dt = M_a C_{p_a} dT_a \quad (2.36)$$

Thus, the instantaneous temperature of the air space:

$$\frac{dT_a}{dt} = \frac{[Q_{scv} + Q_{se} + Q_{ht} + Q_{sen.} + Q_{lat.} - Q_{acv} - Q_{mat}]}{M_a C_{p_a}} \quad (2.37)$$

Using D-operator the temperature of the air space can be written as:

$$T_a = \frac{[Q_{scv} + Q_{se} + Q_{ht} + Q_{sen.} + Q_{lat.} - Q_{acv} - Q_{mat}]}{M_a C_{p_a} D} \quad (2.38)$$

The incubator air space gains heat by convection from the infant skin, Q_{scv} , which can be determined using equation (2.26), and from the heating/humidification compartment, Q_{ht} , which will be defined during the modelling of the humidification compartment. An estimation of the incubator air space mass, M_a , will be detailed in the modelling of the circulated-air fan. Also, the water losses from the skin occur via evaporation into the air space and this vaporized energy is defined by Q_{se} , and can be determined using equation (2.32).

In addition, there is a heat and mass transfer associated with infant's respiration. The heat transfer is in the form of sensible heat, Q_{sen} , due to warming the inhaled air, which can be determined by equation (2.8). The mass transfer is in the form of latent heat, Q_{lat} , which is due to the difference in partial pressure of water-vapour between the inhaled and exhaled air, and can be determined by equation (2.9).

In contrast, the air space compartment loses some of its heat to the walls of the incubator by convection Q_{acv} , which can be determined as follows:

$$Q_{acv} = h_{acv} A_{wi} (T_a - T_w) \quad (2.39)$$

The convective heat transfer coefficient, h_{acv} , depends on the geometry of the incubator hood and the regime of the airflow inside the hood. It is also a function of the Nusselt and Reynolds numbers according to equations (2.28) and (2.29).

Since the given air velocity inside the hood is not high (approximately 10 cm/sec, supplied by the manufacturer) the Reynolds number for such a velocity is 4970.6. Therefore the pattern of the airflow regime is turbulent to transitional flow [35]. This calculation was done by assuming the shape of the hood is rectangular rather than with a slanted front, as follows:

The equivalent hydraulic diameter of the incubator, D_h , can be determined using:

$$D_h = \frac{4A_c}{p} \quad (2.40)$$

The Nusselt number for this regime of flow in the incubator can be determined by [35]:

$$Nu_1 = \frac{h_{acv} D_h}{K_a} = \frac{(f/8)(Re-1000)Pr}{1+12.7(f/8)^{0.5}(Pr^{2/3}-1)} \quad (2.41)$$

The friction factor, f , in equation (2.41) is then determined by [35]:

$$\frac{1}{\sqrt{f}} = -2.0 \log \left(\frac{\varepsilon/D_h}{3.7} + \frac{2.51}{Re\sqrt{f}} \right) \quad (2.42)$$

Since the roughness, ε , of the hood material (plexiglass) is zero, the friction factor is around 0.0119 [35].

Likewise, the mattress is convectively heated by the air. Not all of the area of the mattress is convectively heated however, only the area not covered by the infant, which can be determined as follows:

$$Q_{mat} = h_{acv} A_{net} (T_a - T_m) \quad (2.43)$$

In equation (2.43), the convective heat transfer coefficient, h_{acv} , can be determined using equation (2.41). While the net area of the mattress not covered by the infant A_{net} can easily be determined using:

$$A_{net} = A_{mat} - A_s \quad (2.44)$$

where A_s is defined by equation (2.25).

2.4.2 Wall (hood) Modelling

The compartment of the incubator walls ‘hood’ is made of transparent plexiglass and has 6 port doors plus a front panel for care giving purposes. One of the front sides also has a slanted surface. The incubator wall is considered as a single thin one-lump of 6 mm thickness. Thus, the temperature gradient within such thickness is not significant and the conduction resistance of the wall is negligible.

The following assumptions are made to simplify the modelling:

1. The material of the wall is homogenous and uniform.
2. There is a uniform temperature distribution across and over the internal and external surfaces of the wall.

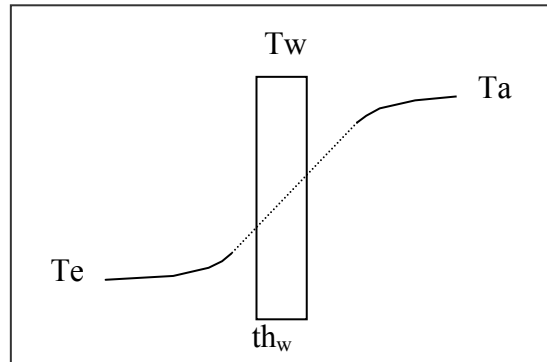


Figure 2-9 Temperature difference across the wall

Figure 2-9 shows the anticipated temperature gradient between the inside of the incubator (T_a) and the outside environment (T_e). Since air is the only medium crossing the inner and outer surfaces, heat losses are therefore in forms of convection and radiation as shown in Figure 2-10.

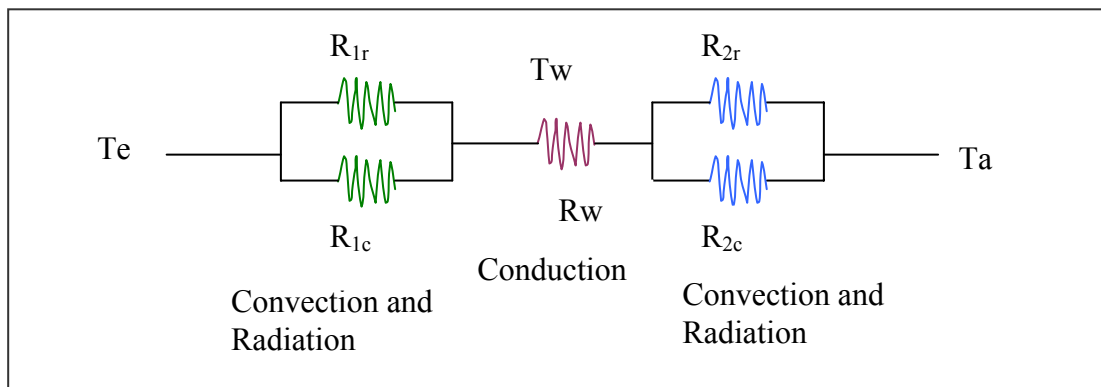


Figure 2-10 Heat transfer diagram

In this figure, R_{2r} and R_{2c} represent the convective and irradiative heat gains to the internal surface of the walls respectively. Likewise, R_{1r} and R_{1c} represent the heat losses

from the external walls to the environment by radiation and convection respectively. R_w , represents the heat transfer by conduction between the inner and outer surfaces of the wall, which in this case is considered negligible. Figure 2-11 illustrates the rates of heat transfer within the wall compartment.

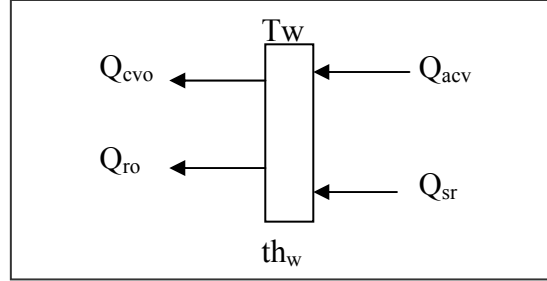


Figure 2-11 Block diagram for heat exchange across the wall

From Figure 2-11, in a period of dt the heat balance equations for the incubator walls can be written using equation (2.1) as:

$$[Q_{acv} + Q_{sr} - Q_{cvo} - Q_{ro}]dt = M_w C_{pw} dT_w \quad (2.45)$$

Therefore, the instantaneous temperature of the wall can be written as:

$$\frac{dT_w}{dt} = \frac{[Q_{acv} + Q_{sr} - Q_{cvo} - Q_{ro}]}{M_w C_{pw}} \quad (2.46)$$

Using D-operator, the wall temperature can be written as:

$$T_w = \frac{[Q_{acv} + Q_{sr} - Q_{cvo} - Q_{ro}]}{M_w C_{pw} D} \quad (2.47)$$

The inner surface of the incubator wall gains heat by convection from the incubator air space, Q_{acv} , which is determined using equation (2.39). The wall also gains heat from the skin of the infant by radiation, the rate of radiative heat transfer, Q_{sr} , being determined by equation (2.34).

Due to the temperature gradient between the inside incubator and environment, the wall of the incubator loses heat to the environment (room) in the form of radiation and convection.

For convective heat losses, free (natural) convection occurs from the walls to the environment. Thus, convective heat loss is a function of the Nusselt and Prandtl numbers, which can be determined by [35]:

$$Nu_{inc} = \frac{h_{cvo} L_c}{K_a} = C (Gr_L Pr)^n = CRa_L^n \quad (2.48)$$

where Gr_L is the Grashof number defined by [35]:

$$Gr_L = \frac{g\beta(T_w - T_e)L_c^3}{\nu^2} \quad (2.49)$$

and Ra_L is the Rayleigh number defined by [35]:

$$Ra_L = Gr_L Pr = \frac{g\beta(T_w - T_e)L_c^3}{\nu^2} Pr \quad (2.50)$$

The fluid properties related to the above equations are evaluated at the average temperature of the inner wall's temperature and room temperature as follows [35]:

$$T_{avg} = \frac{1}{2}(T_w + T_e) \quad (2.51)$$

Since the incubator hood has approximately horizontal and vertical surfaces, the Nusselt number will be determined as follows [35]:

For the horizontal (lower) surface of the incubator:

$$Nu_{hzt} = 0.27 Ra_L^{1/4} \quad (2.52)$$

For the four vertical-sides, the Nusselt number is given by [35]:

$$Nu_{vrt} = \left\{ 0.825 + \frac{0.387 Ra_L^{1/6}}{\left[1 + (0.492 / Pr)^{9/16} \right]^{8/27}} \right\}^2 \quad (2.53)$$

For the Grashof number in equation (2.49), L_c is given by [35]:

$$L_c = \frac{A_c}{p} \quad (2.54)$$

Based on the equations (2.52) and (2.53), two different values of convective heat transfer coefficients are determined for each surface. Using these coefficients, the rate of convective heat transfer is determined by:

$$Q_{cvo} = h_{cvo} A_{wi} (T_w - T_e) \quad (2.55)$$

The total convective heat losses from the four vertical-sides of the incubator Q_{cvt} (i.e. two long sides and two short sides) are added together to give:

$$Q_{cvt} = Q_{c_{het}} + 2[Q_{c_{vrt}}]_{long} + 2[Q_{c_{vrt}}]_{short} \quad (2.56)$$

For the radiation loss, the rate of radiant heat transfer from the walls to the environment is determined as follows [35]:

$$Q_{ro} = A_w \times \sigma \times \varepsilon_w \times [(T_w + 273.15)^4 - (T_e + 273.15)^4] \quad (2.57)$$

The mass of the incubator walls, M_w , is determined using:

$$M_w = \rho_w th_w A_{wi} \quad (2.58)$$

where ρ_w , th_w and A_{wi} are the wall material density (in kg/m³), wall thickness (in m) and the surface area of the incubator walls (in m²) respectively.

2.4.3 Mattress Modelling

The mattress gains heat by conduction with the skin of the infant, and is convectively heated by the incubator air space. Since the two thin support plates carry the mattress, and the contacted area is considered small, the conductive heat transfer from the mattress to the incubator, Q_{ic} , is not significant and can be ignored.

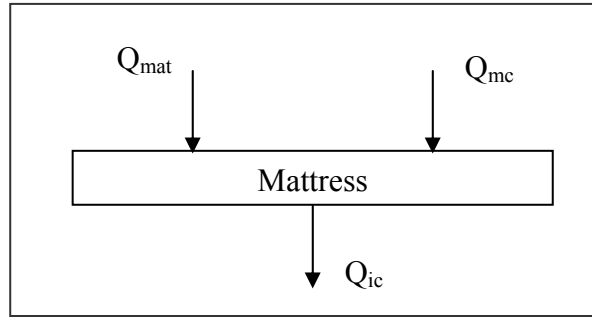


Figure 2-12 Block diagram for the mattress

From Figure 2-12 , in a period of dt , the heat balance equation for the mattress can be written using equation (2.1) as follows:

$$[Q_{mc} + Q_{mat} - Q_{ic}]dt = M_m C_{p_m} dT_m \quad (2.59)$$

Thus, the instantaneous mattress temperature can be written as:

$$\frac{dT_m}{dt} = \frac{[Q_{mc} + Q_{mat} - Q_{ic}]}{M_m C_{p_m}} \quad (2.60)$$

Using D-operator, the mattress temperature T_m can be written as:

$$T_m = \frac{[Q_{mc} + Q_{mat} - Q_{ic}]}{M_m C_{p_m} D} \quad (2.61)$$

Both Q_{mc} and Q_{mat} can be determined using equations (2.24) and (2.43) respectively.

Similarly, and as for the modelling of the infant with four segments, the related parameters of the modelling equations of the incubator (2.36)-(2.61) would be subscripted with i to symbolise the local segment of the infant body.

2.5 Heating Element Modelling

Figure 2-13 illustrates the parts of the heating compartment. Several assumptions are made to simplify the modelling of this compartment as follows:

1. The material of the heater is assumed to be homogenous with constant characteristics such as the specific heat C_p , cross-sectional area of the coil and the gaps between the coils.

2. The distribution of the temperature is uniform.
3. The specific heat of the mixed heated air C_{p_m} is as for normal air.

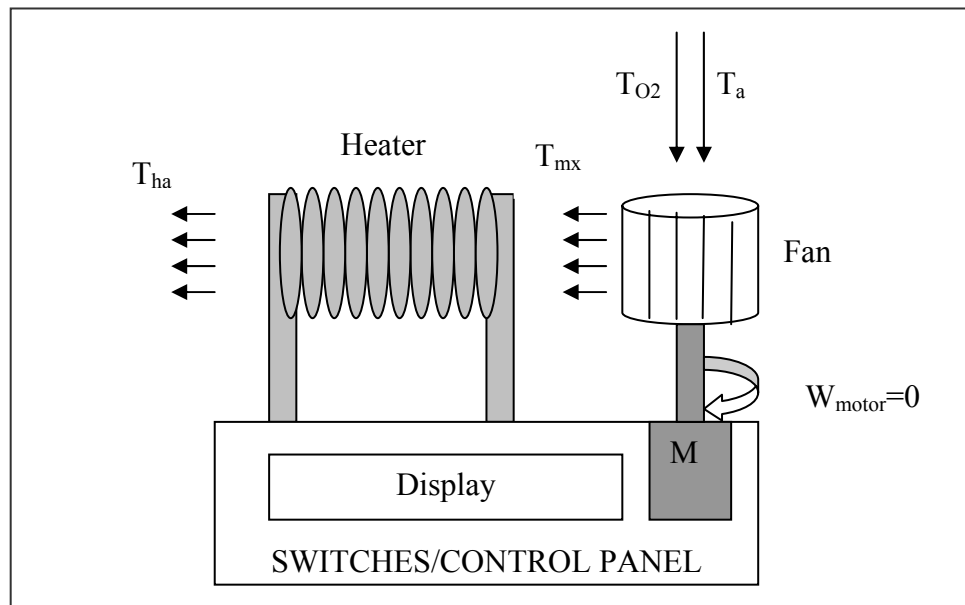


Figure 2-13 Schematic diagram for Fan/Heater compartment

The oxygen flow rate to the incubator depends on the required concentration level of O_2 (i.e. O_2 %) and is given by the manufacturer in Table 2-1:

Table 2-1 Oxygen flow rates and concentrations

Oxygen flow rate (l/min)	2	3	4
Concentration %	28-31	32-36	37-40

This concentration level is reached within 20-30 min. The above scheme for oxygen concentration illustrates that the air space inside the incubator comprises of at least 28% oxygen and 72% nitrogen. Therefore, this air can consider as an ambient air which normally has concentrations of 21% oxygen and 79% nitrogen.

Neglecting the work done by the fan motor (i.e. $W_{motor}=0$) and considering the process to be adiabatic (i.e. no heat added to the system), the heat balance equation for the fan can be written using equation (2.1) as:

$$\dot{m}_a C_{p_a} T_a + \dot{m}_{O_2} C_{p_{O_2}} T_{O_2} = \dot{m}_{mx} C_{p_{mx}} T_{mx} \quad (2.62)$$

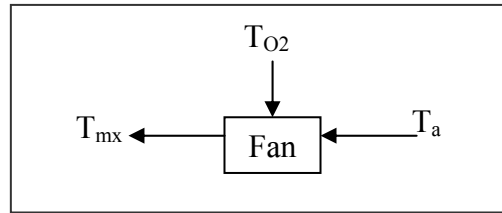


Figure 2-14 Block diagram for the Fan

This is illustrated in Figure 2-14. Using equation (2.62), the mixed air temperature is given by:

$$T_{mx} = \frac{\dot{m}_a C_{p_a} T_a + \dot{m}_{O_2} C_{p_{O_2}} T_{O_2}}{\dot{m}_{mx} C_{p_{mx}}} \quad (2.63)$$

The mass flow rate of the mixed air, \dot{m}_{mx} , is the summation of the returned air plus the mass flow rate of the added oxygen. In terms of the volumetric air and oxygen flow rates, equation (2.61) can be re-written as:

$$T_{mx} = \frac{q_{air} \rho_a C_{p_a} T_a + q_{O_2} \rho_{O_2} C_{p_{O_2}} T_{O_2}}{(q_{air} \rho_a + q_{O_2} \rho_{O_2}) C_{p_{mx}}} \quad (2.64)$$

Since the variation range of the incubator air temperature is between 25 - 40°C, the specific heat of the mixed air $C_{p_{mx}}$ is assumed as C_{p_a} , and thus $C_{p_a} = 1007 \text{ J/kg} \cdot ^\circ\text{C}$ [35].

The mass flow rate of the mixed air, \dot{m}_{mx} , depends on the final density of the air inside incubator, which depends on the concentration of the oxygen added to the incubator air as well as the variation of the returned air temperature T_a [35].

The incubator air is assumed to be a perfect gas, and the mixed mass, \dot{m}_{mx} , is then determined as follows [35]:

The final density of the incubator air is estimated on the basis of the final concentration of the both nitrogen and oxygen gases. Since the incubator air is assumed to comprise of 21% oxygen and 79% nitrogen, the final concentration of the both gases is easily determined [35]:

For nitrogen:

$$Y_{N_2\%} = 0.79 - O_2\% \quad (2.65)$$

And for oxygen:

$$Y_{O_2\%} = 0.21 + O_2\% \quad (2.66)$$

The density of each of oxygen and nitrogen is calculated on a per mole basis and using the perfect gas law [35]:

$$P_t V_{inc} = N_t R_u T_a \quad (2.67)$$

where N_t is the total number of the moles, R_u is the molar gas constant (8.31447 kJ/kmol.K). V_{inc} is the volume of the incubator air space, and P_t is the atmospheric pressure.

Since the air is assumed to be an ideal gas, equation (2.67) can be written in terms of the percentage of the concentration of each gas $Y_{gas\%}$ [35]:

$$\frac{P_{gas}}{P_t} = \frac{N_{gas} R_u T_a / V_{inc}}{N_t R_u T_a / V_{inc}} = \frac{N_{gas}}{N_t} = Y_{gas\%} \quad (2.68)$$

Therefore, the molar concentration, C , for each gas (in kmol per unit volume) can be determined using [35]:

$$C = \frac{N_{gas}}{V_{inc}} \quad (2.69)$$

Finally, the density of each gas in terms of molar weight M and concentration C can be written as [35]:

$$\rho = C \times M \text{ Kg/m}^3 \quad (2.70)$$

The molar weights for oxygen and nitrogen are 32 and 28 kg/kmol respectively [35].

Equation (2.68) is employed to estimate the mass of the incubator air space, M_a , mentioned earlier in section 2.4.1 as follows:

Using the general form of the ideal gas law for each gas (N_2 and O_2) [35]:

$$P_{gas} V_{inc} = M_a R_{gas} T_a \quad (2.71)$$

where R_{gas} is the gas constant which equals to 0.2968 kJ/kg.K and 0.2598 kJ/kg.K for N_2 and O_2 respectively, and T_a is the temperature in Kelvin. P_{gas} can be defined from equation (2.68) as [35]:

$$P_{gas} = Y_{gas\%} \times P_t \quad (2.72)$$

and $Y_{gas\%}$ for N_2 and O_2 can be determined using equations (2.65) and (2.66) respectively.

Thus, the mass of the incubator air, M_a , can be determined using [35]:

$$M_a = \left[\left(\frac{Y_{N_2\%} P_t}{R_{N_2}} \right) + \left(\frac{Y_{O_2\%} P_t}{R_{O_2}} \right) \right] \times \frac{V_{inv}}{T_a} \quad (2.73)$$

For the heater modelling, assuming adiabatic processes (i.e. no heat losses) and that all of the heat generated is absorbed by the air, the heat balance equation for the heater can be written using equation (2.1) as follows:

$$\dot{m}_a C_{p_a} T_{mx} + Q_{heater} = \dot{m}_a C_{p_a} T_{ha} \quad (2.74)$$

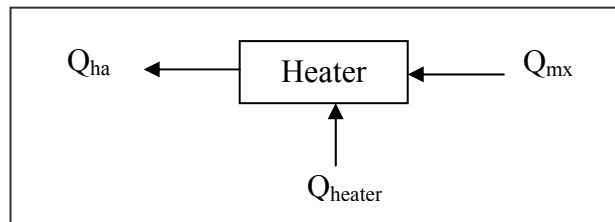


Figure 2-15 Block diagram for the heater

This is illustrated in Figure 2-15. Using equation (2.71), the heated air temperature can be written as:

$$T_{ha} = T_{mx} + \frac{Q_{heater}}{\dot{m}_a C_{p_a}} \quad (2.75)$$

where \dot{m}_a is mass flow rate of the incubator air, kg/sec.

2.6 Humidification System Modelling

The humidification system is the last compartment in the incubator system, where system water vapour is added to the air from the humidifier.

The design specifications of the manufacturer place the humidification system inside a separate housing from the heated air duct. The system comprises of a plastic container and a finned-aluminium block that is placed inside the container as shown in Figure 2-16 and Figure 2-17. The water level is specified by the manufacturer.

Heated air enters the water chamber via an opening in the lid of the chamber, which is also placed at the end of the duct of the heated air. The moist air leaves the water chamber from an opening at the far side of the chamber and past the aluminium block. Both openings are 80×50 mm wide [measured]. Therefore, the volumetric air flow rate, Q_{ah} , undergoing heat exchange with the water surface is a function of both air velocity and the size of the openings (in & out) on the lid, can be determined as follows:

$$Q_{ah} = A_{op} \times V_a \quad (2.74)$$

where V_a is equal to 0.1 m/sec [from the manufacturer] and A_{op} is equal to 0.004 m². Thus, the volumetric air flow rate from equation (2.74) is calculated to be 0.0004 m³/sec.

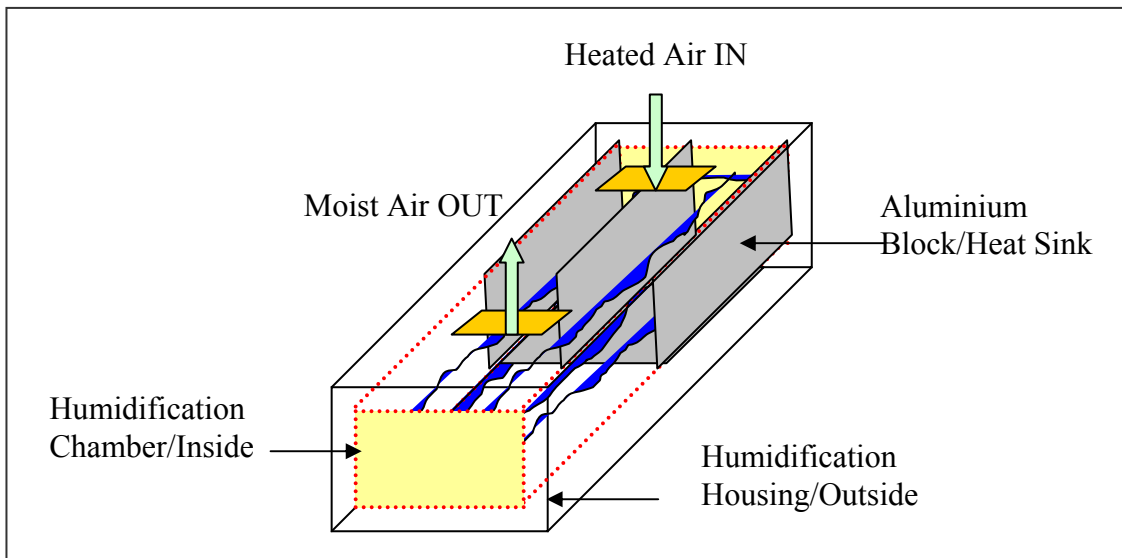


Figure 2-16 Humidification system diagram

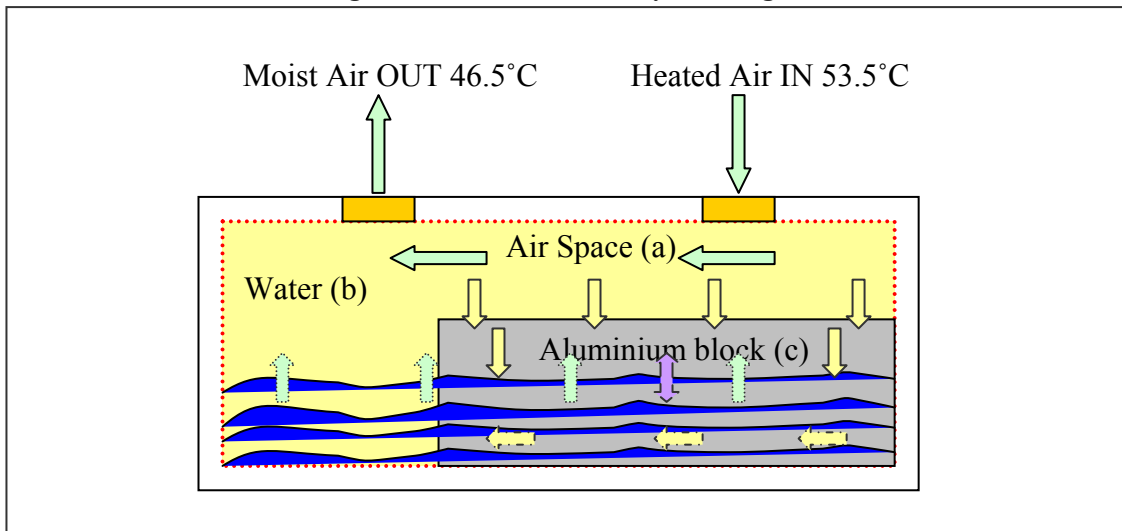


Figure 2-17 Water chamber-Heat exchange/Cross-sectional diagram

The purpose of the finned-aluminium block is to store heat and exchange it with the water and air. The finned-aluminium block is half-immersed in water, and the exposed parts of it exchange heat with the heated air by convection. There is also heat transfer within the aluminium block by conduction between the exposed and the immersed parts. This heat exchange occurs rapidly between the submerged parts and vice versa with a high efficiency estimated at around 99.5% [35].

Therefore, it is reasonable to assume that the temperature gradient between the exposed parts of the aluminium block and the submerged parts is zero (i.e. $T_{al1} = T_{al2} = T_{al}$) [35], and the finned-aluminium block acts as a heat sink. As a result, the heat energy of the heated air is accumulated in the aluminium block and within the mass of the water accordingly.

For this reason, the water in the container will constantly be warmed as the heated air continues entering the water chamber, and this will cause a mass flow of water vapour to the air in form of latent heat via evaporation.

Several assumptions are made to simplify the modelling of this system, as follows:

1. Uniform temperature distribution all over the control system.
2. Water, air and aluminium block have constant thermal characteristics.
3. Conduction between the exposed and immersed parts of the finned-aluminium block is negligible. This is due to the high efficiency of the heat transfer between these parts, estimated at 99.5% [35].
4. Heat losses by convection or conduction from the water container to the humidification housing and to the environment are considered to be negligible.
5. Since the base of the aluminium block is fully contacted with the plastic water container, the heat flow along the bottom surface of the base is negligible.
6. The entire heat exchange process is about heat and mass transfer under forced convection for the parts exposed to the heated air and natural convection for the immersed parts.
7. The water chamber comprises of 3 parts: air space, water and aluminium block, and heat exchange between these three parts are correlated as follows:

From Figure 2-18, the air space gains heat from the heated air that enters the chamber. Since there is a temperature difference between the heated air and the wetted surface, some of the heat energy of this heated air will be dissipated in the form of sensible heat into the water surface and the exposed part of the aluminium block via convection. Due to the temperature difference, there will also be a difference in the saturation pressure and the partial pressure of water vapour. Thus, some mass of water will evaporate from the water surface and the vaporization energy needed for this process is in form of latent heat [34]. The moist air that leaves the water chamber at T_{wet} will directly enter the hood with no further heat processes.

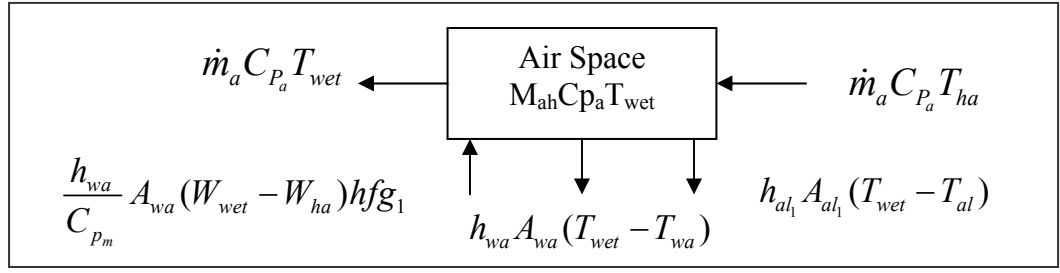


Figure 2-18 Air space above water surface (a)

Thus, in a period of dt , the heat balance equation for the air space inside the water chamber can be written using equation (2.1) as:

$$\begin{aligned} & \left[\dot{m}_a C_{pa} T_{ha} \right] dt + \left[\frac{h_{wa}}{C_{pm}} A_{wa} (W_{wet} - W_{ha}) hfg_1 \right] dt - \left[h_{wa} A_{wa} (T_{wet} - T_{wa}) \right] dt - \\ & \left[h_{al_1} A_{al_1} (T_{wet} - T_{al}) \right] dt - \left[\dot{m}_a C_{pa} T_{wet} \right] dt = M_{ah} C_{pa} dT_{wet} \end{aligned} \quad (2.77)$$

Therefore, the instantaneous temperature of the air inside the water chamber can be determined by:

$$\begin{aligned} & \left[\dot{m}_a C_{pa} T_{ha} \right] + \left[\frac{h_{wa}}{C_{pm}} A_{wa} (W_{wet} - W_{ha}) hfg_1 \right] - \left[h_{wa} A_{wa} (T_{wet} - T_{wa}) \right] - \\ \frac{dT_{wet}}{dt} = & \frac{\left[h_{al_1} A_{al_1} (T_{wet} - T_{al}) \right] - \left[\dot{m}_a C_{pa} T_{wet} \right]}{M_{ah} C_{pa}} \end{aligned} \quad (2.78)$$

and using D-operator gives:

$$\begin{aligned} & \left[\dot{m}_a C_{pa} T_{ha} \right] + \left[\frac{h_{wa}}{C_{pm}} A_{wa} (W_{wet} - W_{ha}) hfg_1 \right] - \left[h_{wa} A_{wa} (T_{wet} - T_{wa}) \right] - \\ T_{wet} = & \frac{\left[h_{al_1} A_{al_1} (T_{wet} - T_{al}) \right] - \left[\dot{m}_a C_{pa} T_{wet} \right]}{M_{ah} C_{pa} D} \end{aligned} \quad (2.79)$$

where W_{wet} and W_{ha} are the humidity ratios of the wetted surface and heated air respectively, and can be determined from equations (2.10), (2.11) and (2.12).

\dot{m}_a can be estimated using:

$$\dot{m}_a = A_{in/out} V_a \rho_{ha} \quad (2.80)$$

where $A_{in/out}$ is the opening area where the heated air enters and leaves the water chamber and is estimated to be around 0.004 m^2 [measured], Va is the incubator air velocity which equals to 0.1 m/sec [from the manufacturer], and ρ_{ha} , density of the heated air is determined using the same technique described in equations (2.65) to (2.70).

Experimentally, and in an empty incubator, the heated air T_{ha} enters the water chamber at around 53.5°C and leaves T_{wet} at around 46.5°C , while the water temperature T_{wa} is approximately 30°C . The heated and wetted air properties could also be evaluated at the film temperature (which gives an average temperature of 50°C and 40°C respectively for the heated air in and out the water chamber). For the sake of this project however, equation (2.13) is again employed to determine the precise air properties inside the water chamber as the temperature of the heated air varies over time.

The area of the water surface A_{wa} is determined using the equation:

$$A_{wa} = L_{con}W_{con} - N_f(th_f \times l_f) \quad (2.81)$$

while the area of the exposed parts of the aluminium block A_{al1} is calculated as:

$$A_{al1} = 2N_f l_f w_l \quad (2.82)$$

The mass of the air in the water chamber M_{ah} can be estimated using:

$$M_{ah} = \rho_{wet} w_l L_{con} W_{con} \quad (2.83)$$

and the specific heat of the moist air C_{P_m} is determined by [34]:

$$C_{P_m} = C_P + W_{wet} C_{ps} \quad (2.84)$$

Since the flow regime of the air inside the water chamber is laminar (due to a Reynolds number of around 1112.6 for the aluminium and 1863.6 for the water surface), the Nusselt number for the aluminium and water can be determined using equation [35]:

$$Nu = 0.664 \text{Re}_L^{0.5} \text{Pr}^{1/3} \quad (2.85)$$

Therefore, h_{wa} and h_{al_1} can be determined by the general form of Nusselt equation [35]:

$$Nu = \frac{hL_c}{K_a} \quad (2.86)$$

Both the Reynolds and Prandtl numbers in equation (2.85) are defined as [35]:

$$Re = \frac{\rho_a V_a L_c}{\mu_a} \quad (2.87)$$

$$Pr = \frac{\mu_a C_{P_a}}{K_a} \quad (2.88)$$

Similarly, in Figure 2-19, in a period of dt , the heat balance equation for the mass of the water in the chamber can be written using equation (2.1) as follows:

$$\begin{aligned} & [h_{wa} A_{wa} (T_{wet} - T_{wa})] dt + [h_{al_2} A_{al_2} (T_{al} - T_{wa})] dt - \\ & \left[\frac{h_{wa}}{C_{P_m}} A_{wa} (W_{wet} - W_{ha}) hfg_1 \right] dt = M_{wa} C_{P_{wa}} dT_{wa} \end{aligned} \quad (2.89)$$

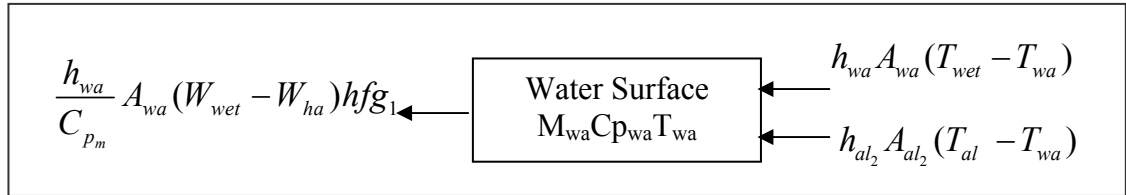


Figure 2-19 Water surface (b)

The instantaneous temperature of the water mass can be determined using:

$$\frac{dT_{wa}}{dt} = \frac{[h_{wa} A_{wa} (T_{wet} - T_{wa})] + [h_{al_2} A_{al_2} (T_{al} - T_{wa})] - \left[\frac{h_{wa}}{C_{P_m}} A_{wa} (W_{wet} - W_{ha}) hfg_1 \right]}{M_{wa} C_{P_{wa}}} \quad (2.90)$$

Using D-operator, the temperature of the water mass is determined as follows:

$$T_{wa} = \frac{\left[h_{wa} A_{wa} (T_{wet} - T_{wa}) \right] + \left[h_{al_2} A_{al_2} (T_{al} - T_{wa}) \right] - \left[\frac{h_{wa}}{C_{P_m}} A_{wa} (W_{wet} - W_{ha}) h f g_1 \right]}{M_{wa} C_{P_{wa}} D} \quad (2.91)$$

where A_{al_2} is determined as follows:

$$A_{al_2} = 2N_f l_f w_{iw} + n_g W_g l_f \quad (2.92)$$

Since no agitator or stirrer is used in the water chamber, the mechanism of heat transfer that occurs between the submerged parts of the aluminium block and the water is natural convection. Therefore, the temperature difference between the water and the aluminium is the buoyancy force that drives the convective heat exchange. The convection heat transfer coefficient h_{al_2} depends on the geometry of the submerged parts of the aluminium block and can be determined using equation (2.86) [35]:

$$h_{al_2} = \frac{Nu \times k_{wa}}{S} \quad (2.93)$$

where k_{wa} the thermal conductivity of water and S is the spacing between adjacent fins (21.63 mm). The Nusselt number, Nu , is a function of Raleigh number, R_a , and can be expressed as follows [35]:

$$Nu = \left[\frac{576}{(Ra_s S/L)^2} + \frac{2.873}{(Ra_s S/L)^{0.5}} \right]^{-0.5} \quad (2.94)$$

and Ra_s is determined by [35];

$$Ra_s = \frac{g \beta (T_s - T_\infty) S^3}{\nu^2} Pr \quad (2.95)$$

The properties of the water are evaluated at a film temperature T_f equal to 40 °C and L the height of the fin (200 mm). This yields h_{al_2} equal to 433.80 W/m².°C.

Likewise, the two partitions of the aluminium block are convectively heated by both the air space and water. The conduction between the exposed and immersed parts is considered to be negligible [35].

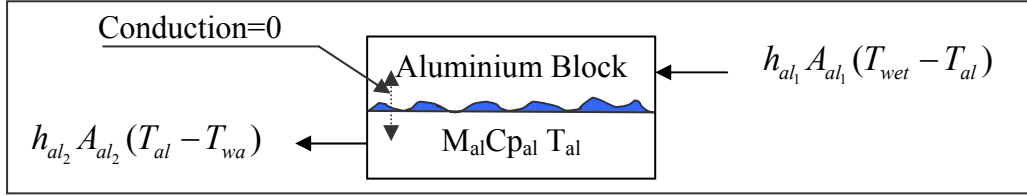


Figure 2-20 Finned-aluminium block/exposed and immersed parts (c)

From Figure 2-20, the heat balance equation for the aluminium block can be written as:

$$\left[h_{al_1} A_{al_1} (T_{wet} - T_{al}) \right] dt - \left[h_{al_2} A_{al_2} (T_{al} - T_{wa}) \right] dt = M_{al} C_{p_{al}} dT_{al} \quad (2.96)$$

Then,

$$\frac{dT_{al}}{dt} = \frac{\left[h_{al_1} A_{al_1} (T_{wet} - T_{al}) \right] - \left[h_{al_2} A_{al_2} (T_{al} - T_{wa}) \right]}{M_{al} C_{p_{al}}} \quad (2.97)$$

Using D-operator, the temperature of the aluminium block can be written as:

$$T_{al} = \frac{\left[h_{al_1} A_{al_1} (T_{wet} - T_{al}) \right] - \left[h_{al_2} A_{al_2} (T_{al} - T_{wa}) \right]}{M_{al} C_{p_{al}} D} \quad (2.98)$$

where A_{al_1} , h_{al_1} , A_{al_2} and h_{al_2} can be determined by equations (2.82), (2.86), (2.92) and (2.93) respectively.

The amount of the heated air as well as the moist air that enter the hood is adjusted by a mechanical lever (manually), which slides over the two side openings (i.e. one for the moistened air and the other for the heated air) at the end of the heated air duct (Figure 2-21). The setup position of the slider lever is based upon the required level of humidity inside the hood, and is graded from 20-99% in steps of 10%.

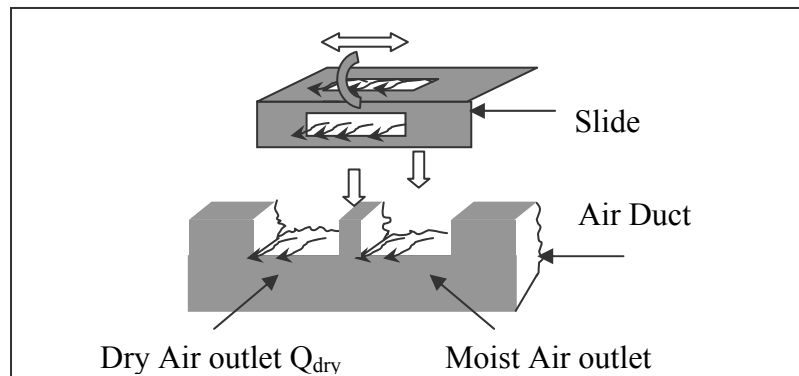


Figure 2-21 Slider/Air outlets assembly

The amount of wetted and heated air is proportional to the area of the openings they flow through, which is accordingly a function of the relative humidity $RH\%$.

This is experimentally evaluated against each level of $RH\%$ and the best fit equations for the areas of the moist air outlet and the dry air outlet are shown in Figure 2-22.

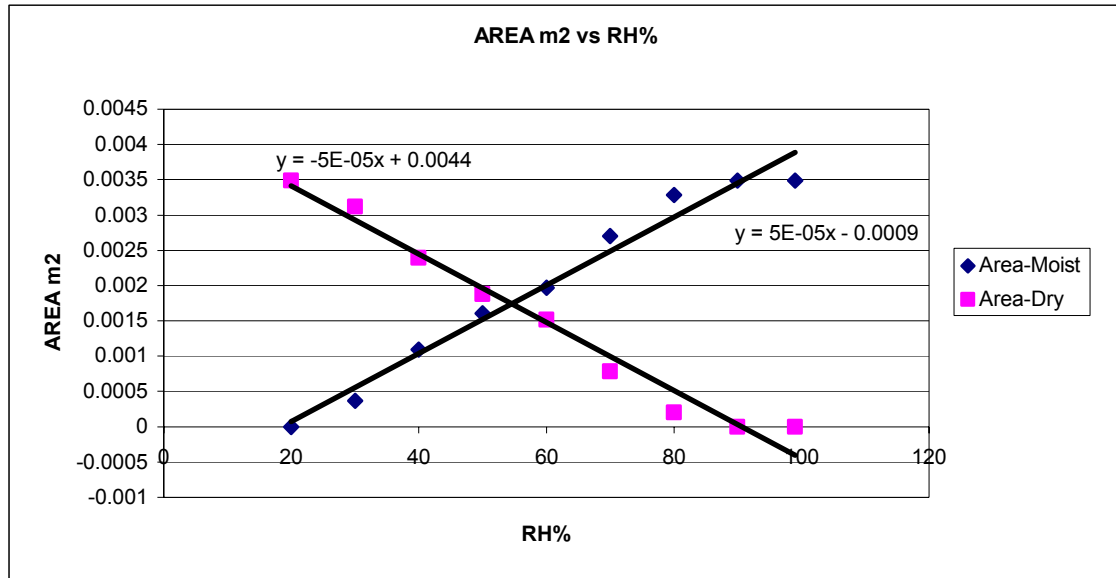


Figure 2-22 Area m2 vs. RH%

From Figure 2-22 the area of the moist air can be written as:

$$A_{wet} = 5 \times 10^{-5} (RH\%) - 0.0009 \quad (2.99)$$

and for the dry air:

$$A_{dry} = 0.0044 - 5 \times 10^{-5} (RH\%) \quad (2.100)$$

Thus, the supplied air temperature to the hood can be evaluated by the following equation:

$$\dot{m}_{wet} C_{p_a} T_{wet} + \dot{m}_{dry} C_{p_a} T_{ha} = (\dot{m}_{wet} + \dot{m}_{dry}) C_{p_a} T_{sply} \quad (2.101)$$

Since the heat capacity C_{p_a} is same for wetted air and heated air ($1007 \text{ J/kg} \cdot ^\circ\text{C}$), equation (2.101) can be re-written as:

$$T_{sply} = \frac{\dot{m}_{wet} T_{wet} + \dot{m}_{dry} T_{ha}}{(\dot{m}_{wet} + \dot{m}_{dry})} \quad (2.102)$$

where \dot{m}_{wet} and \dot{m}_{dry} are estimated as follows:

$$\dot{m}_{wet} = \rho_{wet} A_{wet} V_a \quad (2.103)$$

$$\dot{m}_{dry} = \rho_{ha} A_{dry} V_a \quad (2.104)$$

The variables ρ_{wet} and ρ_{ha} are evaluated at T_{wet} and T_{ha} respectively.

The convective heat energy supplied to the hood Q_{ht} (i.e. incubator's air space) can be determined by the equation:

$$Q_{ht} = \dot{m}_a C_{p_a} (T_{sply} - T_a) \quad (2.105)$$

Equation (2.105) is associated with section 2.4.1. Thus, equations (2.1)-(2.105) describe a comprehensive detailed model of the infant-incubator system, with the infant described as either a one lump or four-lump system with 2 layers.

Chapter 3 Development of SIMULINK Model

3.1 Introduction

In this chapter, a computer simulation for each compartment of the infant-incubator system that was mathematically modelled in chapter 2 model will be developed. The model is being developed in MATLAB[®]/SimuLink environment for each part of the system. These Simulink models are then interlocked via internal loops (called iterations) in one block known as the Plant. In other words, the output of one compartment is the input to another compartment.

The plant basically has a single variable input which is the heating power and another constant input which is the desired humidity level inside the hood. However, all the other variables and constants related to the model are already being identified in a separate M-file given in appendix 1.

The plant is then plugged into a closed-loop system (feedback system) with a PID (Proportional-Integral-Derivative) controller (compensator) and a reference input (i.e. reference temperature: air or skin temperature) with a comparator. Figure 3-1 illustrates the general principle of the simulation model.

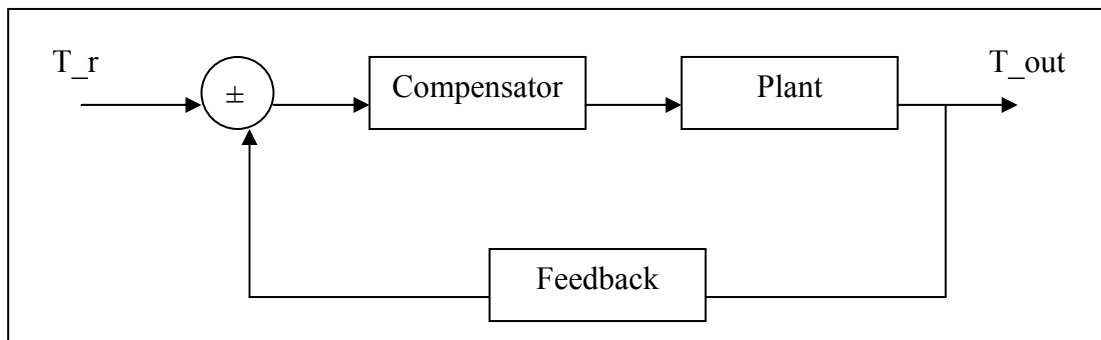


Figure 3-1 Feedback block diagram

The components of control system (i.e. the PID and the feedback elements) are thoroughly investigated in terms of the overall system stability, and the response of applying a step input to the whole system will be demonstrated. This will be implemented using an available function in MATLAB called ‘single input-single output tool’, or so called ‘*sisotool*’, which is based on the root locus method. The virtual parameters of the PID are determined by the modified Zeigler-Nichols method [41].

The results of the simulation model are in terms of temperature variation associated with the infant itself and for each of the incubator compartments such as: the core and skin temperatures, incubator wall temperature, mattress temperature and incubator air space temperature. The simulation also incorporates the modelling of the humidification chamber with its three divisions: water, aluminium block (the heat sink) and the air space above the water surface.

The overall simulation model of the infant-incubator system is shown in Figure 3-2. In the following sections detailed figures of each compartment of the infant-incubator system will be developed.

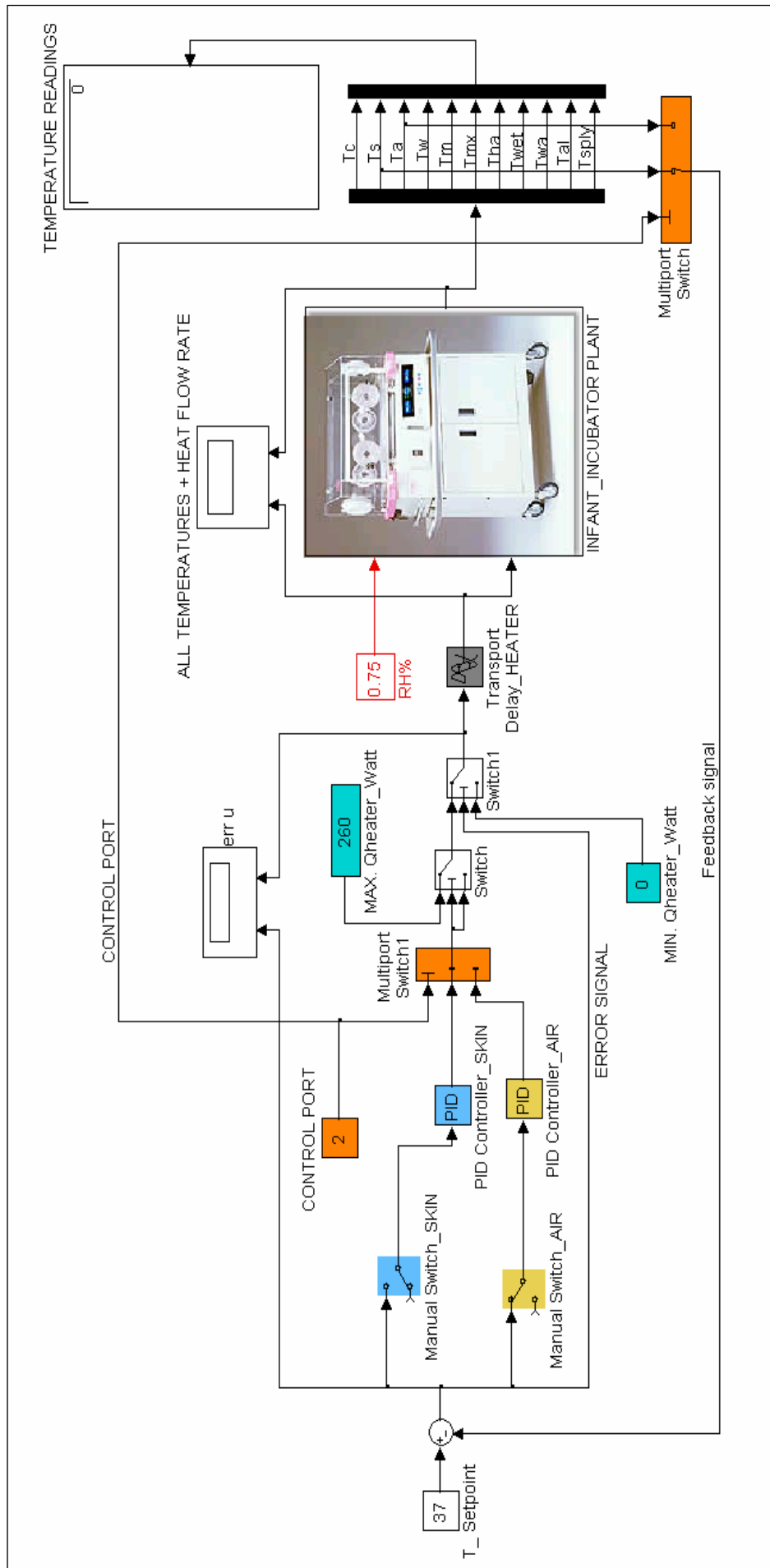


Figure 3-2 Overall simulation model

3.2 Infant-Incubator System Compartments (PLANT)

The infant-incubator system (PLANT) comprises of 11 compartments in total as shown in Table 3-1 .

Table 3-1 Number of components of the simulation model

<i>S</i>	<i>Designation</i>	<i>Compartments</i>
1	Infant, one-lump	Core
		Skin
2	Incubator	Incubator air space
		Incubator walls
		Mattress
		Fan
		Heater
		Air space above water surface
		Water surface
		Aluminium block-heat sink
		Supplied air temperature

The combined Simulink model for all compartments of the ‘PLANT’ is demonstrated in Figure 3-3. For each of the listed compartments in Table 3-1, a Simulink model will be developed.

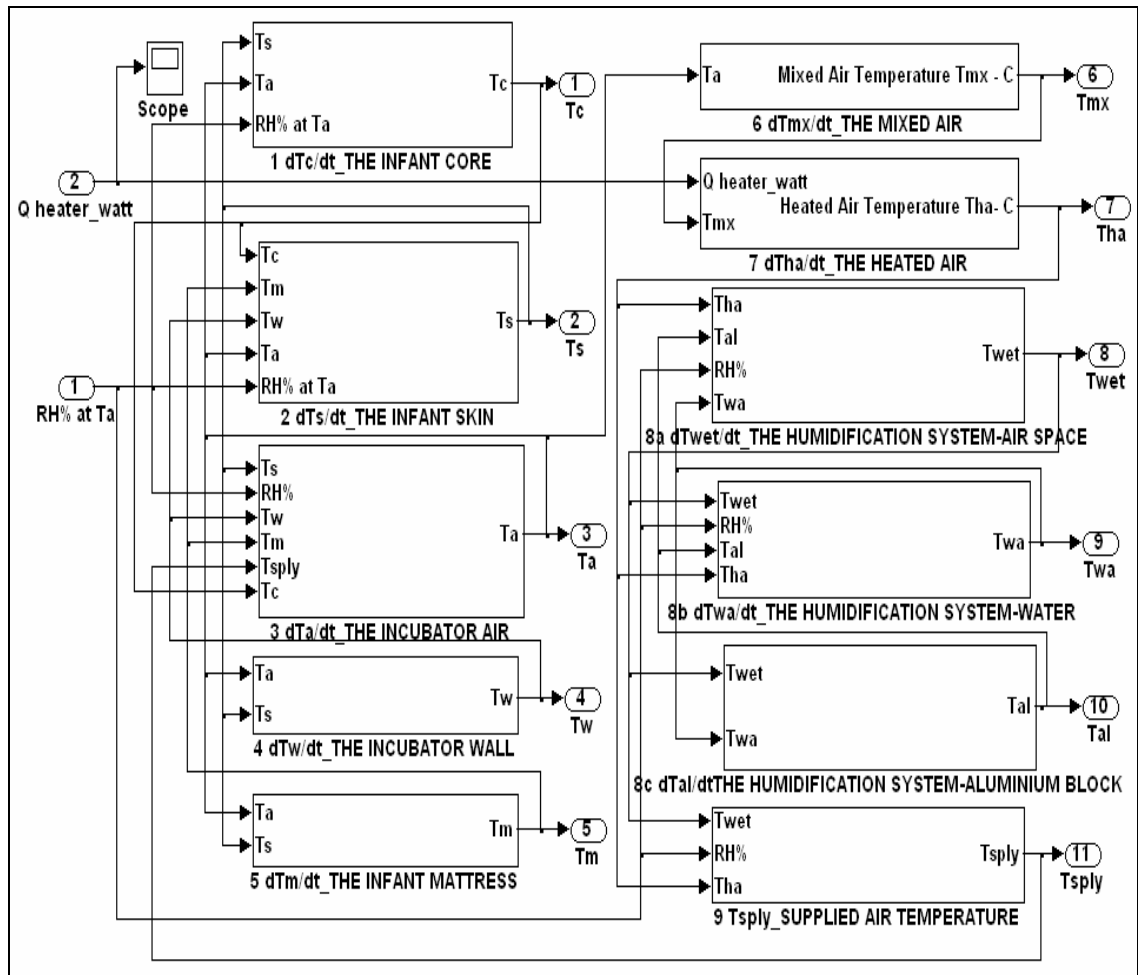


Figure 3-3 Combined system compartments

3.2.1 The Infant Core Compartment

The Simulink model for this compartment is shown in Figure 3-4. Each of the sub-systems shown in this figure represents the rate of the heat exchange over time in the core compartment which was described in equation (2.3).

These sub-systems are listed in Table 3-2 with the input name and input source. A Simulink model will be developed for each sub-system.

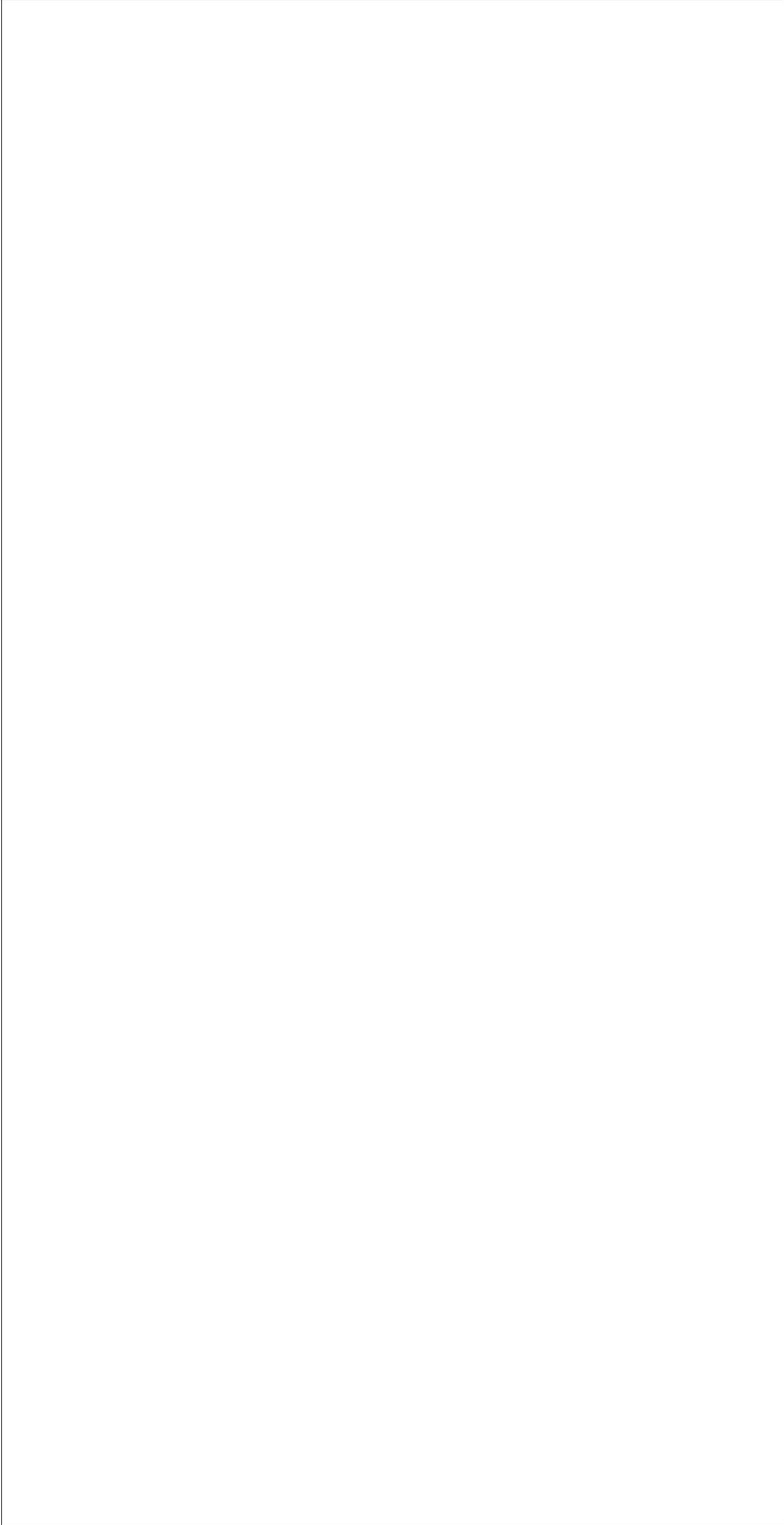


Figure 3-4 The infant core compartment

Table 3-2 Sub-systems of the infant core compartment

<i>S</i>	<i>Sub-System designation</i>	<i>Input Name</i>	<i>Input Source</i>
1	Heat production of the infant core	Mass of the infant	Matlab file
2	Core-skin conduction	Core and skin temperatures	Core and skin compartments
3	Core-skin blood convection		
4	Sensible heat losses	Core temperature	Core compartment
		Air temperature	Incubator air space compartment
5	Latent heat losses	Core temperature	Core compartment
		Air temperature	Incubator air space compartment
		Relative humidity	Constant input to the parent system
6	Mass of the infant core	Mass of the infant	Constant in M-file
7	Specific heat capacity of the core	Cpc	Constant in M-file
8	Initial core temperature	Tci	Constant in M-file

3.2.1.1 Heat Production of the Infant Core

The Simulink model for this sub-system is illustrated in Figure 3-5 and the output (in Watts) represents the rate of the heat production from the infant, which is a function of the infant surface area in terms of infant mass and rate of heat production per surface area, as described in equation (2.5).

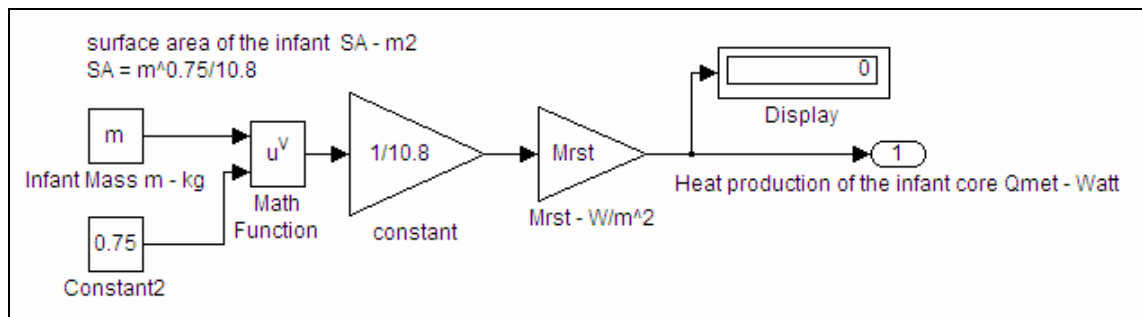


Figure 3-5 Heat production sub-system

3.2.1.2 Core-Skin Conduction

Figure 3-6 represents the Simulink model for the rate of the conduction heat transfer between the core and the skin layers, which was described in equation (2.14) (. The inputs to this sub-system are the core and skin temperatures.

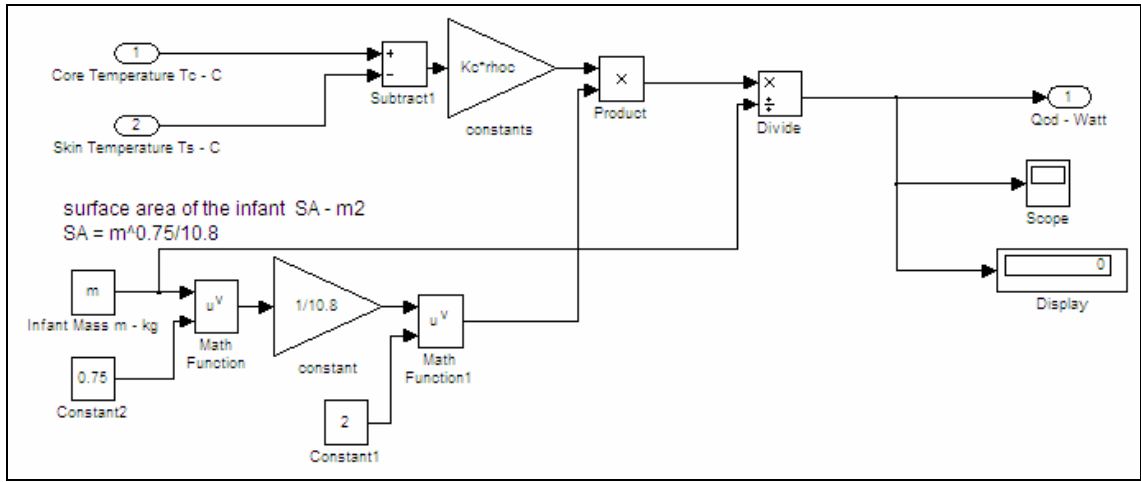


Figure 3-6 Core-skin conduction subsystem

3.2.1.3 Core-Skin Blood Convection

Figure 3-7 demonstrates the simulation of the convective heat transfer between the core and the skin layers via the blood, as described in equation (2.15). The input source is similar to the previous subsystem (Core-Skin Conduction).

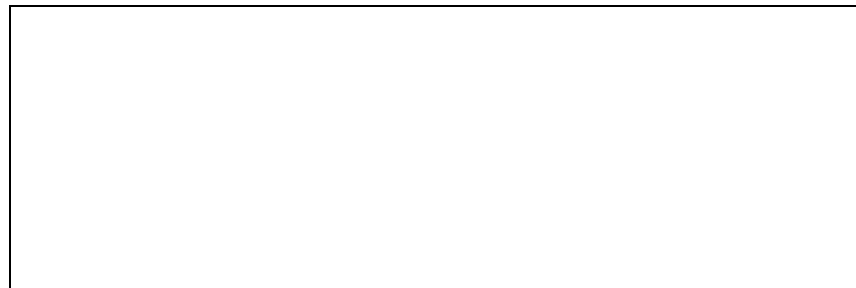


Figure 3-7 Core-skin blood convection subsystem

3.2.1.4 Sensible Heat Losses

The rate of the sensible heat loss via respiration is due to the temperature difference between the inhaled air and the exhaled air, which is described in equation (2.8), and is simulated as shown in Figure 3-8.



Figure 3-8 Sensible heat losses subsystem

3.2.1.5 Latent Heat Losses

The Simulink model for this subsystem is represented as in Figure 3-9.

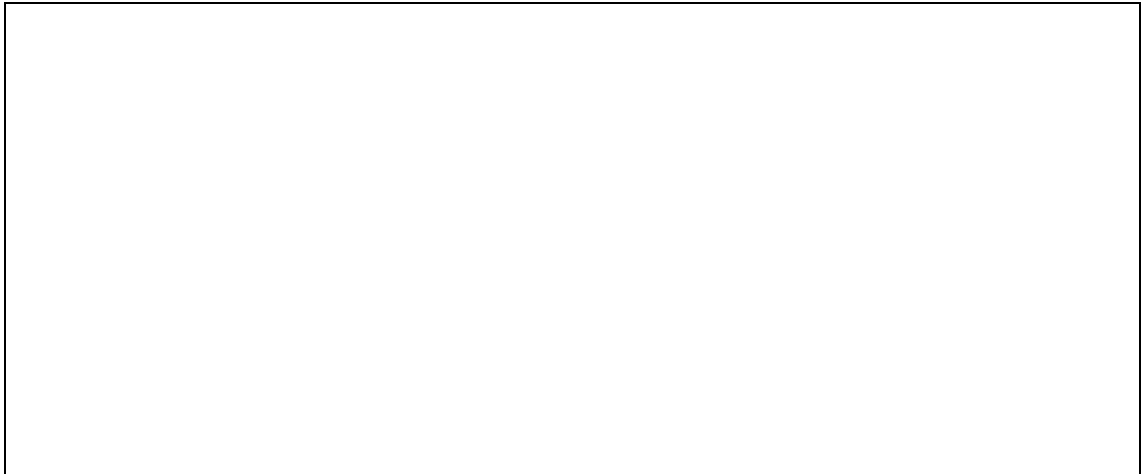


Figure 3-9 Latent heat losses subsystem

The latent heat loss is in terms of the difference in humidity ratio between the exhaled and inhaled air as described in equation (2.9). Since the humidity ratio, W_a , is function of water vapour pressure, it depends on the temperature difference between the core (i.e. exhaled air temperature) and the ambient air (i.e. inhaled air temperature) as well as the relative humidity level inside the hood. The relative humidity level inside the hood (RH %) is preset on the parent model (i.e. Figure 3-2).

The humidity ratio of the exhaled air, W_{ex} , and the ambient pressure were considered constants in chapter 2, and therefore appear as a gain (RH1) and (Pt) respectively in the above Simulink model.

In this subsystem exhaled air temperature is represented by the core temperature, which varies over time as can be seen from Figure 3-9. This hypothesis is consistent with the assumptions made in chapter 1, as the preterm infant in particular can not maintain its body temperature.

3.2.1.6 Mass of the Infant Core

This subsystem is simulated as in Figure 3-10, the mass of the infant core is determined by subtracting the infant mass from the skin mass of the infant, which is described in equation (2.18). While the infant mass is given as a constant parameter in an M-file, the

skin mass is estimated from the thickness of the skin, the skin density and the total surface area of the infant which is function of the infant mass.

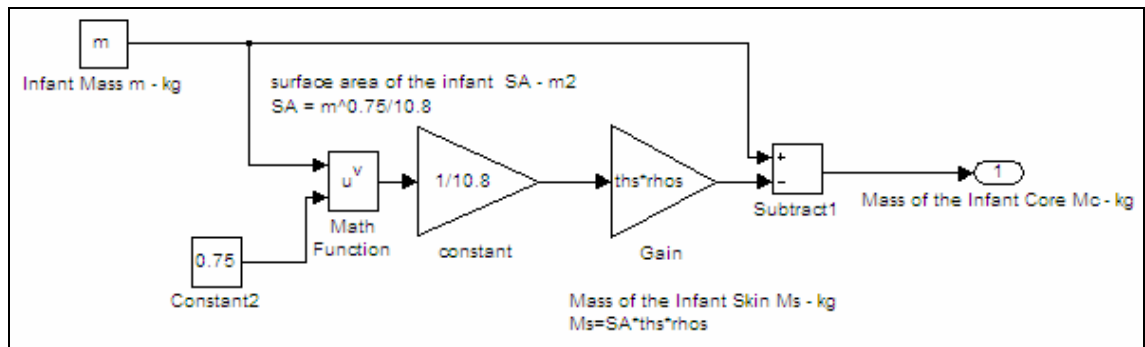


Figure 3-10 The mass of the infant core subsystem

The other parameters shown in Figure 3-4, C_{pc} and T_{ci} , are considered constants given in the M-file. The D-operator in equation (2.4) is represented by $1/s$, the integrator. Thus, the output T_c represents the core temperature that varies over time.

As can be seen from Figure 3-4, there are four inputs with three of them being external: skin temperature (T_s), incubator air space temperature (T_a) which are the outputs of the skin and incubator air space compartments respectively, and relative humidity ($RH\%$) is a constant input through the parent model. The fourth input is the internal input T_c which feeds the incorporated subsystems via internal loops called ‘iterations’.

As a result, the output T_c will be the input that feeds the other system compartments. Sections 3.2.1.1 to 3.2.1.6 explain in detail the infant core compartment.

The above description is applicable for the other compartments of the infant-incubator system with some attention to the notations used in each compartment.

3.2.2 The Infant Skin Compartment

A Simulink model is developed to represent the skin temperature variation over time as in equation (2.22). Figure 3-11 illustrates the Simulink model of the infant core compartment. Some of the subsystems in this figure have been described earlier within the core compartment such as, core-skin conduction and core-skin blood convection (as in Figure 3-6 and Figure 3-7, respectively).

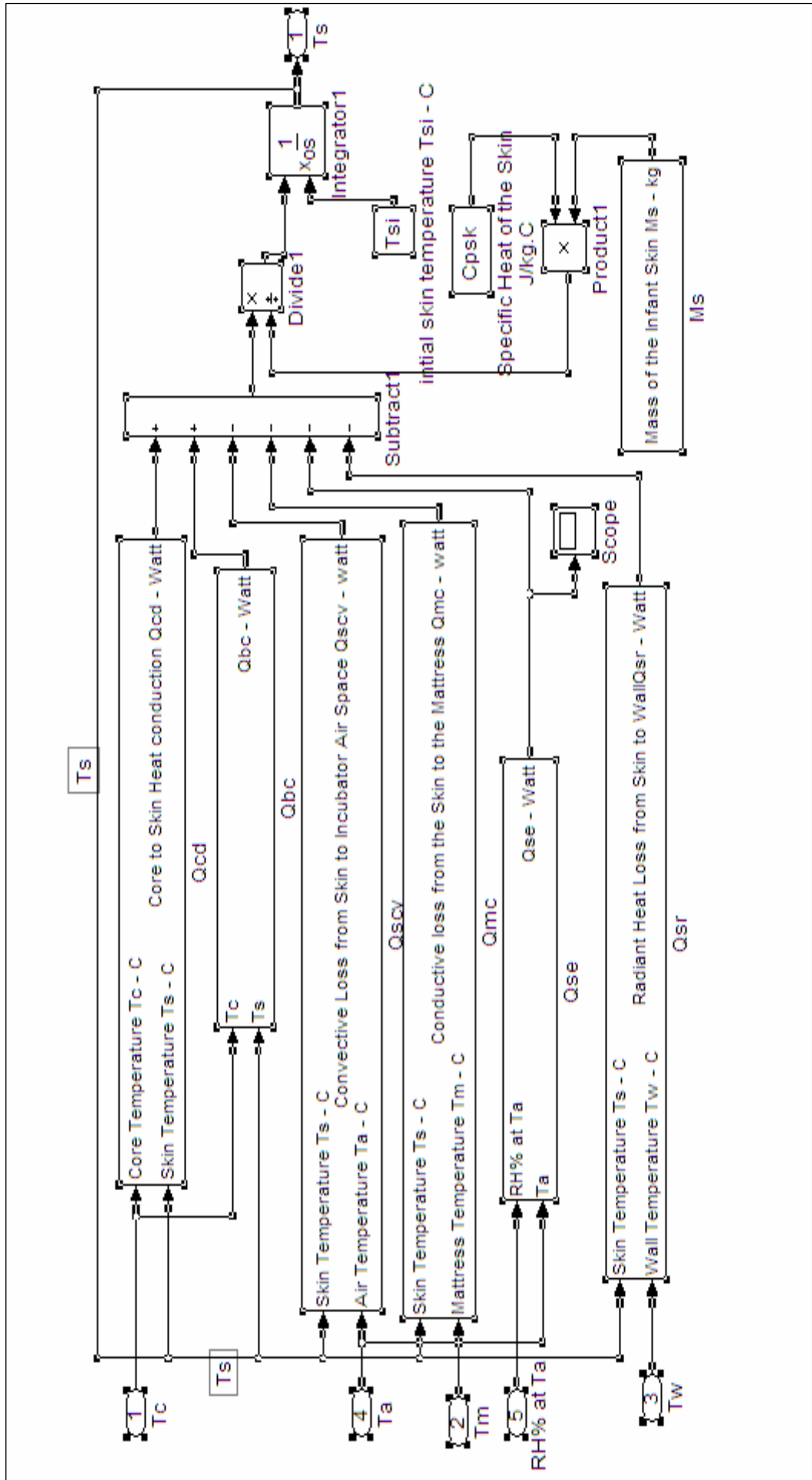


Figure 3-11 The infant skin compartment

Table 3-3 shows the sub-systems of the Simulink model of the infant skin compartment with the input name and the source of that input:

Table 3-3 Sub-systems of the infant skin compartment

<i>S</i>	<i>Sub-System designation</i>	<i>Input Name</i>	<i>Input Source</i>
1	Core-skin conduction	Core and skin temperatures	Core and skin compartments
2	Core-skin blood convection		
3	Convective loss from skin to incubator air space	Skin temperature	Skin compartment
		Air temperature	Incubator air space compartment
4	Conductive loss from skin to mattress	Skin temperature	Skin compartment
		Mattress temperature	Mattress compartment
5	Evaporation loss from skin to incubator air space	Relative humidity	Constant input to the parent system
		Air temperature	Incubator air space compartment
6	Radiation loss from skin to incubator walls	Skin temperature	Skin compartment
		Wall temperature	Wall compartment
7	Mass of the infant skin	Mass of the infant	Constant in M-file
8	Specific heat capacity of the skin	Cpsk	Constant in M-file
9	Initial skin temperature	Tsi	Constant in M-file

For each of the above sub-systems a Simulink model is developed in the following sections.

3.2.2.1 Skin-Incubator Air Space Convection

Figure 3-12 demonstrates the Simulink model for the convection rate in Watts for the heat exchange between the infant skin and the incubator air space, as described in equation (2.26). The convective heat transfer coefficient for the infant h_{scv} is a function of Nusselt number and the diameter of the cross-sectional area of the cylinder which is a sphere, the Nusselt number is determined separately within an M-file.

The infant surface area exposed to the incubator air space in this Simulink model is considered to be 90% of the total surface area. The other two inputs are the skin temperature itself (which is internally iterated within the Simulink model of the infant skin compartment) while the air temperature is externally fed from the incubator air space compartment (Figure 3-11). All other gains in Figure 3-12 are constant parameters defined in an M-file.

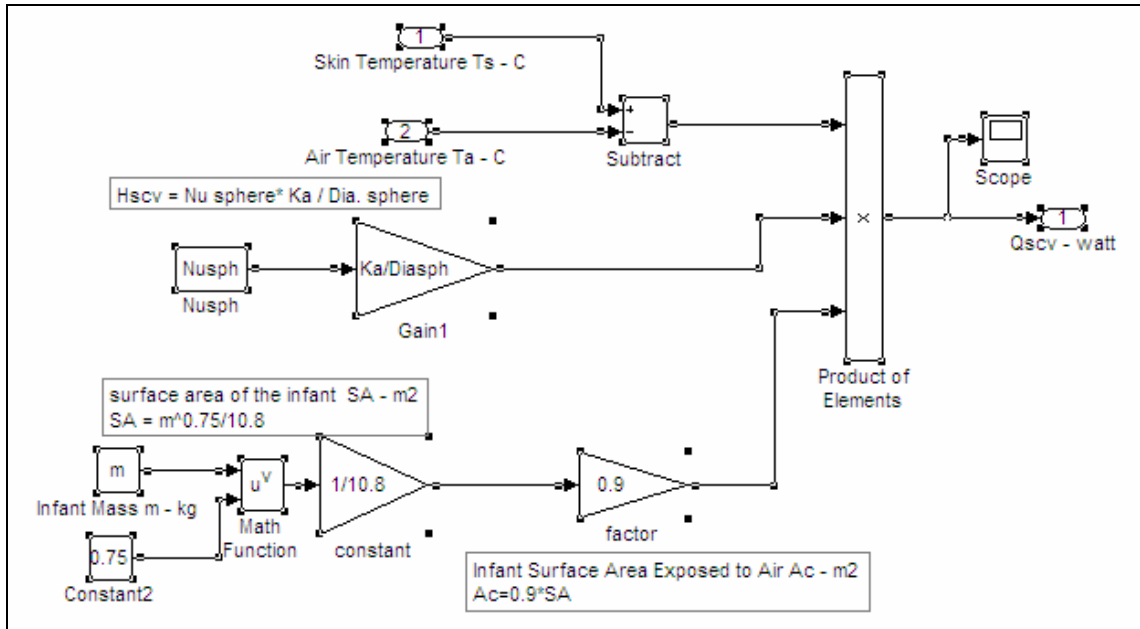


Figure 3-12 Skin–air convective heat exchange

3.2.2.2 Skin-Mattress Conduction Subsystem

Figure 3-13 illustrates the Simulink model for this sub-system which is described in equation (2.24), as follows:

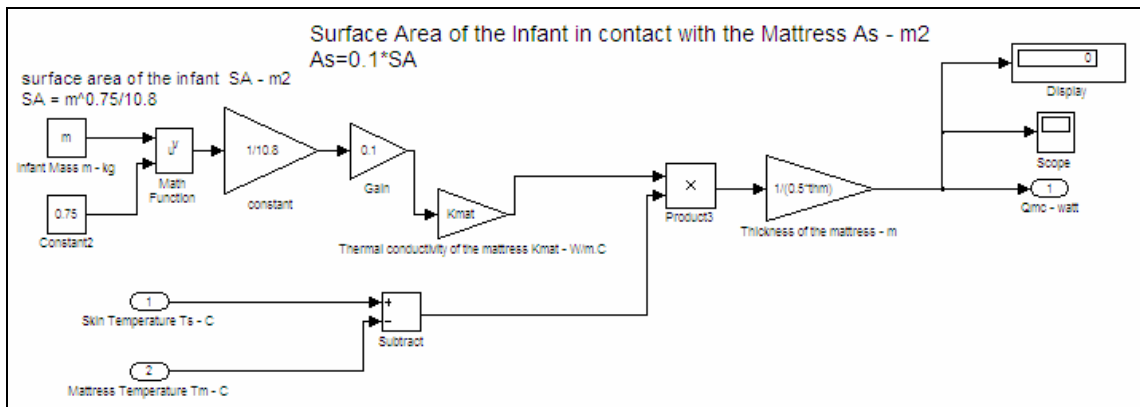


Figure 3-13 Skin-mattress conduction

The inputs are the iterated skin temperature fed from the infant skin compartment, and the mattress temperature (externally supplied from the mattress compartment). The contacted surface area with the mattress is considered to be 10% of the total surface area of the infant skin. The thickness of the mattress th_m is halved since the average mattress temperature is feasibly taken in the middle of the thickness. Likewise, all other gains are considered constant parameters defined in an M-file.

3.2.2.3 Evaporative Loss from the Skin

The Simulink model for this sub-system that is described in equation (2.32) is shown in Figure 3-14.

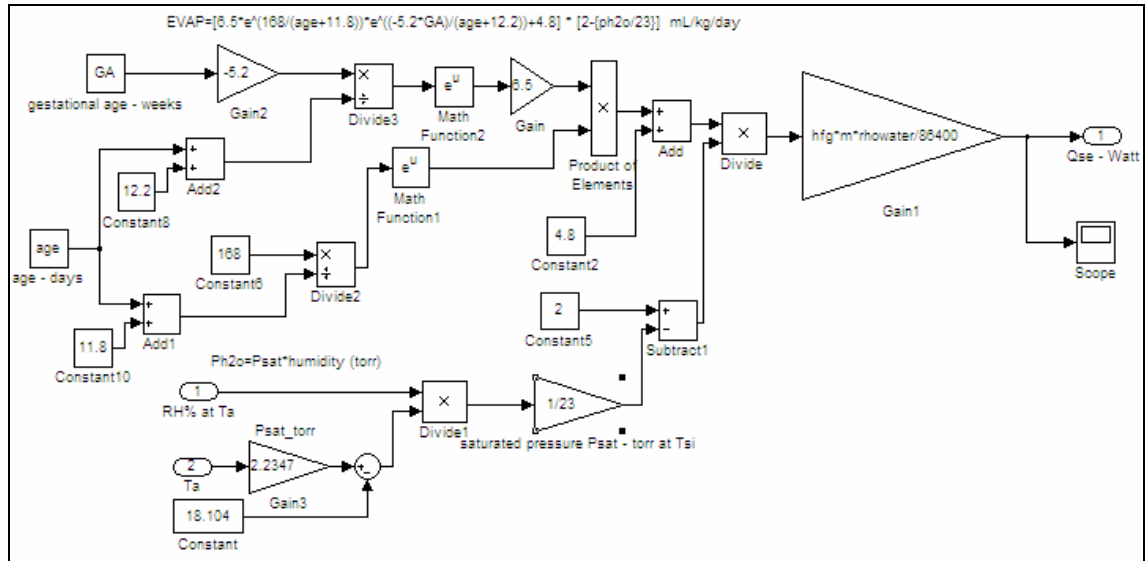


Figure 3-14 Evaporative loss from the skin

The evaporation rate formula (equation (2.33)) in terms of mL/kg/day is a function of gestational age and postnatal age of the infant as well as the partial pressure of water-vapour. The latter is a function of saturation pressure which depends on air temperature as a first input supplied from the incubator air space compartment, and the relative humidity as second input which is fed as a constant input in the parent model.

All other boxes Figure 3-14 are constants given by equation (2.33). Thus, the evaporation rate in mL/kg/day is then converted into Watts by multiplication with the gain shown in Figure 3-14 to represent the evaporative heat loss from the skin Q_{se} .

3.2.2.4 Skin-Wall Radiation

Radiant heat exchange that occurs between the infant skin and the incubator walls as described in equation (2.34) is simulated in Figure 3-15. Radiation usually takes place between any two surfaces no matter the geometry and regardless of their directions or inclination onto each other. Since in our case the shape of the infant is not uniform and has various view factors normal to the incubator walls, fractions used (as of the total surface area of the infant skin exposed to the incubator air space) were stated in chapter

two). Thus, the total fractions of the overall skin surface area exposed to the air space and normal to incubator walls is 55.5%.

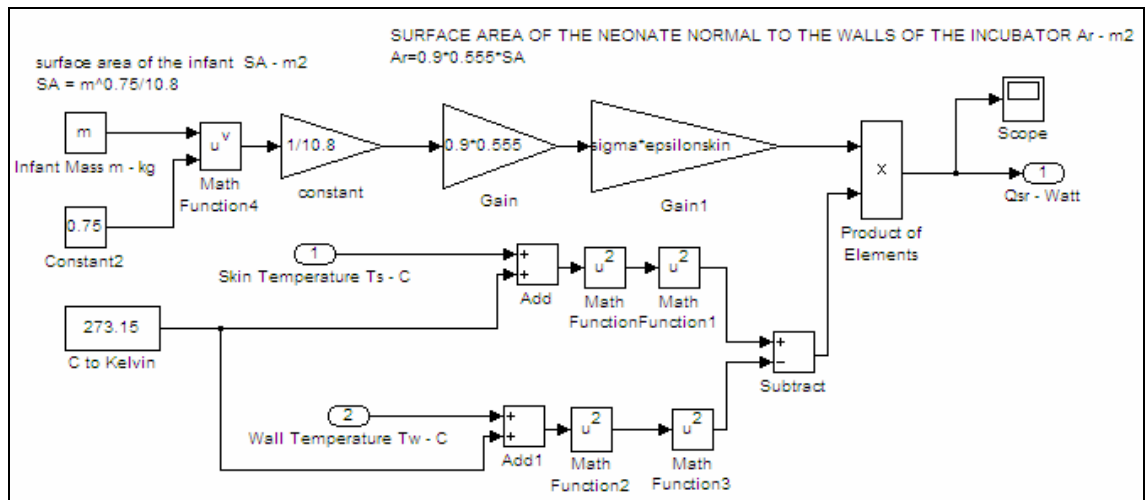


Figure 3-15 Skin-wall radiation

Both the skin temperature and wall temperature inputs are converted into degrees Kelvin and raised to the fourth power due to the nature of the general formula of radiation (Stefan - Boltzmann Law).

Skin temperature is an internally iterated input, while the wall temperature is externally fed from the incubator wall compartment. All other parameters and gains are constants defined in an M-file.

3.2.2.5 Mass of the Infant Skin

Figure 3-16 represents the Simulink model of the infant skin mass as described in equation (2.19). The skin mass is determined from the thickness of the skin, the skin density and the total surface area of the infant which is function of the infant mass.

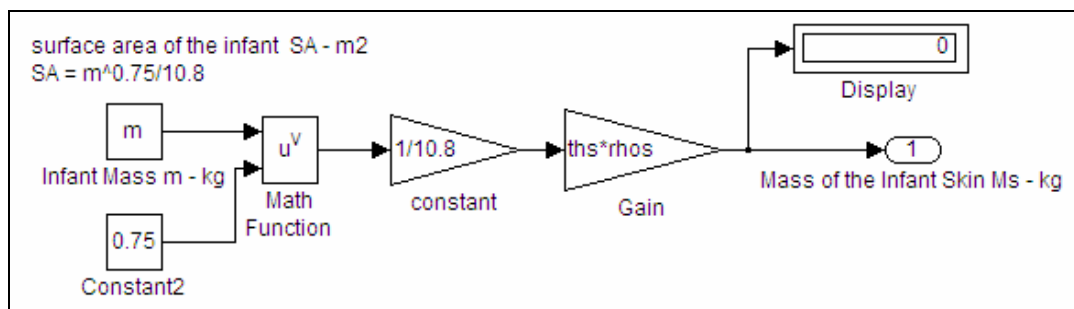


Figure 3-16 Mass of the infant skin

The other parameters shown in Figure 3-11, C_{psk} and T_{si} , are considered constants given in an M-file. The D-operator in equation (2.23) is represented by $1/s$, the integrator. Thus, the output, T_s , represents the skin temperature that varies over time.

3.2.3 The Incubator Air Space Compartment

The Simulink model of this compartment is illustrated in Figure 3-17. It represents the variation of the incubator air space temperature over time, T_a , as in equation (2.38).

A Simulink model for each of the subsystems shown in Figure 3-17 is being developed and each of them represents the rate of the heat exchange in Watts that takes place between the elements associated inside each subsystem.

Some of the subsystems in Figure 3-17 have been detailed earlier in the previous sections and figures in this chapter such as, the skin-air convection (Figure 3-12), the evaporation from the skin (Figure 3-14), sensible heat losses (Figure 3-8) and latent heat losses (Figure 3-9). Table 3-4 lists all the subsystems of Figure 3-17 with the input name and the source for that input.

From Figure 3-17, there are seven variable inputs: five externally fed from other compartments (T_s , T_{sply} , T_c , T_w and T_m), one input a constant variable $RH\%$ provided within the parent system and lastly the internally iterated input T_a .

All other parameters given in equation (2.38) such as: C_{pa} and T_{ai} are constants defined in an M-file. The output T_a represents the variation of the incubator air temperature over time.

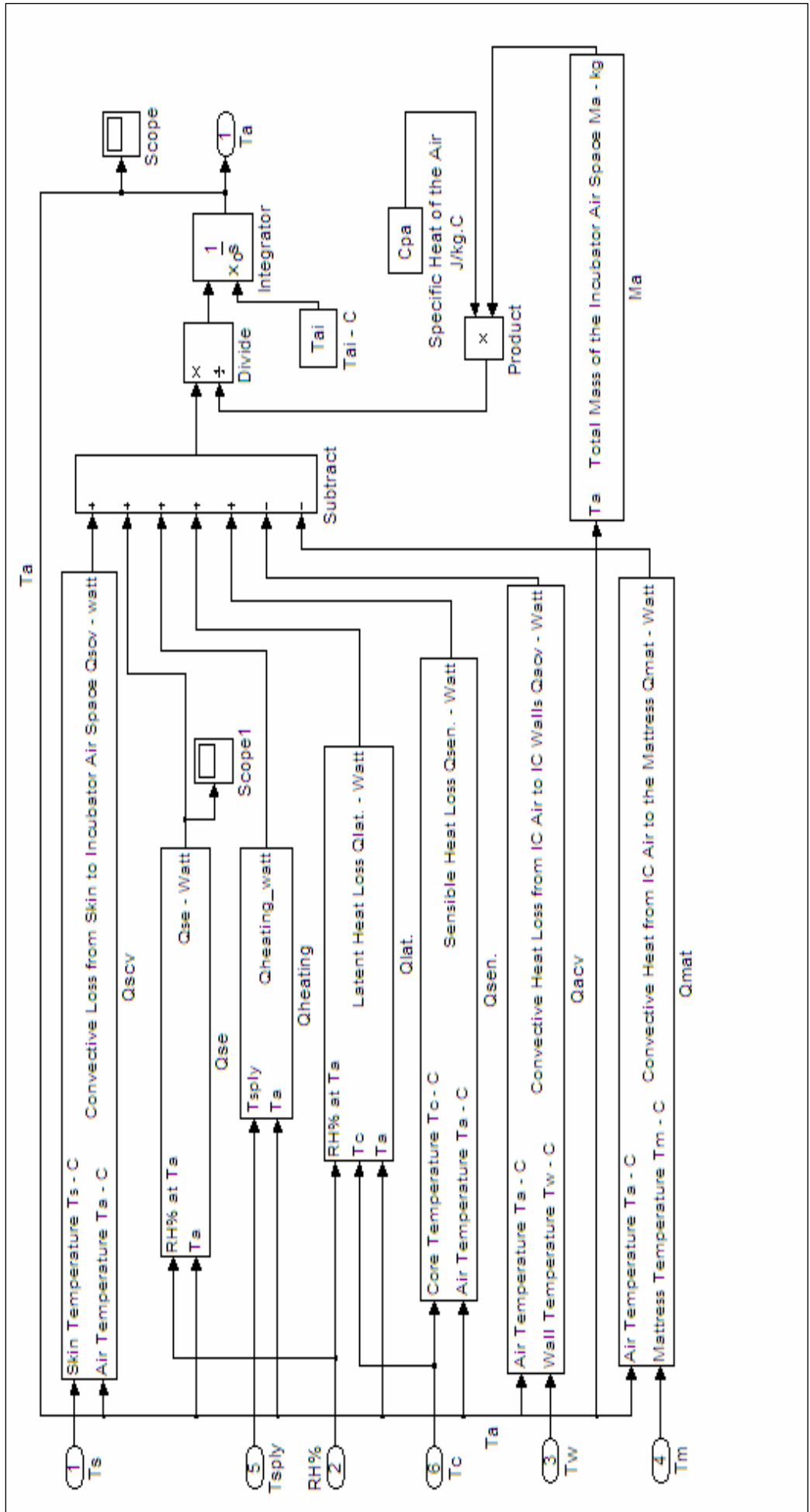


Figure 3-17 The incubator air space compartment

Table 3-4 Sub-systems of the incubator air space

<i>S</i>	<i>Sub-System designation</i>	<i>Input Name</i>	<i>Input Source</i>
1	Convective loss from skin to incubator air space	Skin temperature	Skin compartment
		Air temperature	Incubator air space compartment
2	Evaporation loss from skin to incubator air space	Relative humidity	Constant input to the parent system
		Air temperature	Incubator air space compartment
3	Sensible heat losses	Core temperature	Core compartment
		Air temperature	Incubator air space compartment
4	Latent heat losses	Core temperature	Core compartment
		Air temperature	Incubator air space compartment
		Relative humidity	Constant input to the parent system
5	Heat supply	Supply air temperature	supplied air compartment
		Air temperature	Incubator air space compartment
6	Incubator air space-walls convection	Air temperature	Incubator air space compartment
		Wall temperature	Incubator walls compartment
7	Incubator air space-mattress convection	Air temperature	Incubator air space compartment
		Mattress temperature	Mattress compartment
8	Total mass of the incubator air space	Air temperature	Incubator air space compartment
9	Specific heat of the air	Cpa	Constant in M-file
10	Initial Air temperature	Tai	Constant in M-file

3.2.3.1 Heat Supply Sub-System

This Simulink model as shown in Figure 3-18 illustrates the rate of heat energy supply to the incubator hood that exchanges heat with the infant as well as with the incubator walls and the room environment accordingly, as described in equation (105).

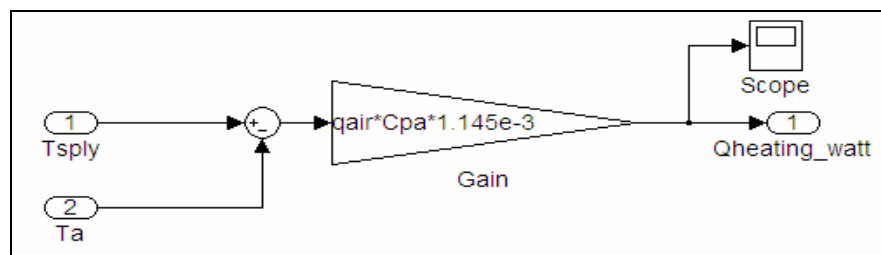


Figure 3-18 Heat supply sub-system

The incubator air density in Figure 3-18 is purposely considered a constant (1.145×10^{-3} kg/L) in order to simplify the Simulink model (i.e. to reduce the size of the subsystem and minimise the time needed by the computer to implement the process). The density variation upon the variation of both T_{sply} and T_a is also not significant, although, it should technically be calculated at T_{wet} and T_{ha} as in equations (2.101) and (2.102), respectively.

3.2.3.2 Incubator Air-Walls Convection Heat Transfer Sub-System

This sub-system is represented in Figure 3-19. Convective heat exchange occurs between the incubator walls and the air space inside the incubator, as described in equation (2.39). The pattern of the air flow is forced convection due to the circulated-air fan.

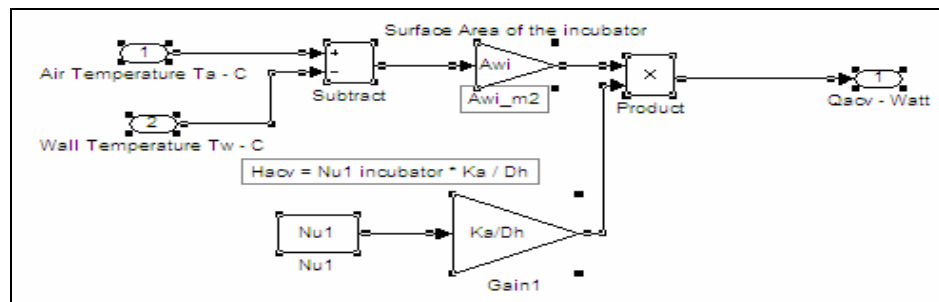


Figure 3-19 Incubator air-walls convection sub-system

The surface area of the incubator walls, A_{wi} , as well as the Nusselt number, Nu_1 , are required to estimate the convective heat transfer coefficient, h_{acv} , and are given in an M-file along with other constant parameters and gains. This A_{wi} represents all areas of the transparent plexiglass hood.

The thermal conductivity of the air, Ka , is estimated at 35 °C. The hydraulic diameter of the incubator, Dh , is a function of both incubator area and perimeter based on the airflow direction. All parameters required to determine Nu_1 are detailed in an M-file.

3.2.3.3 Incubator Air-Mattress Convection Heat Transfer Sub-System

Figure 3-20 represents the convective heat exchange that occurs between the air space and the mattress due to the temperature difference between them, as described in equation (2.43). Only 90% of the mattress area contributes in this convective heat

exchange, as the remaining 10% is in contact with the infant skin and undergoes conduction.

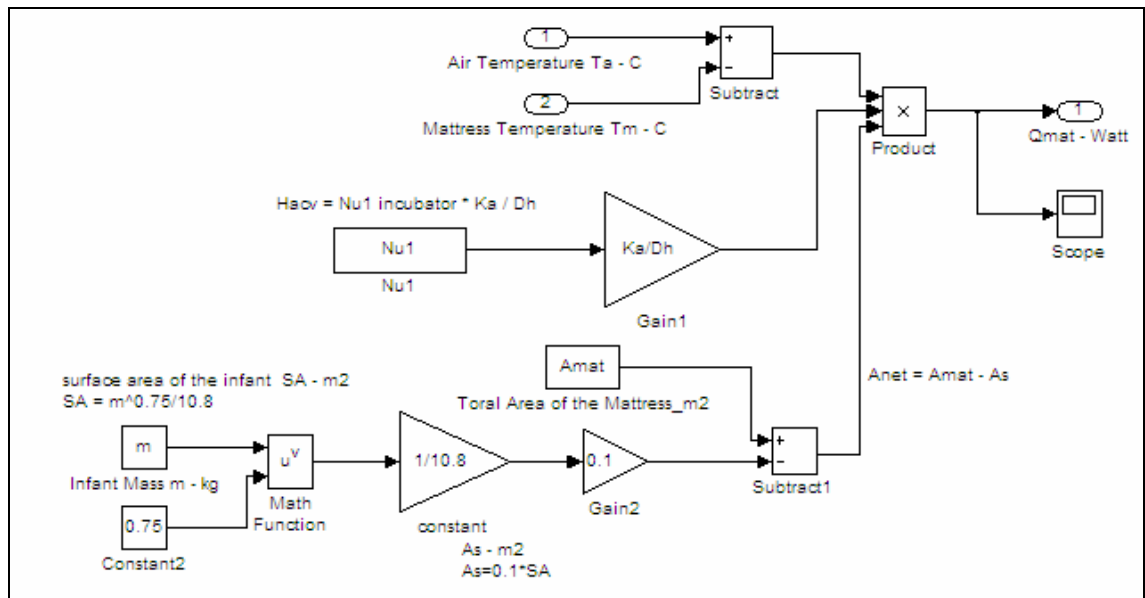


Figure 3-20 Incubator air-mattress convection sub-system

This 10% mattress area is a function of infant mass and is determined as shown in Figure 3-20. The total area of the mattress is quantifiable at around 0.21045 m^2 , the $Nu1$ and Dh are explained in the previous section. All other parameters shown in Figure 3-20 such as $Amat$ are detailed in an M-file.

3.2.3.4 Mass of the Incubator Air Space Sub-System

The Simulink model for this subsystem is illustrated in Figure 3-21, which represents equation (2.73). The mass of the incubator air varies upon the variation of air temperature inside the incubator (i.e. the return air temperature) and the concentrations of N_2 and O_2 . The temperature of the air is converted into degrees Kelvin as this is a required in the perfect gas law.

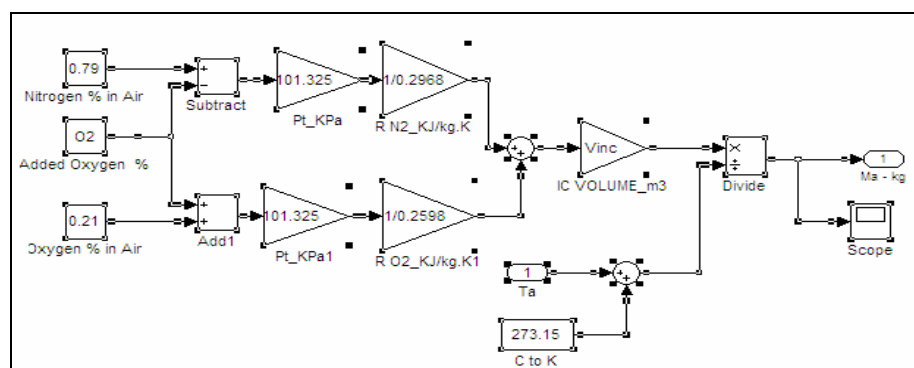


Figure 3-21 Mass of the incubator air space sub-system

Although this Simulink model can technically incorporate the element of added oxygen, to decrease the computation time this was disabled (i.e. O_2 set to zero in the M-file) during simulation. This is justified in that this practice is no longer in use. Therefore, both N_2 and O_2 concentrations in the air remain at their normal level of 79% and 21% respectively.

Thus, the only variable that influences the mass of the incubator air is the variation of the air temperature. However, the simulation results show that this variable has a subtle effect on the air mass. All other parameters and gains are constants and are given within the Simulink model/M-file (e.g. the incubator volume, V_{inc}).

Sections (3.2.3.1 - 3.2.3.4) and 3.2.3 describe the Simulink model sub-systems of the incubator air space compartment as shown in Figure 3-17.

3.2.4 The Incubator Wall Compartment

The Simulink model of this compartment is illustrated in Figure 3-22. It represents the variation of the incubator walls temperature over time T_w as in equation (2.47). The subsystems of this compartment also reflect the relationships between the infant skin and the internal walls of the incubator as well as the external walls with respect to the environment (room) in terms of radiation, forced convection and free convection respectively.

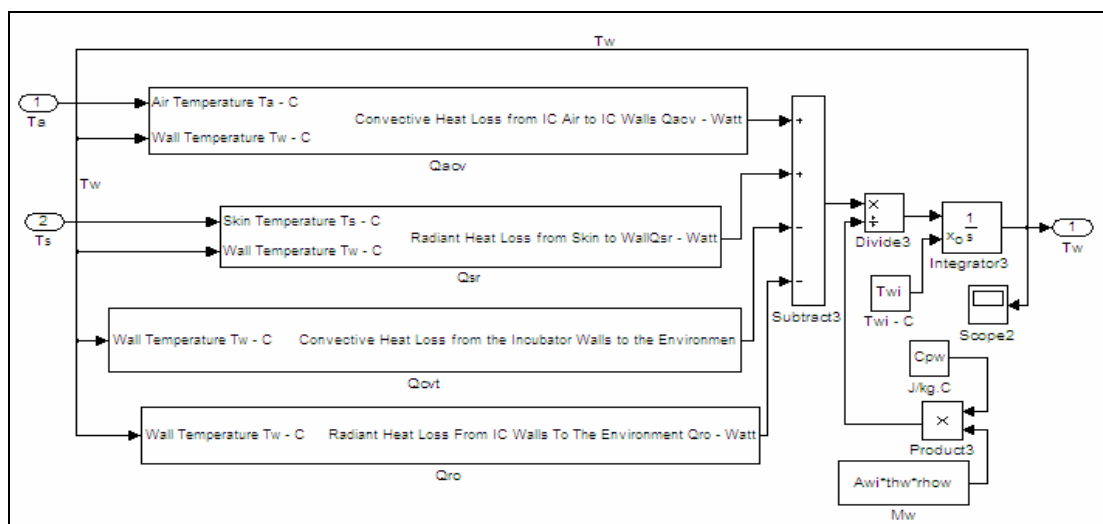


Figure 3-22 The incubator wall compartment

A Simulink model for each of the subsystems shown is being developed, and each of them represents the rate of heat exchange in Watts that takes place between the elements associated inside each subsystem.

Some of the subsystems in Figure 3-22 and Figure 3-17 have been detailed earlier in the previous sections in this chapter. These include the skin-wall radiation as in Figure 3-15 and the incubator air-walls convection in Figure 3-19. These two subsystems are associated with the heat exchange that occurs between the infant and the internal surfaces of the incubator walls. However, the other two subsystems Q_{cvl} and Q_{ro} are for the heat transfer between the external surfaces of the incubator walls and the environment. This will be demonstrated in the following sections.

Table 3-5 lists all the subsystems of Figure 3-22 with the input name and the source for that input as follows:

Table 3-5 Sub-systems of the incubator walls compartment

<i>S</i>	<i>Sub-System designation</i>	<i>Input Name</i>	<i>Input Source</i>
1	Incubator air space-walls convection	Air temperature	Incubator air space compartment
		Wall temperature	Incubator walls compartment
2	Infant skin-walls radiation	Skin temperature	Skin compartment
		Wall temperature	Incubator walls compartment
3	Incubator walls-environment convection	Wall temperature	Incubator walls compartment
4	Incubator walls-environment radiation	Wall temperature	Incubator walls compartment
5	Mass of the incubator walls	wall material properties: density, thickness and total surface area	constants in M-file
6	Specific heat of the wall	Cpw	Constant in M-file
7	Initial wall temperature	Tw _i	Constant in M-file

As can be seen from Figure 3-22, there are three variable inputs: two externally fed from other compartments (T_a and T_s), while T_w is an internally-iterated input.

All other parameters given in equation (2.47), C_{pw} and T_{wi} are constants defined in the M-file. The output T_w represents the variation of the incubator wall temperature over time.

3.2.4.1 Incubator Walls-Room Environment Free-Convection Sub-Systems

The Simulink model for the free convection heat exchange that occurs between the incubator external wall surfaces and the room environment is illustrated in Figure 3-23, as described in equation (2.56). This subsystem comprises of three internal sub-systems of the free convection from the top surface, long sides surfaces (two surfaces) and short sides surfaces (two surfaces). Thus, the entire external surfaces of the incubator walls undergo free convection heat exchange with the room environment.

For each of the three internal subsystems a detailed Simulink model is developed in the following sections.

The only variable input to these three internal subsystems is the internally-iterated wall temperature, T_w . All other parameters given in them are quantifiable constants defined in an M-file.



Figure 3-23 Incubator walls-environment free convection sub-systems

The output, Q_{cvt} , (in Watts) represents the amount of the exchanged heat energy due to free convection occurs between incubator walls and the room environment.

3.2.4.1.1 The hood top surface free convection subsystem

The Simulink model of this subsystem is represented in Figure 3-24. It describes the implementation of equation (2.52). All parameters shown are associated with the horizontal surface of the incubator hood and defined in an M-file.

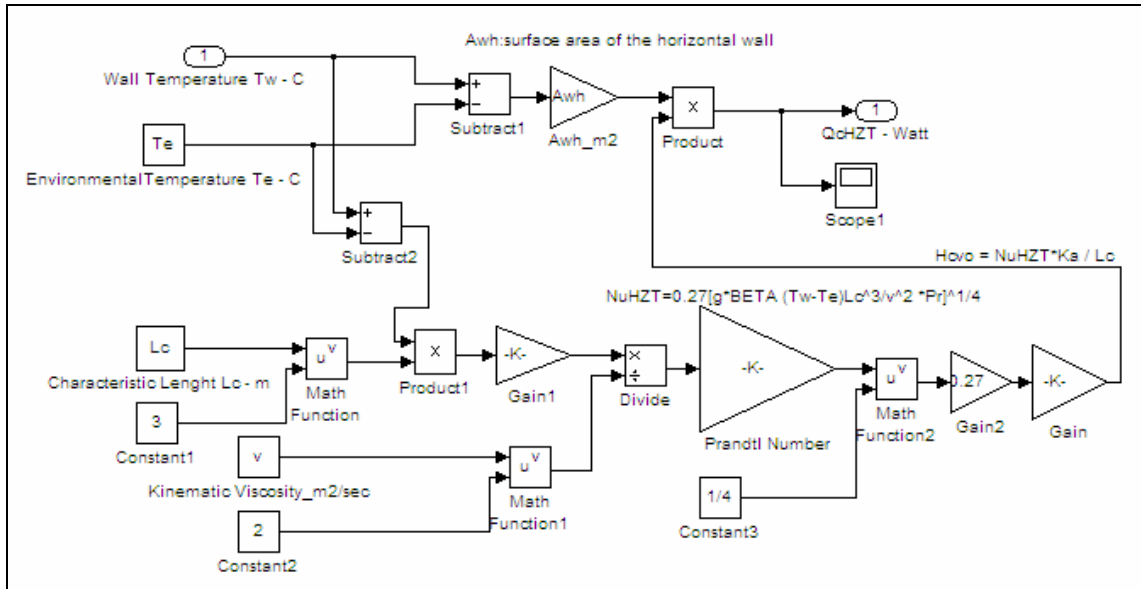


Figure 3-24 Incubator horizontal surface-free convection subsystem

The output Q_{cH2T} in Watts represents the rate of the convective heat exchange of the horizontal surface of the incubator hood. All of the parameters in Figure 3-24 characterise the free convection relationships, in which the Rayleigh, Prandtl and Nusselt numbers are determined in order to estimate the convective heat transfer coefficient for free convection, h_{cvo} . The variable input for this subsystem is the wall temperature while the environment (room) temperature, Te , is considered to be constant.

3.2.4.1.2 The hood vertical surfaces free convection subsystem

The free convective heat energy exchange from the external vertical sides of the hood on both the long and the short sides are simulated as shown in Figure 3-25 and Figure 3-26, respectively.

The parameters shown in these two figures are almost identical, except the surface area associated with each side is different. This is A_{wvl} for the long side and A_{wvs} for the short side, both of which are estimated in an M-file along with all other constant parameters and gains shown in Figure 3-25 and Figure 3.26.

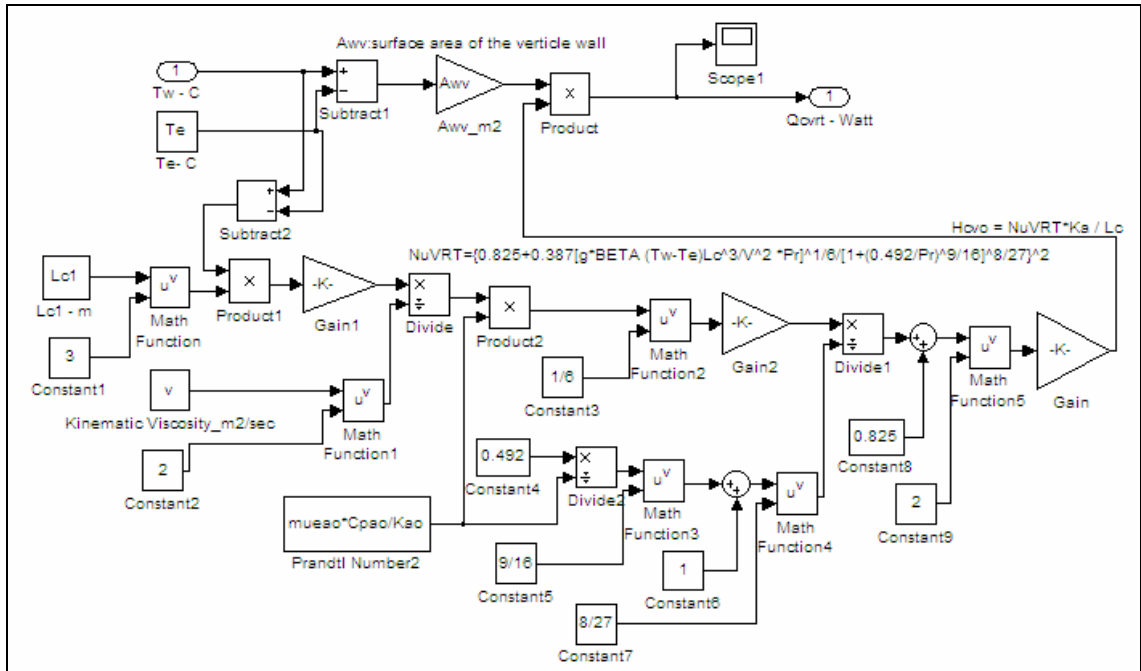


Figure 3-25 Incubator vertical surface free convection-Long side

Figure 3-25 and Figure 3-26 represent the implementation of equation (2.52) with all other related factors given in that equation.

The outputs, Q_{ovrt} , (in Watts) from Figure 3-25 and Figure 3-26 are only for one short side and one long side. Therefore, both outputs from these two sides are multiplied by two in order to obtain the four vertical sides of the incubator walls.

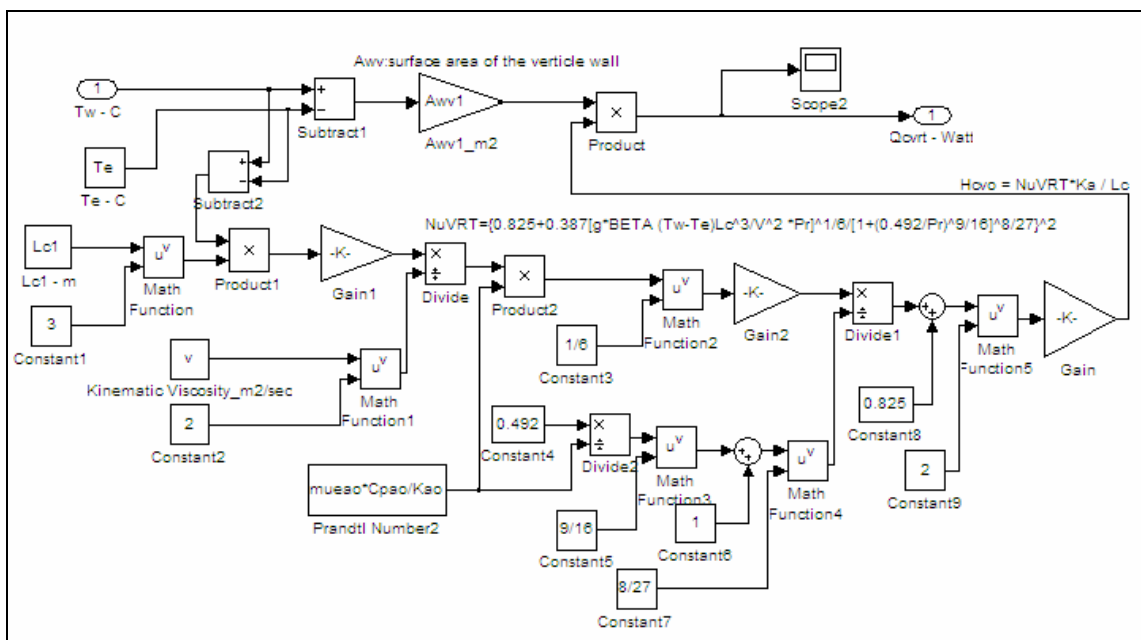


Figure 3-26 Incubator vertical surface free convection-Short side

As in section 3.2.4.1.1, Figure 3-25 and Figure 3-26 demonstrate the free convection relationships, in which the Rayleigh, Prandtl and Nusselt numbers are determined in order to estimate the convective heat transfer coefficient for free convection, h_{cvo} . The variable input is the wall temperature whereas the temperature of the environment (room), T_e , is constant.

Thus, in sections 3.2.4.1.13.2.4.1.2 and 3.2.4.1.2 the total convective heat energy of the external surfaces of the incubator walls by free-convection was determined and with the integration of other subsystems (shown in Figure 3-22), the final wall temperature, T_w , can be estimated.

3.2.4.2 Incubator Walls- Room Environment Radiation Sub-System

The Simulink model for this subsystem is illustrated in Figure 3-27, which represents equation (2.57). The variable input wall temperature, T_w , as well as the room temperature, T_e , are converted into degrees Kelvin to comply with the unit measure of the Stephan-Boltzmann constant (i.e. $W/m^2 \cdot K^4$). Clearly, the amount of the radiative energy depends on that temperature difference raised to the fourth power. The room temperature, T_e , is considered to be constant, and all other parameters in Figure 3-27 are defined in an M-file.

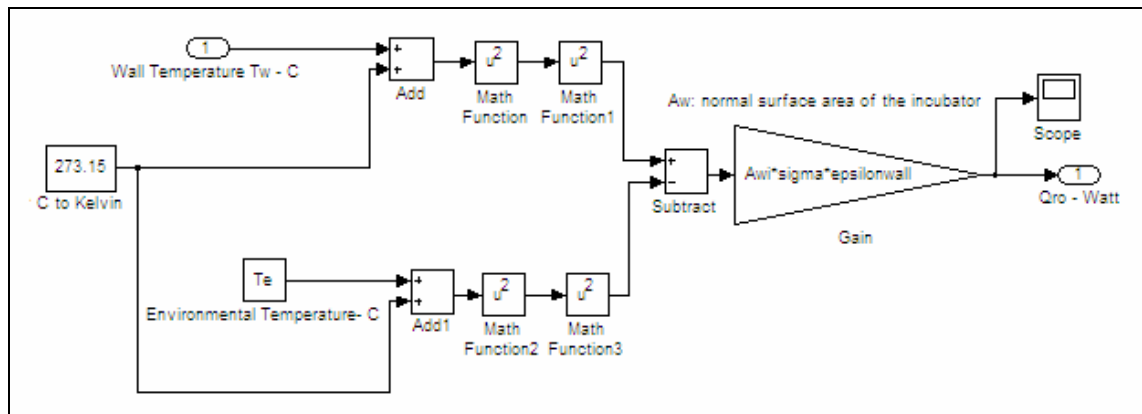


Figure 3-27 Incubator walls-room environment radiation

3.2.5 The Incubator Mattress Compartment

The Simulink model of this compartment is shown in Figure 3-28, and represents equation (2.60). The subsystems of this compartment include the infant skin-mattress conduction sub-system and the subsystem of incubator air space-mattress. Both of these subsystems have already been stated as in Figure 3-13 and Figure 3-20, respectively.

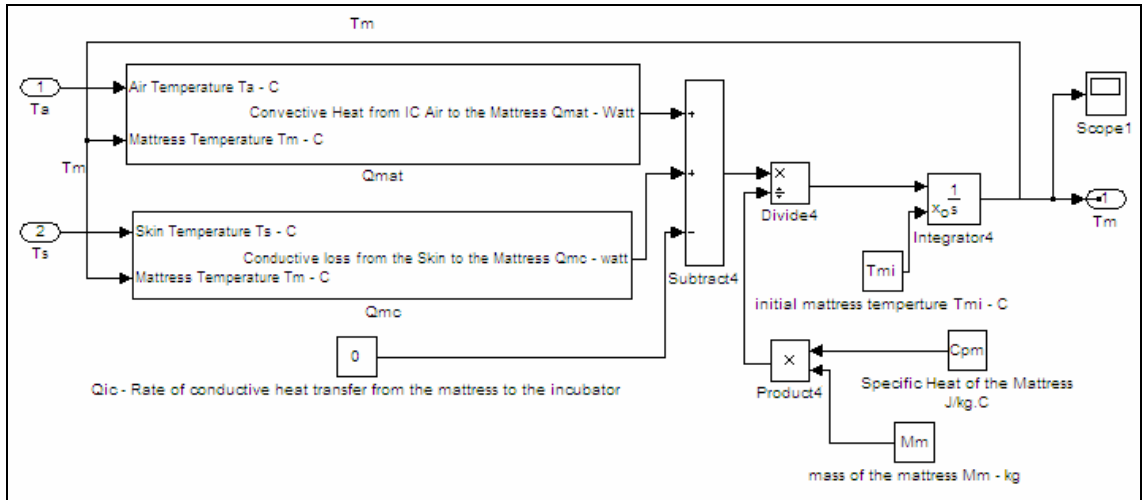


Figure 3-28 The incubator mattress compartment

The third subsystem is shown in Figure 3-28 (conduction that occurs between the incubator and the mattress) is considered to be zero.

As can be seen from Figure 3-28, there are three inputs into this compartment. Two of them are externally fed (T_a and T_s) from the incubator air and infant skin compartments, whereas the third input, T_m , is internally iterated. All other parameters given in Figure 3-28 are constants defined in an M-file.

The output, T_m , is the final estimated temperature of the mattress in degrees Celsius, which also represents the variation of the mattress temperature over time.

Table 3-6 lists all the subsystems of Figure 3-28 with the input name and the source for that input as follows:

Table 3-6 Sub-systems of the incubator mattress compartment

<i>S</i>	<i>Sub-System designation</i>	<i>Input Name</i>	<i>Input Source</i>
1	Incubator air space-mattress convection	Air temperature	Incubator air space compartment
		Mattress temperature	Incubator mattress compartment
2	Infant skin-mattress conduction	Skin temperature	Skin compartment
		Mattress temperature	Incubator mattress compartment
3	Incubator-mattress conduction	zero	zero
4	Mass of the incubator mattress	Mm	constants in M-file
5	Specific heat of the mattress	Cpm	Constant in M-file
6	Initial mattress temperature	Tmi	Constant in M-file

3.2.6 The Circulated - Air Fan Compartment (Mixed Air Compartment)

The Simulink model of this compartment is illustrated in Figure 3-29. It represents the mixed air temperature, T_{mx} , as described in equation (2.63). This Simulink model demonstrates the variation of the output, T_{mx} , in response to variation in the concentration of added oxygen, as well as the variation in the densities of N_2 and O_2 as the incubator air space temperature varies.

This has purposely been implemented in this project to acquire more accuracy in the T_{mx} . The simulation results show that the margin between T_{mx} and T_a is small since the element of the added oxygen plus the volumetric oxygen flow rate are both disabled (i.e. added O_2 and q_{O_2} are set to zero in the M-file) during simulation. Thus, N_2 and O_2 concentrations in the incubator air remains normal at 79% and 21% respectively. The mixer here is the circulating-air fan described in section 2.5.

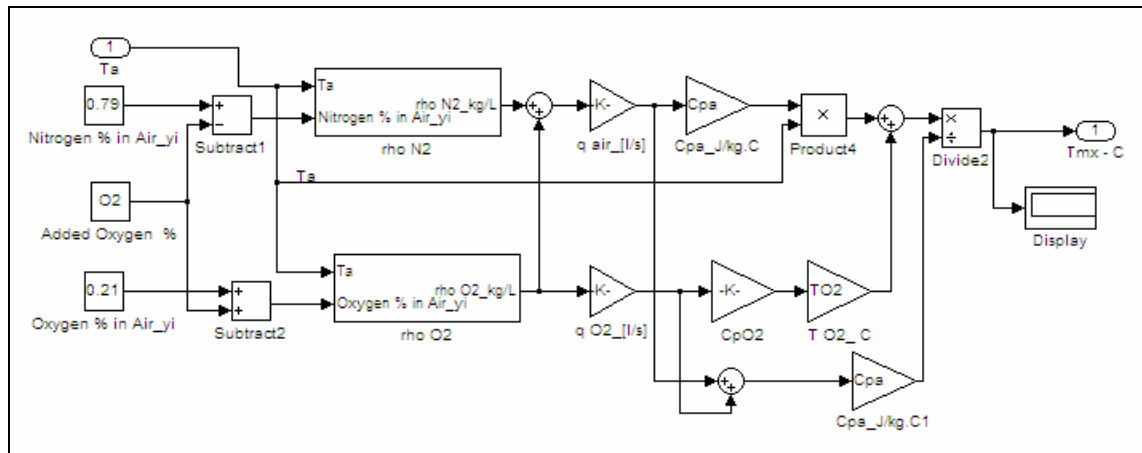


Figure 3-29 The circulated-air fan compartment

Therefore, the only input to this Simulink model is the incubator air temperature, T_a (i.e. the return air temperature). For each of the subsystems shown in Figure 3-29, a Simulink model is developed in the following sections. All other parameters given in Figure 3-29 are defined in an M-file.

3.2.6.1 The Nitrogen Density Sub-System

Figure 3-30 describes the Simulink model of the density variation of N_2 upon the variation of the incubator air temperature, T_a . The output, ρ_{N_2} , is given in kg/L. This Simulink model is entirely based on the perfect gas law described in section 2.5, and in particular equations (2.62) to (2.67).

All other constant parameters and gains shown in Figure 3-30 are defined the M-file.

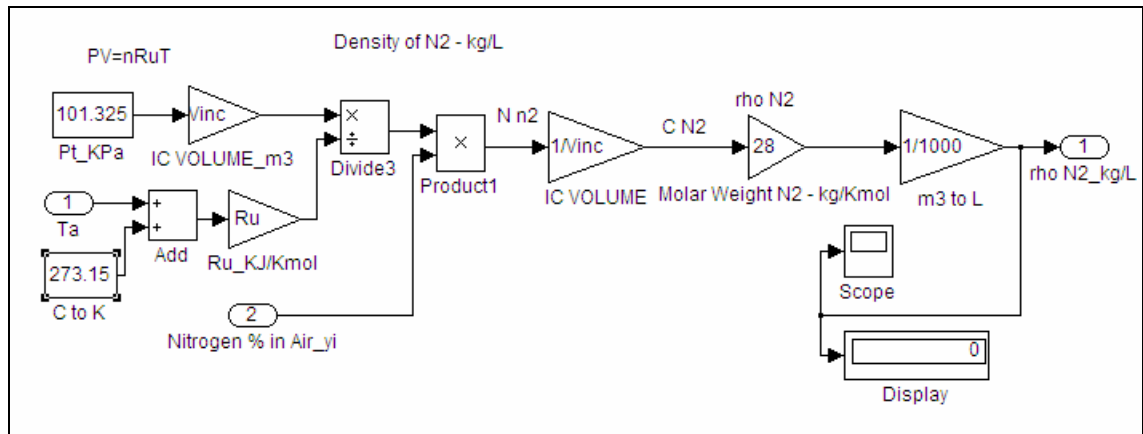


Figure 3-30 The nitrogen density sub-system

3.2.6.2 The Oxygen Density Sub-System

The Simulink model of this sub-system is illustrated in Figure 3-31. The way that this Simulink model is implemented in terms of the components and elements shown is similar to Figure 3-30 in the previous section. However, in Figure 3-30 all of the parameters used are related to the oxygen density.

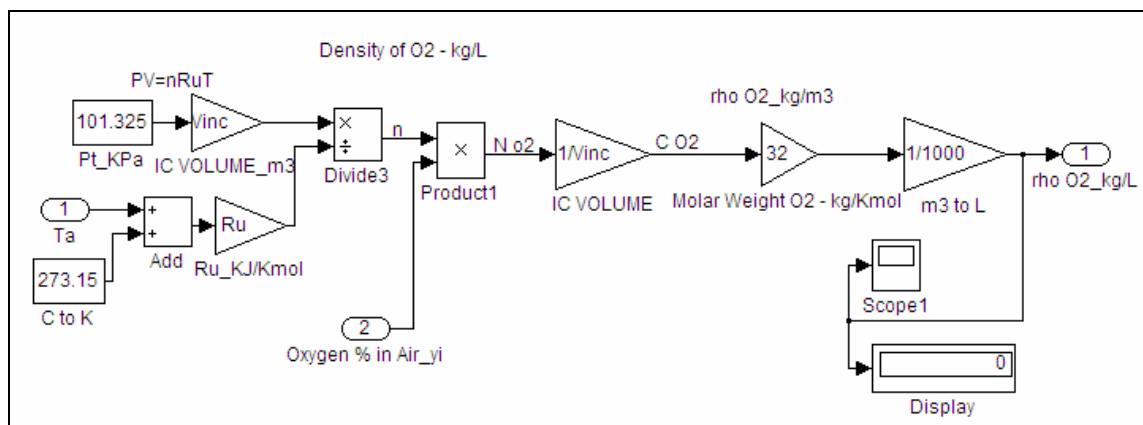


Figure 3-31 The oxygen density sub-system

3.2.7 The Heated Air Compartment (Heater Element Compartment)

Figure 3-32 illustrates the Simulink model of the heated air temperature. It represents equation (2.75). In this Simulink model, the heated air temperature varies upon the variation of T_{mx} , the percentage of the added oxygen which varies the density of N_2 and O_2 and thus the density of the circulated air. It also adjusts the power rating of the heater element (i.e. maximum and minimum power limits), which for this element is between

0-260 Watts. This latter factor is part of the closed-loop system shown in Figure 3-2. In this Simulink model the air density is assumed to be a constant, 1.145×10^{-3} kg/ml to simplify the simulation process (i.e. to reduce the size of the subsystem and minimise the time needed by the computer to implement the process).

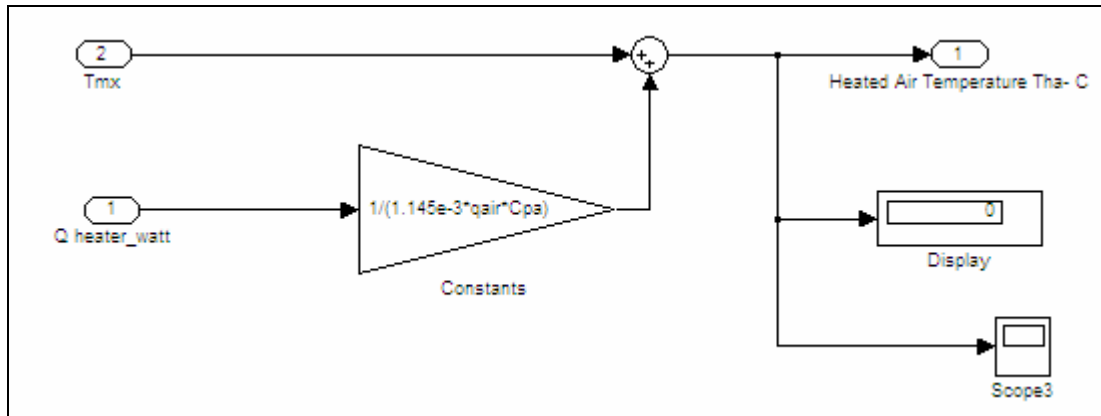


Figure 3-32 The heater element compartment

The power rating of the heater element fluctuates (i.e. increase or decrease between 0-260 watts) upon the variation in the corrected output signal from the controller element (i.e. the PID element). This controller element transforms the input (i.e. the difference value between the feedback and the reference temperatures) into a voltage signal which is sent to the heater. Thus, the power ratings of the heater fluctuates based upon that voltage signal.

The Simulink model of the heater compartment has two inputs; the T_{mx} from the mixed air compartment and the Q_{heater} from the closed-loop system. The added oxygen element (as was discussed earlier in the previous sections) is technically incorporated within the modelling but is disabled during simulation. Both subsystems related to the density of N_2 and O_2 shown in Figure 3-32 are adapted from the previous sections 3.2.6.1 and 3.2.6.2 respectively. All other parameters given are defined in an M-file.

3.2.8 The Humidification System Compartment

The humidification system compartment is the water chamber which consists of three parts: an air space inside the water chamber, water, and the aluminium block or ‘heat sink’. For each of these parts, a Simulink model is developed in the following sections. These three parts interact with each other and their combination creates the

humidification process that has a significant influence on the overall thermo neutrality environment of the infant incubator.

3.2.8.1 The Air Space Inside the Water Chamber Compartment

The Simulink model of this part (air space) in the water chamber is demonstrated in Figure 3-33, and represents equation (2.78). There are four external inputs fed from other system compartments: heated air temperature, T_{ha} , aluminium temperature, T_{al} , water temperature, T_{wa} , and incubator relative humidity, $RH\%$, and single internally iterated input, the wetted air temperature that leaves the water chamber, T_{wet} .

The output, T_{wet} , represents the variation in the wet air temperature, that leaves the water chamber over time. All constant parameters and are gains shown in Figure 3-33 (such as $Nu2$, $Nu3$, $A_{in/out}$, Va , Cpa , Cps , A_{all} , M_{ah}) and are related to equations (2.80) to (2.88) and evaluated in an M-file.

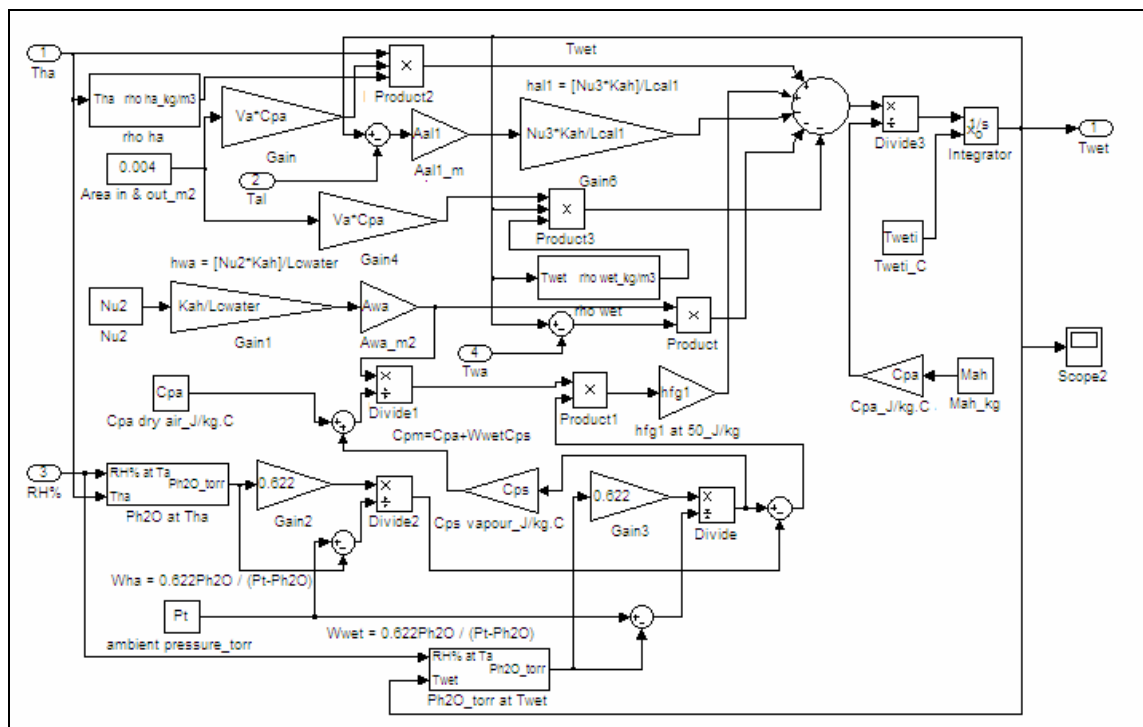


Figure 3-33 Humidification process-air space simulink model

There are also four other Simulink subsystems shown in Figure 3-33: two Simulink subsystems for the air density at T_{ha} and T_{wet} , and two Simulink subsystems for the water-vapour partial pressure at T_{ha} and T_{wet} . The subsystems for densities of the air are the heated air temperature, ρ_{ha} , and wet air temperature, ρ_{wet} , which are simulated in Figure 3-34 and Figure 3-35 respectively.

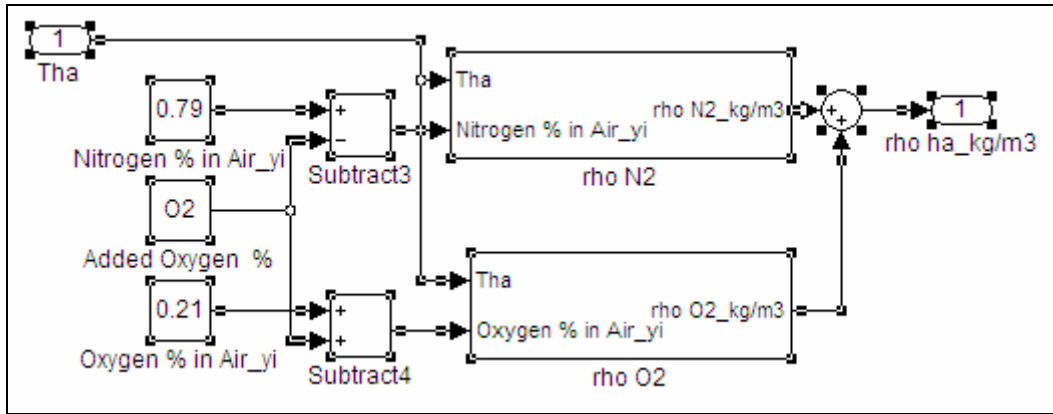


Figure 3-34 Air density variation at heated air temperature

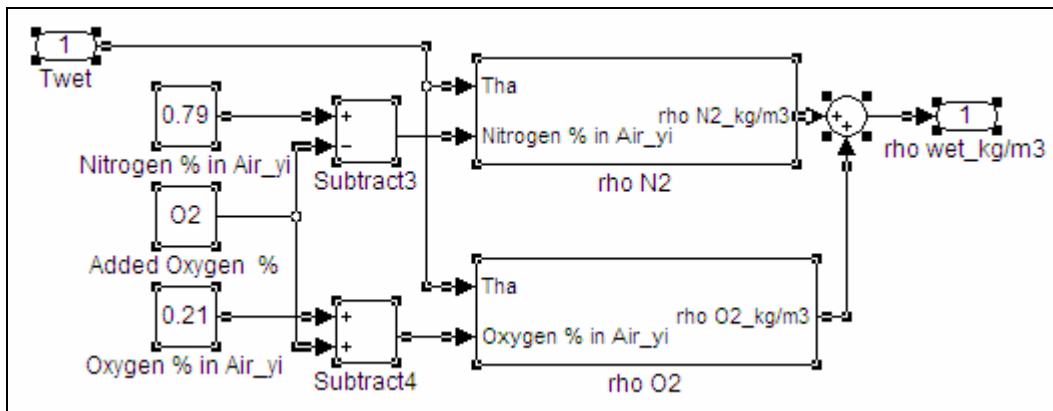


Figure 3-35 Air density variation at wet air temperature

Figure 3-34 and Figure 3-35 describe the variation of the air density upon the variation of the heated air, the wetted air temperatures and the change of the concentrations of the gases in the air in case added oxygen is considered. (As discussed previously, this latter part is disabled during simulation).

Both Figure 3-34 and Figure 3-35 have a single input which is the temperature of the heated air or the wetted air. The subsystems for the density variation upon the change in gases percentages for N_2 and O_2 are detailed earlier in sections 3.2.6.1 and 3.2.6.2 and demonstrated in Figure 3-30 and Figure 3-31 respectively.

The other two subsystems in Figure 3-33 are for the partial pressure of water-vapour at T_{ha} and T_{wet} as illustrated in Figure 3-36 and Figure 3-37 respectively.

Figure 3-36 and Figure 3-37 demonstrate the variation of water-vapour partial pressure upon the variation of relative humidity, $RH\%$, of the incubator air and the variation of either the heated air or wetted air temperatures.

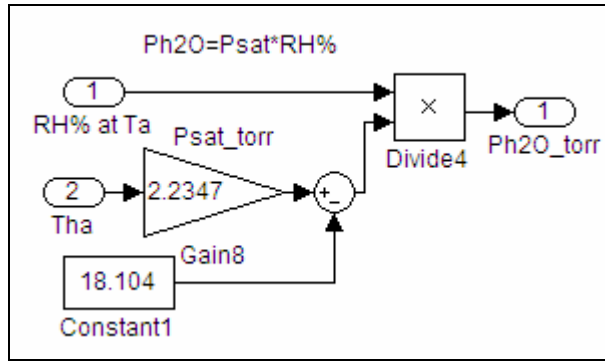


Figure 3-36 Water-vapour partial pressure at T_{ha}

Moreover, Figure 3-36 and Figure 3-37 represent a combined Simulink model of equations (2.12) and (2.13). Since the $RH\%$ is considered to be a constant input in the parent Simulink model (Figure 3-2) which does not change during simulation, the only variable input into these two subsystems is the heated air and wetted air temperatures. Thus, the output, P_{H_2O} , (in torr) represents the variation of water-vapour pressure upon the variation of T_{ha} , and T_{wet} over time.

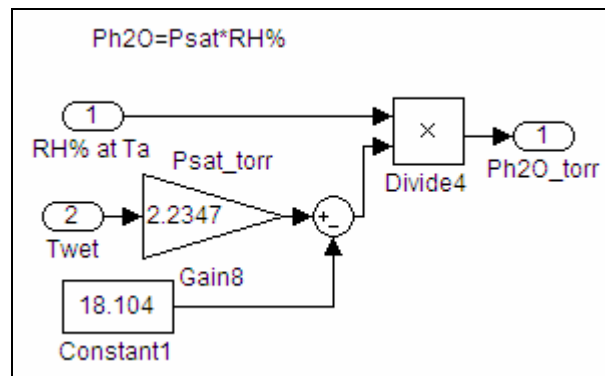


Figure 3-37 Water-vapour partial pressure at T_{wet}

In Figure 3-36, T_{ha} , is fed from the heated air compartment (Figure 3-32), whereas T_{wet} is internally iterated as shown in Figure 3-33.

3.2.8.2 The Water Mass in the Water Chamber Compartment

The Simulink model of this part of the humidification process is illustrated in Figure 3-38, and represents equation (2.91). The output T_{wa} represents the variation in the water mass temperature over time.

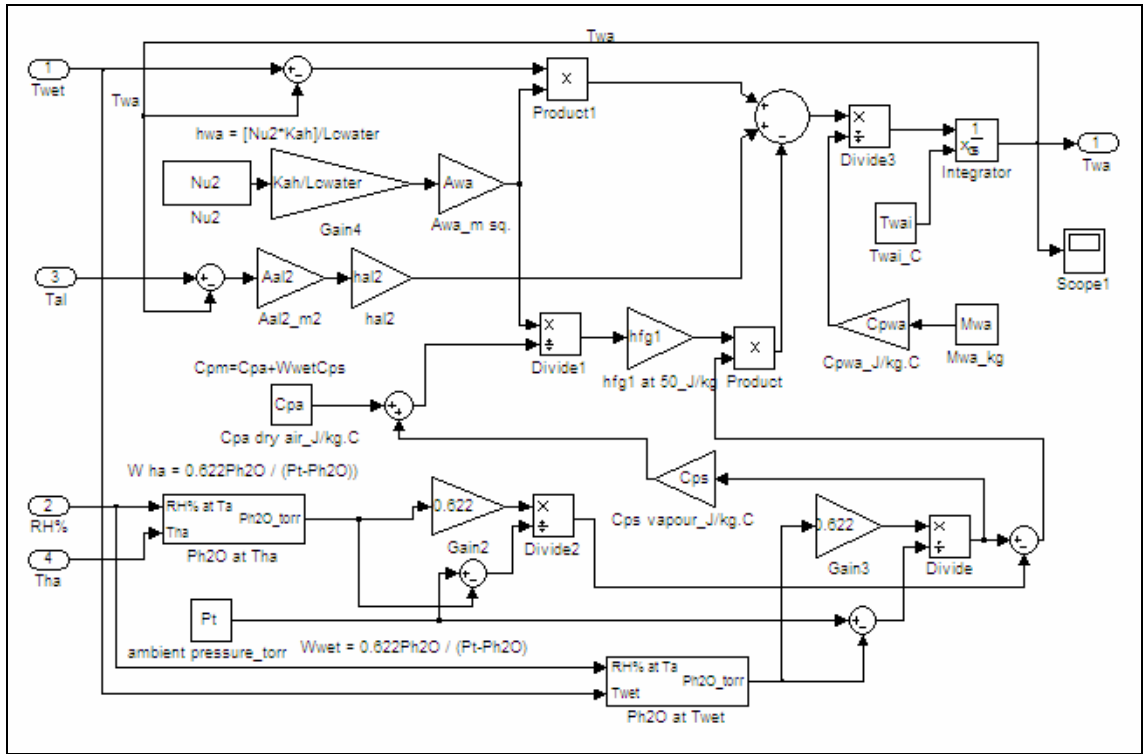


Figure 3-38 Humidification process-water mass simulink model

This Simulink model is simpler in components, although it has some similarity with Figure 3-33 in terms of the two subsystems of water-vapour partial pressure at T_{ha} and T_{wet} , which have been stated previously in Figure 3-36 and Figure 3-37 respectively. All other constants and gains shown in Figure 3-38 were demonstrated in section 3.2.8.1 (such as $Nu2$, A_{wa}). While the rest of the constants and gains (such as A_{al2} , h_{al2}) are related to equations (2.92) to (2.95), and are evaluated in an M-file.

Similar to section 3.2.8.1, there are four inputs in Figure 3-38: the wetted air temperature, T_{wet} , (which is an internally iterated input), aluminium temperature, T_{al} , heated air temperature, T_{ha} , (which are externally fed into this compartment) and incubator air relative humidity, $RH\%$ (which is fed as a constant input during simulation in the parent Simulink model as shown in Figure 3-2). Thus, this subsystem (Figure 3-38) has three variable inputs which change over time during simulation and a single input, ($RH\%$) that does not change during simulation.

3.2.8.3 The Aluminium Block the Water Chamber Compartment

The aluminium block is the last part in the water chamber compartment and acts as a heat sink. The Simulink model of the heat exchange occurs in this part as illustrated in

Figure 3-39 and represents equation (2.98). The output, T_{al} , represents the variation of the aluminium block temperature over time.

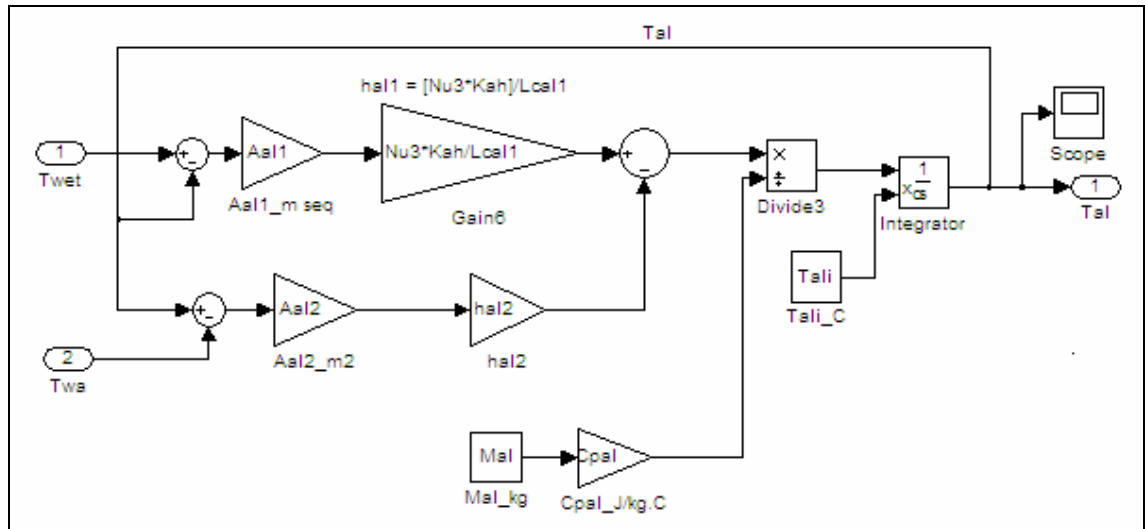


Figure 3-39 Humidification process-aluminium block simulink model

As can be seen from Figure 3-39, there are two external inputs: T_{wet} and T_{wa} which are fed from air space-water chamber and water mass-water chamber compartments plus one internally iterated input, T_{al} . The other constant parameters shown in Figure 3-39 are similar to those used in sections 3.2.8.1 and 3.2.8.2 which are defined in an M-file.

Thus, sections 3.2.8.1 to 3.2.8.3 describe a detailed Simulink model of the humidification processes. All heat exchange relationships that occur between the parts incorporated, are shown, and generate the required humidity inside the infant incubator.

3.2.9 The Supplied Air Temperature Compartment

This compartment is the last component of the infant-incubator system that describes the modelling of the final temperature entering the hood. The supplied air temperature compartment also incorporates the modelling of the mixing processes between the heated air temperature and wetted air temperature. This is demonstrated in Figure 3-40, and represents equation (2.102). The output, T_{sply} , represents the final temperature of the air that enters the hood as T_{wet} and T_{ha} vary over time.

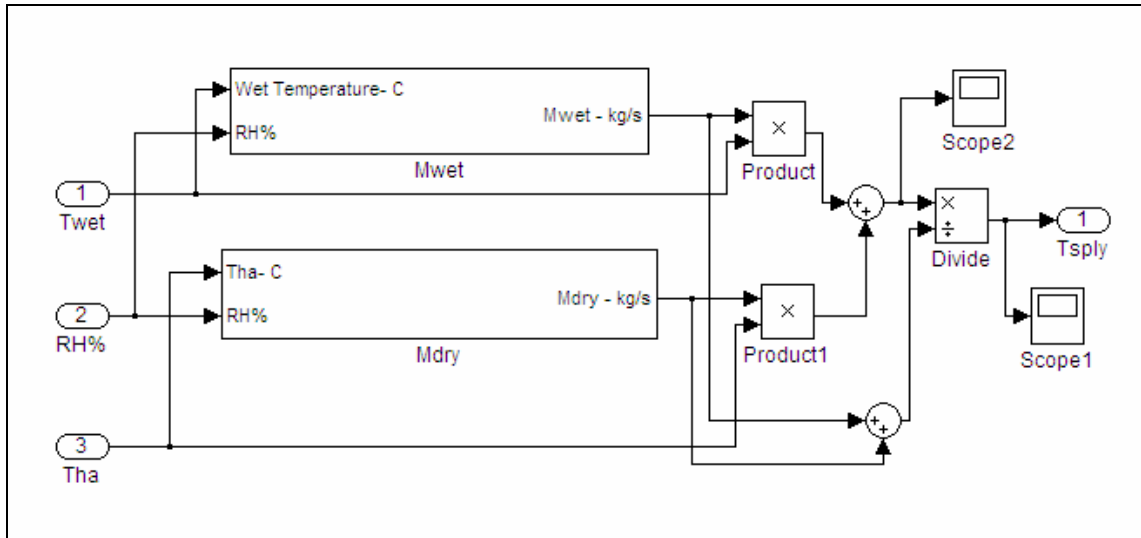


Figure 3-40 Supplied air temperature compartment

As can be seen from Figure 3-40, there are two variable inputs: T_{wet} and T_{ha} which vary over time during simulation and one constant input, $RH\%$, that does not change during simulation time. However, the setting of $RH\%$ alters the mass air flow rate of both the wet air and dry air as stated in equations (2.103) and (2.104) respectively. The density of the air will only be varied upon the variation of T_{wet} and T_{ha} since the added oxygen is considered to be disabled during the simulation.

A Simulink model is developed for each of the subsystems described above in Figure 3-40.

3.2.9.1 The Wet Air Mass Flow Rate Subsystem

For the wet air mass flow rate, M_{wet} the Simulink model is illustrated in Figure 3-41, and represents equations (2.99) and (2.103). The output M_{wet} (in kg/sec) represents the variation in the mass flow rate of the wet air that enters the hood. The variable input, T_{wet} changes the density of the wet air over time, whereas the $RH\%$ input varies the area of the opening of the wet air as demonstrated in Figure 3-22.

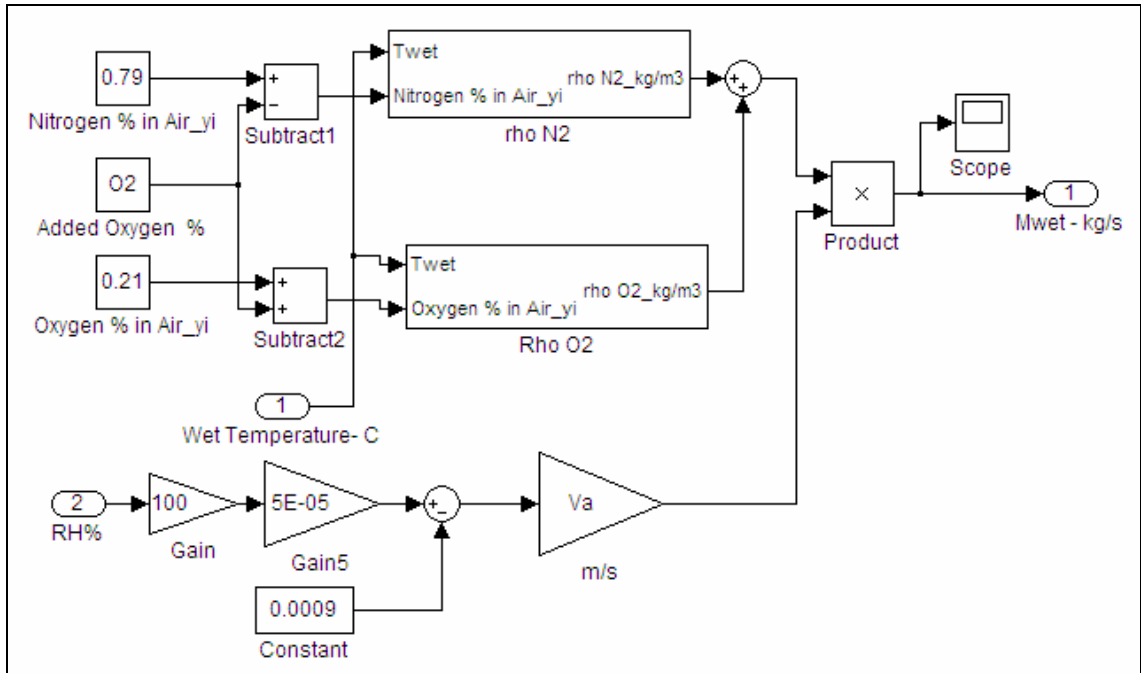


Figure 3-41 Wet air mass flow rate subsystem

Both subsystems of the N_2 and O_2 densities have already been stated in Figure 3-30 and Figure 3-31 respectively.

3.2.9.2 The dry air mass flow rate subsystem

The Simulink model of this subsystem is illustrated in Figure 3-42. It represents equations (2.100) and (2.104). The output M_{dry} (in kg/sec) represents the variation in the mass flow rate of the dry air that enters the hood. The variable input, T_{ha} , changes the density of the dry air over time, whereas the $RH\%$ input varies the area of the opening of the dry air as demonstrated in Figure 2-22.

Likewise, the subsystems of the N_2 and O_2 were previously detailed in Figure 3-30 and Figure 3-31 respectively.

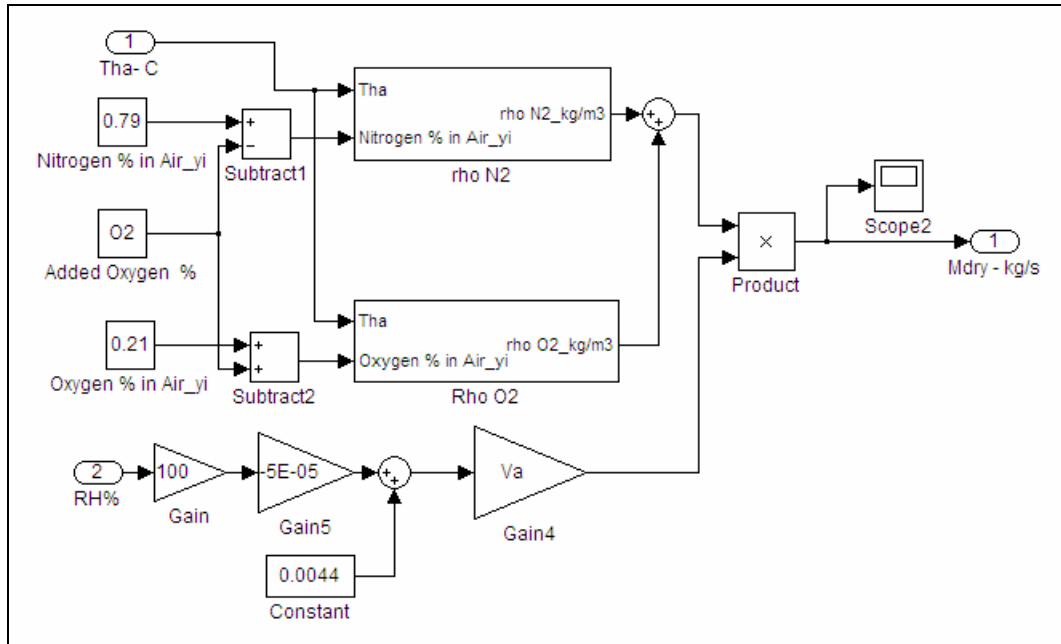


Figure 3-42 Dry air mass flow rate subsystem

Thus, sections 3.2.1 to 3.2.9 describe a completely detailed Simulink model of the infant-incubator system compartments (PLANT) as illustrated in Figure 3-3 with all the sub-systems associated with each compartment. All the compartments in Figure 3-3 can be contained in a sub-system called the open-loop system as shown in Figure 3-43.

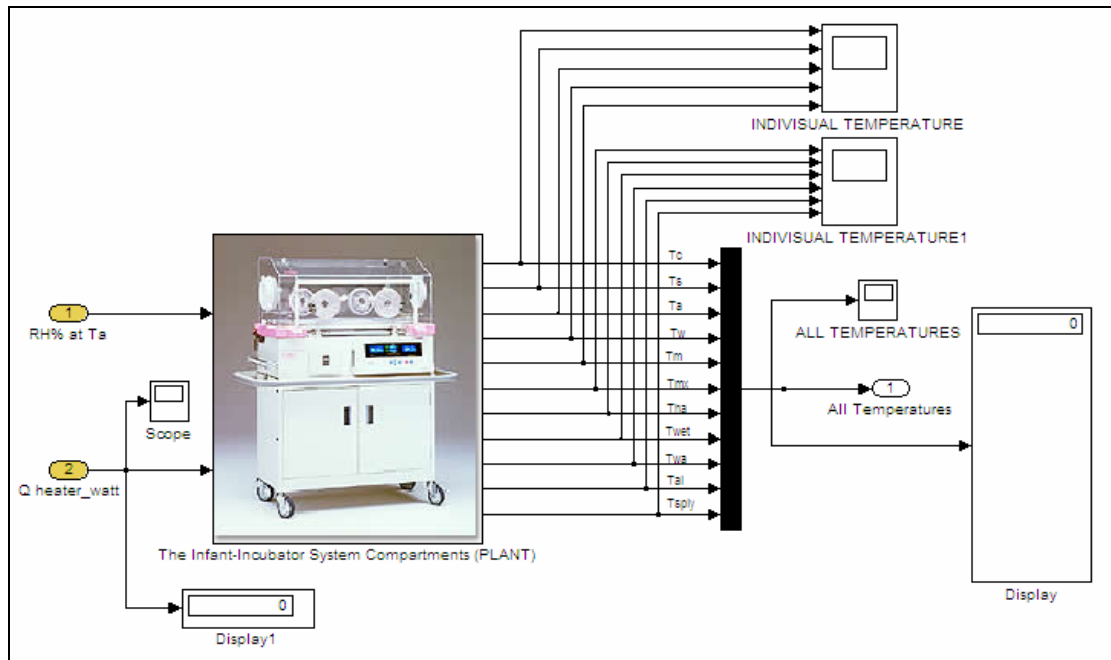


Figure 3-43 Open-Loop sub-system

The subsystem in Figure 3-43 has only two inputs: the heater power, Q_{heater} , (in Watts) which varies upon the variation in the feedback signal (i.e. the controlled temperature either skin or air mode) and incubator air relative humidity, $RH\%$, which is considered to be a constant parameter during simulation. The outputs are all final temperatures of the compartments demonstrated in Figure 3-3.

The input, Q_{heater} , in Figure 3-43 will be connected onto a feedback system with all related elements such as switches, comparator, feedback signal and compensator (controller) as shown in Figure 3-2 so that it can respond to the variation of the feedback signal and change the power ratings consequently. This process is called the temperature control process and will be described in detail in section 3.3.

3.3 Feedback System and Temperature Control

As it explained earlier (section 3.1), the infant-incubator system has two modes to provide a feedback signal - skin (T_s) and incubator air (T_a) modes, as shown in Figure 3-2. Each of these modes works independently, which means each mode has its own circuitry components, although they look similar in names and location in Figure 3-2 but they perform differently up on the requirements of each mode. Especially, the elements for the *PID* and the *Manual Switch* associated with each mode.

Since the parameters as well as the type of the controller element of the incubator ATOM V-850 are difficult to determine due to manufacturer confidentiality, also the control box of this incubator is sealed and thus it is impractical to extract the controller to determine its configuration, as this exercise may cause permanent damage to the entire electrical circuitry of the incubator.

Therefore, in this work it is assumed that the simulation model of this incubator ATOM V-850 has a PID type controller for each mode, skin and air. The PID controller provides a more convenient improved response to the feedback signal (i.e. T_s and T_a) in terms of fast rise time, minimised settling time and reduced oscillations [42]. Thus, the performance of the incubator is enhanced to the optimum.

The parameters of the PID system are virtual and selected using the Ziegler-Nichols method available in several control engineering textbooks such as, [43], [44] and [45]. However, in this work a modified Ziegler-Nichols method given by [41] is employed with some adjustments applied to the calculated values in order to obtain more desirable

outputs. Hence, the parameters for the PID controller of the air mode are different to those selected for the skin mode. These parameters will be given in the results chapter (Chapter 4).

The output signal from the PID represents the corrected (tuned) signal, and its magnitude varies upon the difference (the error signal) between the feedback signal (i.e. the final output temperature, skin (T_s) or air (T_a)) and the reference temperature input (i.e. the setting temperature, T_{set}). Then, this output signal passes with some time delay to the PLANT, which is essential to reflect the behaviour of the heater element in real world, although the exact value for ATOM V-850 is unknown, it is assumed to be 0.2 second. This PID output signal also represents the magnitude of the heater power that fluctuates from 0-260 Watts.

The purpose of the *Switch* and *Switch1* blocks shown in Figure 3-2, is to control the signal that passes out into the PLANT and varies between 0-260 Watts, only if the set up condition inside these blocks is satisfied. Furthermore, the *Multiport Switch* block shown in Figure 3-2 indicates the type of the control mode, this is to put 1 and 2 in the *CONTROL PORT* block in Figure 3-2 for the skin and air modes respectively.

The outputs represent the temperatures of all of the 11 compartments. The scopes in Figure 3-2 are to display the responses of the related signals.

3.4 Overall System Stability and Transfer Function

The overall system stability is verified using the Matlab function called Single Input – Single Output Tool, (or as ‘*Sisotool*’). *Sisotool* allows the analysis and tuning of feedback control systems and design of the compensator (controller) parameters.

The overall system stability is in terms of response of the input and the output to a step input applied onto the feedback system. In this work, the input to the system (i.e. the infant-incubator system) is the heater power that varies between 0-260 Watts and the output is the controlled temperature of each mode (i.e. the skin and air temperatures).

An open-loop Simulink model is developed for each mode (skin and air) as shown in Figure 3-44 and Figure 3-45, respectively. This developed model includes all 11 compartments of the infant-incubator system mentioned in the previous sections but with only a single input and output.

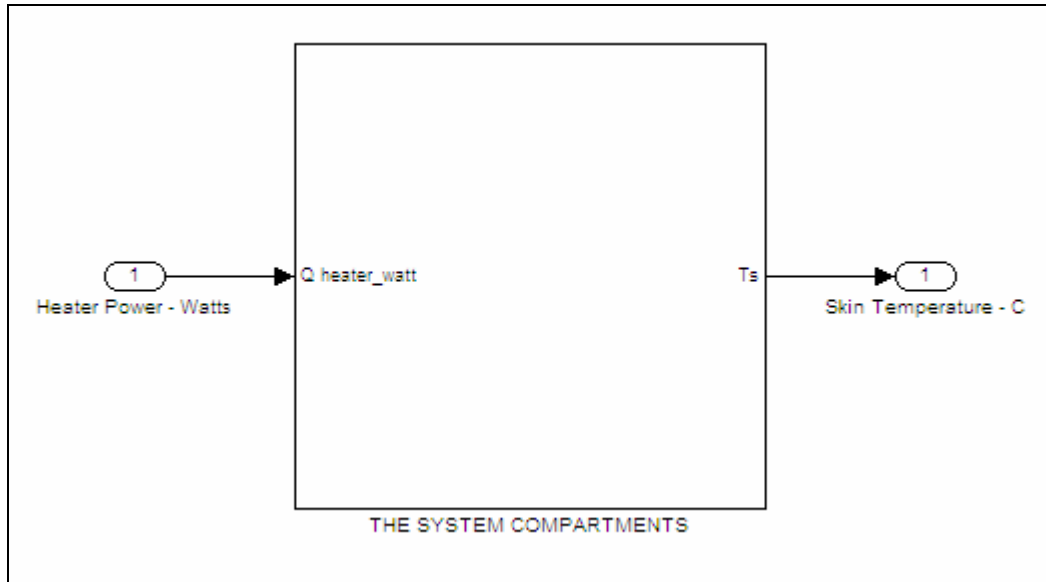


Figure 3-44 Sisotool Simulink Model-Skin Mode

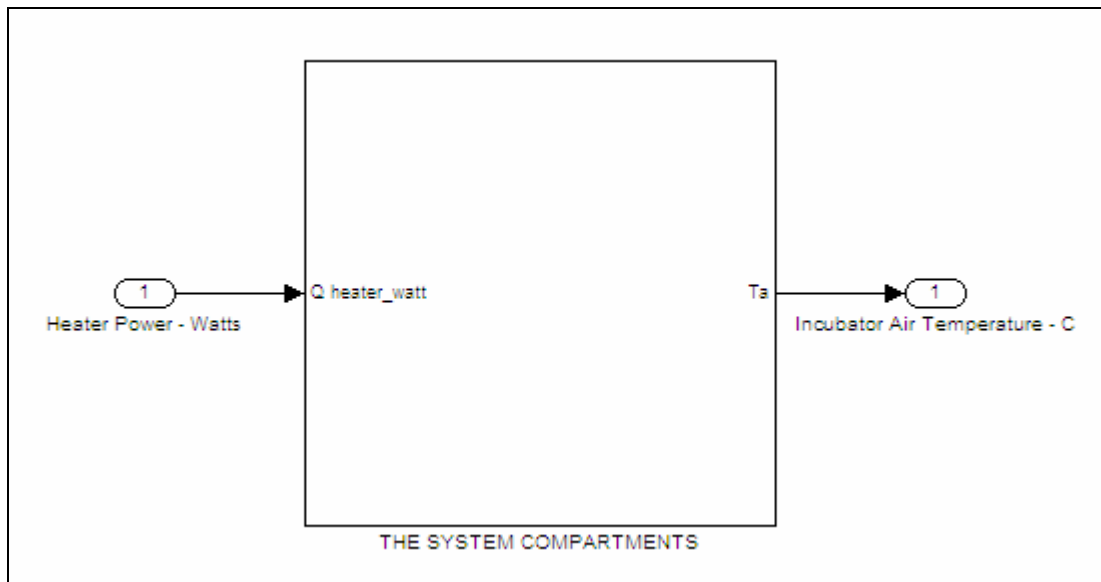


Figure 3-45 Sisotool Simulink Model-Air Mode

The subsystem box shown in Figure 3-44 and Figure 3-45 has the same compartments as previously illustrated in Figure 3-3 but the RH% is set as a constant 0.8 and the outputs are reduced from 11 temperatures into one single temperature, T_s and T_a

Code was written (see Appendix 1) for each mode (skin and air) to linearize the Simulink model and to convert it into a state-space model consistent with the following formulae [45]:

$$\frac{dx}{dt} = Ax + Bu \tag{3.1}$$

$$y = Cx + Du \tag{3.2}$$

where A, B, C, and D are matrices of appropriate dimensions, x is the state vector, and u and y are the input and output vectors .

The open-loop Simulink model for each mode is compiled within the *Sisotool* and the results displayed in the SISO window. The displayed results are analysed using a root locus editor and open-loop bode editor as shown in Figures 3-46 and 3-47 for the skin and air modes respectively. As shown in Figure 3-46 and Figure 3-47, the open-loop system stability is verified. At this stage, neither the compensator or reference input is considered.

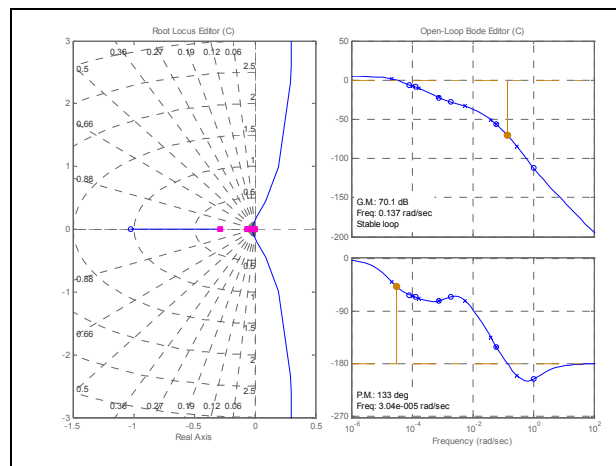


Figure 3-46 SISO Window- Skin Mode/open-loop

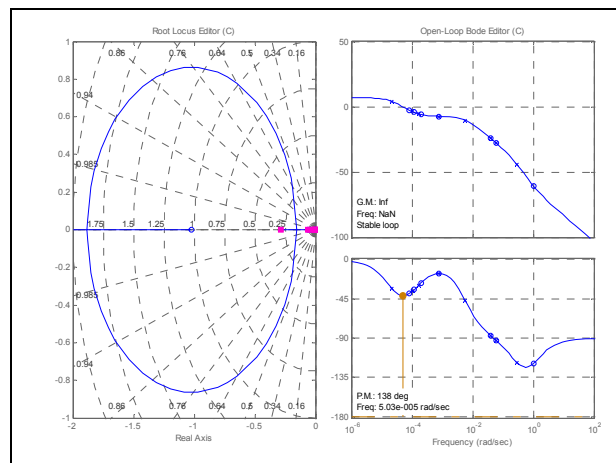


Figure 3-47 SISO Window-Air Mode/open-loop

Using the available features in the *Sisotool* window, the transfer function of the open-loop model for each mode can be generated based on the parameters A, B, C and D

defined in equations (3.1) and (3.2). both modes have proven to be continuous-time models and the transfer functions are in Zero/Pole/Gain format, as follows:

For the Skin Mode, the transfer function is:

$$\frac{1.8862e-006(s+1.021)(s+0.06054)(s+0.001944)(s+0.0007812)(s+0.0001291)(s+8.294e-005)}{(s+0.2871)(s+0.0605)(s+0.04003)(s+0.005754)(s+0.0007712)(s+0.0001649)(s+0.0001025)(s+2.188e-005)}$$

and the transfer function for the Air Mode is:

$$\frac{0.00068991(s+1.021)(s+0.06054)(s+0.03987)(s+0.0007739)(s+0.0001951)(s+0.0001195)(s+8.294e-005)}{(s+0.2871)(s+0.0605)(s+0.04003)(s+0.005754)(s+0.0007712)(s+0.0001649)(s+0.0001025)(s+2.188e-005)}$$

For the closed-loop analysis for each mode, which includes the design and tune of the compensator parameters. We first choose the parameters for the reference input, T_{set} , and the feedback sensor, then we determine the performance responses of the input and output of the infant-incubator system (i.e. the PLANT) by applying a step input. *Sisotool* can implement the following:

For the skin mode, in the SISO window, the feed forward input is chosen to be 36 to represent the skin temperature, whereas the sensor dynamics is set to 1. Thus, a Simulink model in terms of LTI (linear time-invariant) blocks for the entire closed-loop system can be generated from the SISO window as shown in Figure 3-48. Thus, from the MATLAB/workspace window, the transfer functions of each of LTI block shown in Figure 3-48 can be determined in Zero/Pole/Gain format as follows:

For the F_{SKIN} block, the transfer function is: 36.5

and the transfer function of the C_{SKIN} block is:

$$\frac{2.2335 (s^2 + 160s + 9.64e004)}{(s^2 + 160s + 2.89e004)}$$

while for H_{SKIN} block, the transfer function is: 1

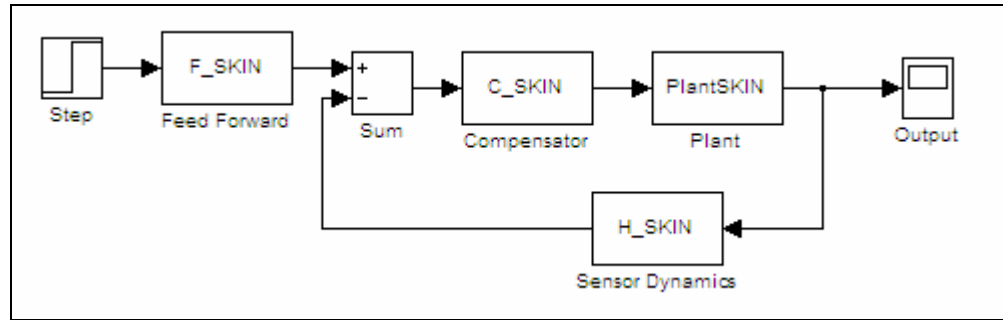


Figure 3-48 Simulink Model-LTI Blocks-Skin Mode

However, the transfer function for the *PlantSKIN* block is as for the open-loop/Skin Mode which has been stated earlier. As shown in Figure 3-48, a step input is applied onto the entire closed-loop system, the output is illustrated in Figure 3-49.

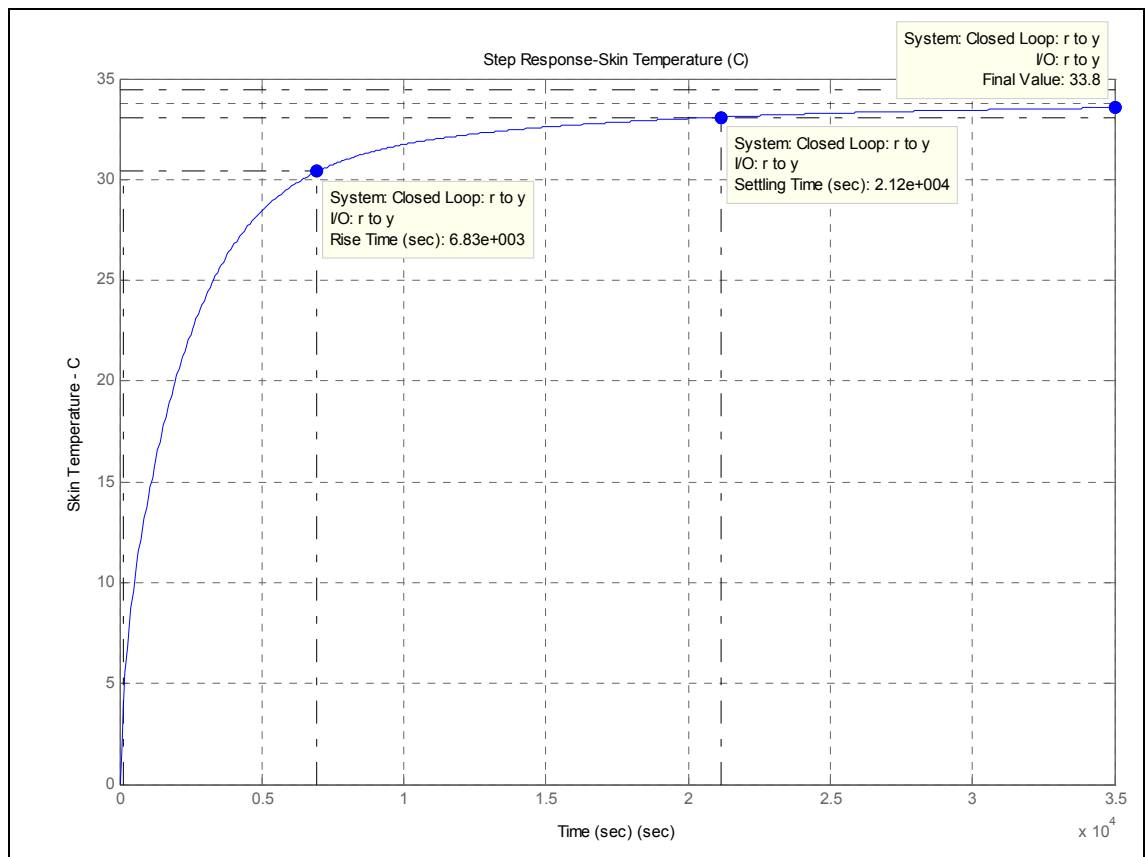


Figure 3-49 Step Response-Skin Temperature/closed-loop

and the step response of the input signal (i.e. post the compensator) that flows to the *PlantSKIN* is demonstrated in Figure 3-50. This signal represents the oscillation of the heater power between 0-260 watts upon the variation of the output temperature (skin temperature).

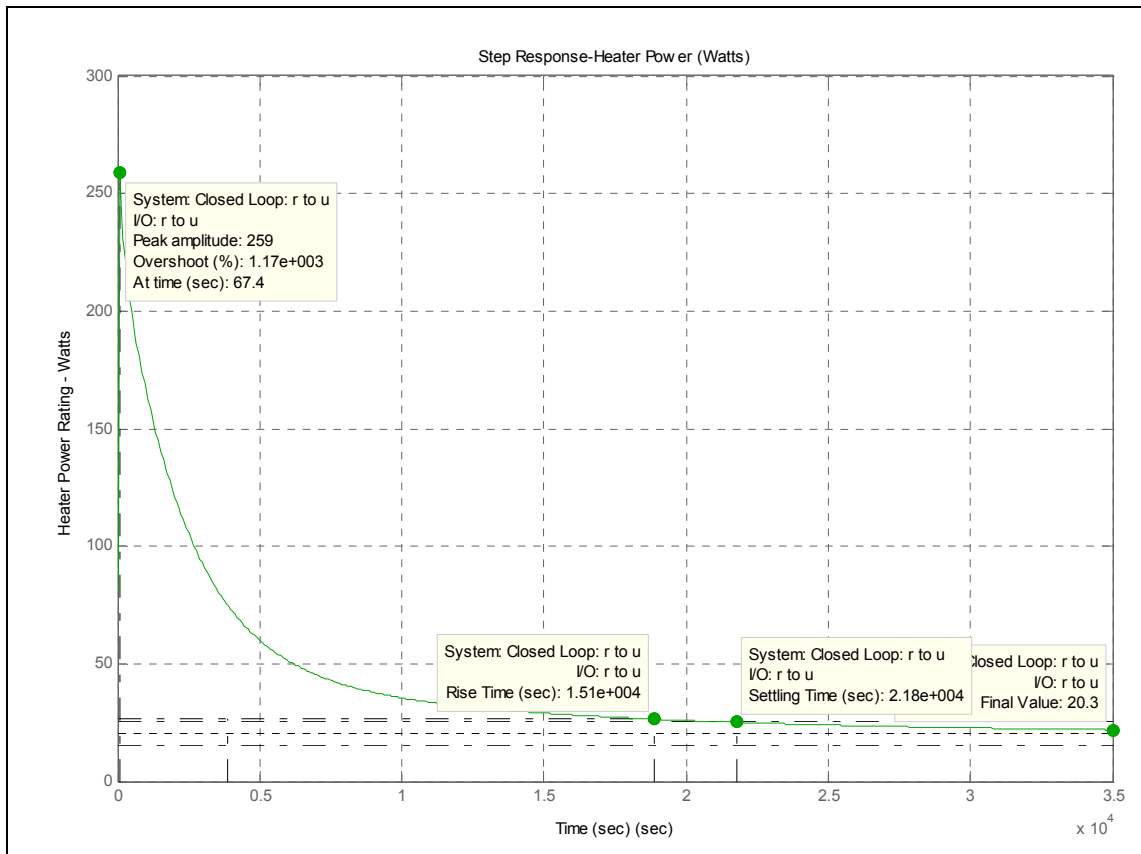


Figure 3-50 Step Response - Heater Power/Skin Mode/closed-loop

The stability of this closed-loop system after adding the new parameters in the SISO window for the feed forward and compensator tabs, as well as tuning the compensator in order to determine the desired outputs, has maintained as it was for the open-loop system. This is illustrated in Figure 3-51.

Similarly, for the air mode, the same procedures followed for the skin mode are applied again but with the following considerations:

The feed forward input is chosen to be 37 to represent the incubator air temperature, whereas the sensor dynamics is also set to 1, and appropriate parameters for the compensator are selected in terms of Zero/Pole/Gain format. Thus, a Simulink model in terms of LTI (Linear Time-Invariant) blocks for the entire closed-loop system can be generated from the SISO window as in Figure 3-52. From the MATLAB/workspace window, the transfer functions of each of LTI blocks shown in Figure 3-52 can be determined in Zero/Pole/Gain format as follows:

For the F_{AIR} block, the transfer function is: 37

and for H_SKIN block, the transfer function is:1

while the transfer function of the $C-AIR$ block is:

$$6.9252 (s^2 + 160s + 9.64e004)$$

$$(s^2 + 160s + 2.89e004)$$

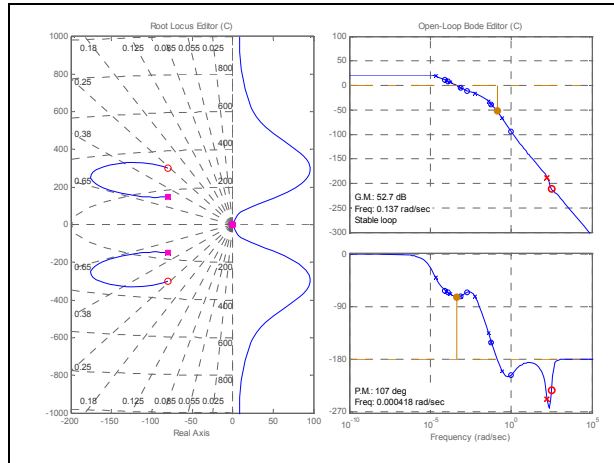


Figure 3-51 System Stability-Skin Mode/closed-loop

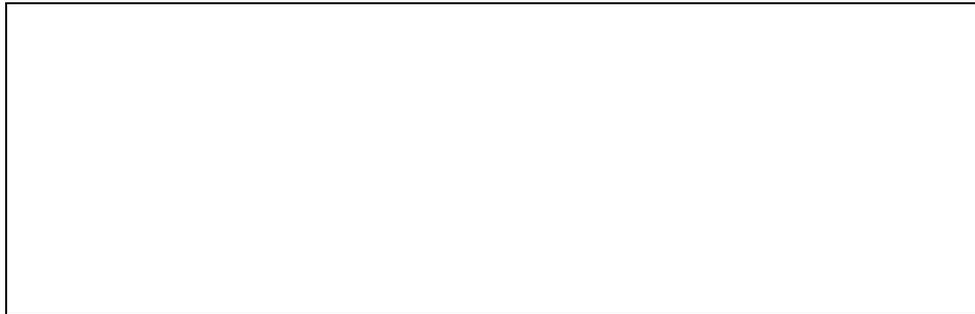


Figure 3-52 Simulink Model-LTI Blocks-Air Mode

Also, the transfer function for the $PlantAIR$ block is as for the open-loop/AIR Mode which has been stated above earlier. Thus, the response of a step input applied onto the entire closed-loop system is illustrated in Figure 3-53. And the step response of the input signal (i.e. post compensator) that flows to the $PlantAIR$ is demonstrated in Figure 3-54. This signal represents the oscillation of the heater power between 0-260 watts upon the variation of the output temperature (incubator air temperature).

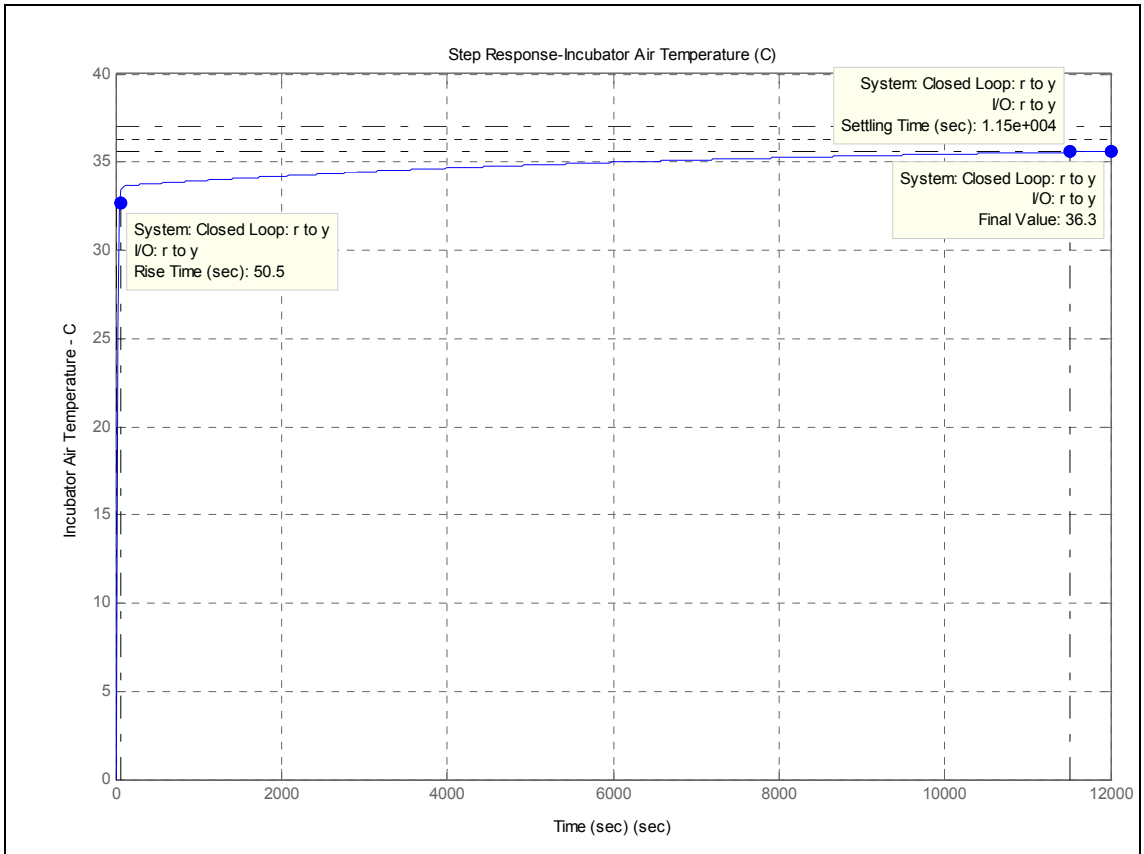


Figure 3-53 Step Response-Incubator Air Temperature/closed-loop

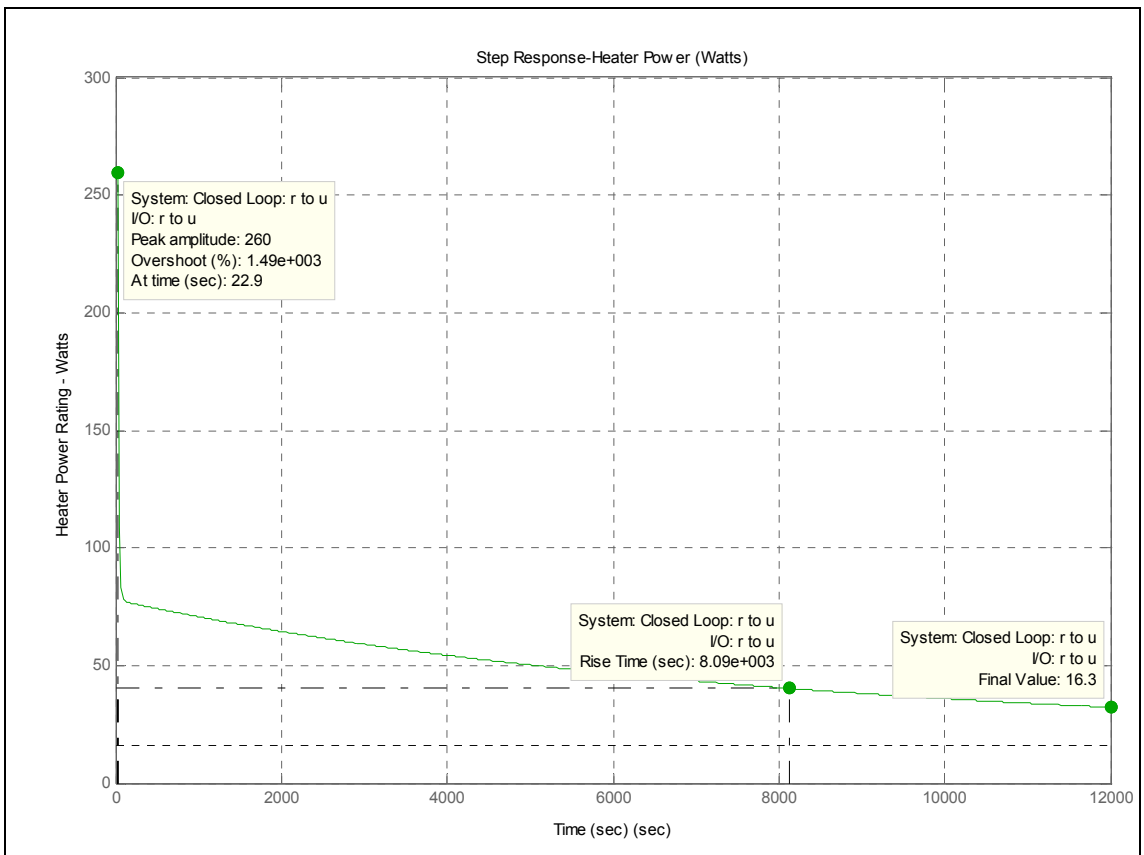


Figure 3-54 Step Response - Heater Power/Air Mode/closed-loop

Likewise, the stability of this closed-loop system after adding the new parameters in the SISO window for the feed forward and compensator tabs, as well as tuning the compensator in order to determine the desired outputs, has maintained as it was for the open-loop system. This is illustrated in Figure 3-55.

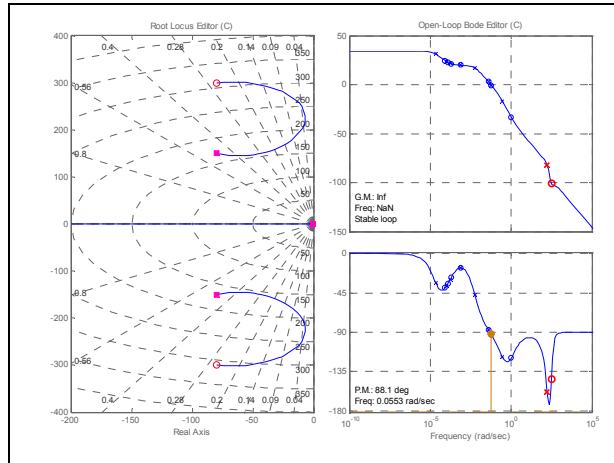


Figure 3-55 System Stability-Air Mode/closed-loop

Thus, section 3.4 has thoroughly demonstrated from control engineering perspective the advantage of using *sisotool* to design, analyse and tune of a feedback system. This is consistent with the nature of this work since the infant incubator is a feedback system.

Chapter 4 Results and Validation

4.1 Introduction

The computer simulation model of the infant-incubator system developed in the MATLAB[®]/Simulink environment provides numerous quantitative results such as the final temperatures for each compartment (i.e. 11 compartments in this work), as well as other results for each subsystem blocks of each compartment. These include the heater power rating, PID responses and the heating energy rates of radiation, convection and evaporation.

In this chapter, the simulation results for the skin and air modes will be presented. These results will be for an infant of 900 grams birth weight and a gestational age of 28 during the first day of life. Other details and initial conditions that are related to both modes will also be illustrated. Examples of these include the PID settings (i.e. PID parameters) that provide the most desirable outputs, time for simulation, and temperature settings for air and skin modes.

The simulation results will be validated against available clinical empirical data in literatures in terms of the pattern of temperature fluctuations for both infant body and environment. Extra results for air and skin modes are included in the Appendix 2 and 3 respectively. [for the heat exchange relationships and feedback signal outputs such as, convection, conduction, radiation, evaporation heat energy, and PID tuning signals].

The validation process will consider the final temperatures of the three compartments of infant-incubator system. These are the infant core, infant skin and incubator air space, as the performance of the compartments is a popular measure described by other authors [3, 4, 8, 10, 11, 17, 19, 22-27].

The initial conditions and parameters given for the Simulink model are not identical with those described in the literature, because each clinical study (literature) is designed for a particular set of conditions in order to achieve its goals. This includes specific parameters and characteristics for the incubator and the infant. Thus, in this work, the initial conditions that are set for the Simulink model will be taken from those described in the literature. This process disregards the incubator brand (other than ATOM V-850) and its parameters, the characteristics of study infants (i.e. gender, birth weight, core

and skin temperatures at admission, gestational and postnatal age), the setting temperatures for each mode (skin/air modes) and finally, with or without added humidity.

However, this model will strongly consider the type (mode) of the feedback system described in the literature, whether skin or air modes, as this is essential in determining the performance of the Simulink model.

4.2 Initial Conditions

The initial conditions for the infant-incubator system for both modes (air and skin) are defined in an M-file given in Appendix 1. This M-file is linked with the Simulink model and set to pre-load all variables and parameters in the Matlab view port, as well as implement some mathematical calculations for the equations defined in the file (e.g. Nusselt numbers for convective heat transfer coefficients related to different compartments within the system before the Simulink model starts).

The initial incubator air temperature, T_{ai} , is chosen to be 37 °C, because the current practice in nursing preterm infants in incubators is to preheat the incubator prior to placing an infant inside it. Thus for both skin and air modes, the incubator is preheated to 37 °C with added humidity of 80% [3, 4, 10]. This temperature (37 °C) also represents the incubator temperature setting, T_{set} , for air mode in the Simulink model.

The operative (neutral) temperature determined by LeBlanc [18] for a 900 grams, 26 weeks gestational age is 37.2 °C, and thus the estimated air temperature (i.e. incubator temperature setting, T_{set}) inside the incubator would be 38.2 °C (as it previously discussed in section 1.1.2 (page 2)). This is outside the temperature range, however a 25-38 °C given by the manufacturer of this incubator (ATOM). Therefore, the selected 37 °C for air mode is justified. Whereas, for skin mode, the T_{set} is set to 36.5 °C, as this is more appropriate for preterm infant with very low birth weight as recommended by other authors [17, 19, 23-25, 27, 46].

The parameters for the PID controller for each mode are virtually set by applying Ziegler-Nichols method [41] for several attempts until desirable (i.e. stabilised) outputs are achieved in two hours simulation time, these selected values as follows:

- Air mode:

$$P = 10, I = 0.9, D = 100$$

- Skin mode:

$$P = 30, I = 0.007, D = 0.0$$

For the sake of validation processes, the simulation time for both modes is set to be two hours (7200 seconds) since most clinical empirical results, in particular, the fluctuated performance in skin and core temperatures are recorded from zero up to eight hours. Within two hours fluctuations in trends of infant body and incubator air temperatures can be stabilised, and thus the performance of the whole system can be determined. Furthermore, the two hour time in incubator is vital to determine the improvement in infant body temperature to reduce the mortality rate.

4.3 Results

The Simulink model is run separately for each mode and the following results are generated:

4.3.1 Air Mode Results

The following results are for the temperatures of the infant core and skin and the incubator air space:

4.3.1.1 Incubator Air Temperature, T_a

The fluctuation in the incubator air temperature is illustrated in Figure 4-1. Initially, the air temperature drops to around 36.52 °C, which is below the set temperature of 37 °C. It rises rapidly again in a very short time at around 100 seconds. However, a constant fluctuation in the incubator air temperature is continued at a range of 37 ± 0.003 °C until the end of simulation time.

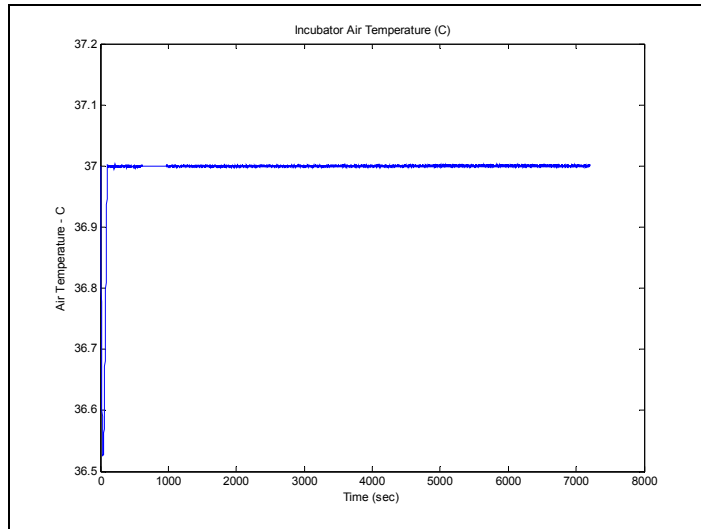


Figure 4-1 Incubator air temperature variation vs. time

The fluctuation pattern in the incubator air temperature is shown in Figure 4-1, particularly, after 100 seconds. This is clearer in Figure 4-2 given by Chessex [17], although the air temperature setting is 34.8 ± 0.6 °C for a double-walled incubator.

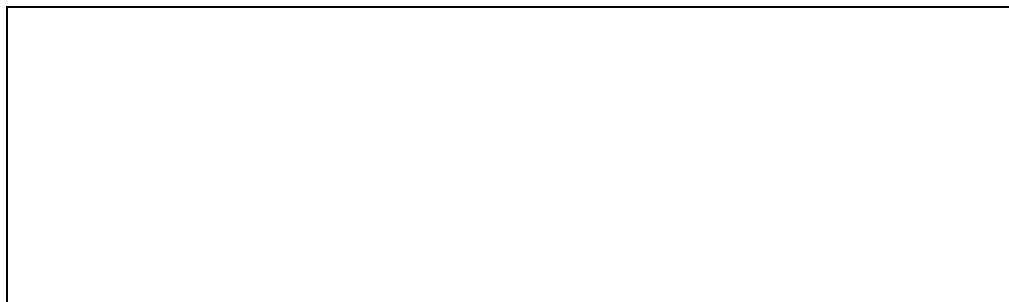


Figure 4-2 Operative temperature of Air Shields C-100 under air servo control (33.8 ± 0.1 °C), A 2-minute incubator opening (*) was performed after 3 hours of recordings [17]

According to the specification of the ATOM V-850 incubator, the fluctuation in the setting temperature is between +1.5 and -3.0 °C in 0.1 steps and thus the ± 0.003 °C fluctuations in the setting temperature of the Simulink model is well within the range given by the manufacturer of this incubator. It can also be said that the Simulink model provides a stabilised thermo-regulated environment, as the incubator air temperature is maintained along the simulation time and this is attributed to the virtual parameters chosen for the PID controller.

4.3.1.2 Infant Core and Skin Temperatures, T_c , T_s .

Figure 4-3 and Figure 4-5 demonstrates the variation of the infant core and skin temperatures respectively, and both are initially set at, 35.5 °C. The core temperature is steadily risen to 36.02 °C from its initial value.

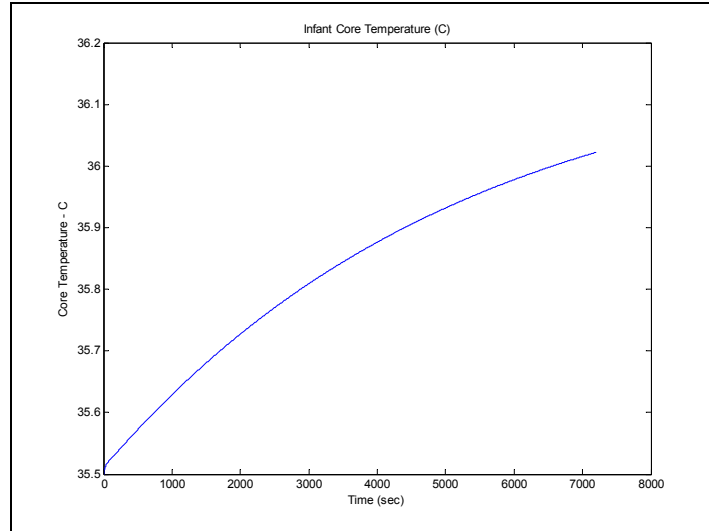


Figure 4-3 Infant core temperature variation vs. time

This core temperature is comparable to the averages of empirical clinical findings reported for preterm infants with gestational age 29 ± 2 weeks and birth weight < 1000 grams [11, 17]. A value of 36.6 ± 0.3 °C (achieved in double-walled incubator) in a four hour period after birth is given by Chessex [17]. For term infants at around 34.4 °C the incubator air temperature at approximately 50 % RH, the core temperature reaches 36.2 ± 0.23 °C in two a hour period [11].

Figure 4-4 given by Miller [11], illustrates the fluctuations in the core temperature for a term infant nursed in incubator with 50% RH. As it can be seen, the core temperature falls rapidly from 37 °C (in our case 35.5 °C) to below 36 °C during the first hour of incubation. Thereafter, it returns to the lower limits of normal level, 36.5 °C, at 3¼ hours. Thus, it can be inferred that the core temperature improved by 0.5 °C in approximately 2¼ hours. This outcome is consistent with the simulation in Figure 4-3, as the margin between the initial and final values of core temperature over two hours simulation is 0.52 °C.

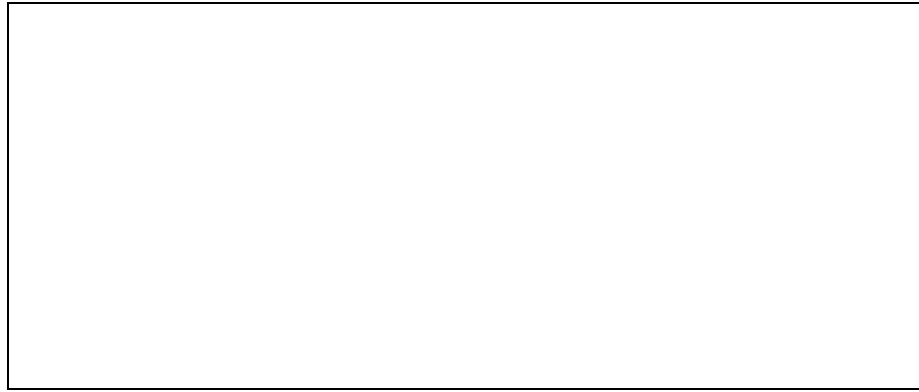


Figure 4-4 Mean core temperature of normal infants during the first 8 hours of postnatal life [11]

The skin temperature (Figure 4-5) falls rapidly to 35.21 °C in 85 seconds, but rises again into 35.67 °C as a final temperature at the end of 2 hours simulation. This is slightly higher than the initial value 35.5 °C.

This final temperature of the skin is similar to the averages of empirical clinical results reported in [3, 11, 17, 26], as 35.9 ± 0.86 °C, 35.8 ± 0.1 °C, and 35.9 ± 0.2 °C respectively. Also, Michael *et al* [3] has reported that the percentage of skin temperature readings in 0-2 hours that are < 36 °C is almost 38%. All these findings were for preterm infants < 1000 grams birth weight nursed in double-walled incubator.

Moreover, for preterm infants < 1000 gram birth weight covered by a plastic sheet and nursed in humidified incubator (80% RH), the percentage of time during the first day of life when the average skin temperature < 36.3 °C is 12.2 % [4].

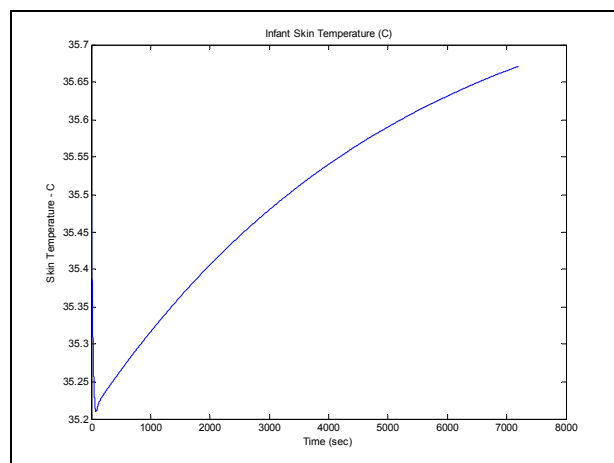


Figure 4-5 Infant skin temperature variation vs. time

From Figure 4-6 (determined by Miller [11]), it can be seen that the skin temperature fell rapidly below the core temperature during the first 30 minutes. However, it rises to

35.15 °C in two hours approximately which is less than the simulation result of 35.67 °C, and after six hours reached around 35.60 °C.

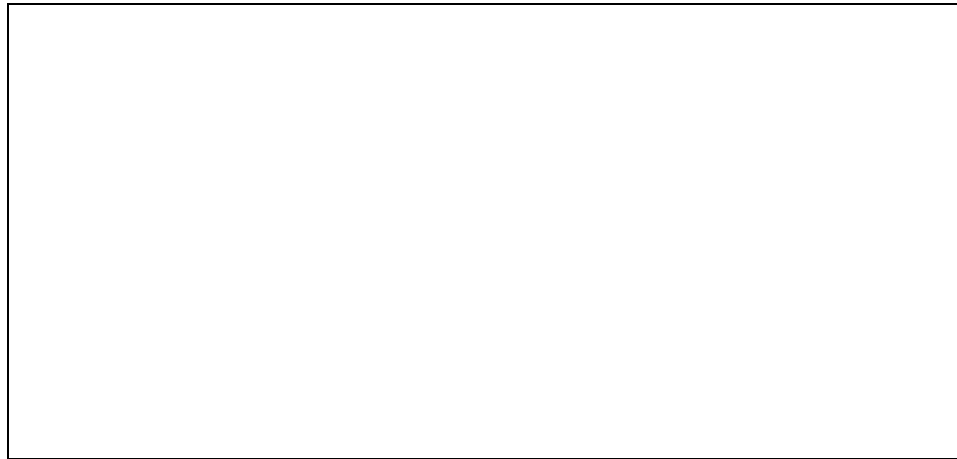


Figure 4-6 Comparison of mean core and abdominal skin temperatures after birth [11]

From Figure 4-6, the margin between the core and skin temperatures is in the range of 0.1 - 0.4 °C, below core temperature [11]. This is comparable to our simulation results for the core and skin temperatures shown in Figure 4-3 and Figure 4-5, as the difference between the final temperatures is 0.35 °C below core temperature. Thus, the performance of our Simulink model under air servo control is satisfactory.

4.3.2 Skin Mode Results

Similarly, the following results are for the temperatures of the infant core and skin and the incubator air space:

4.3.2.1 Infant Core and Skin Temperatures, T_c and T_s

Figure 4-7 illustrates the variations in core temperature which is increased from 35.5 °C into around 36.87 °C over a two hour period. This final value of core temperature is in agreement with the averages of the empirical clinical results reported in [22-25, 27], as 36.9 ± 0.1 °C , 37, 36.7 ± 0.2 °C, 36.2 ± 0.2 °C and 36.9 ± 0.11 °C respectively.

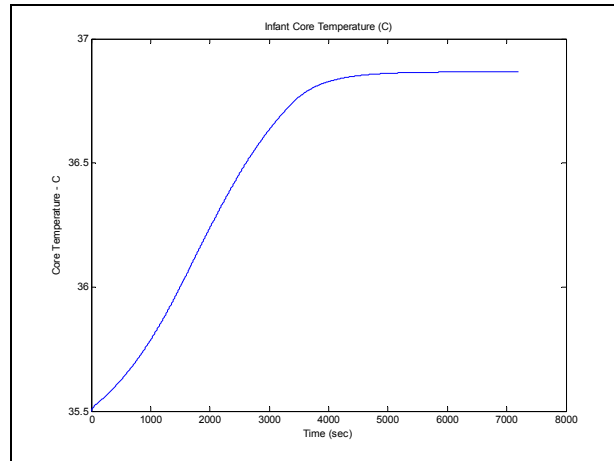


Figure 4-7 Infant core temperature variation vs. time

These clinical values are averages values however were measured for preterm infants nursed in different brands of single-walled incubators set at 36.5 °C on skin servo control. The gestational age ranged from 28-40 weeks and birth weight ranged from < 1000 up to 3800 grams, whereas postnatal age ranged from 1-30 days. The ambient relative humidity level, $RH\%$, ranged from 26-35% without added water for humidification.

Moreover, the core temperature reported by LeBlanc [8] as 36.93 ± 0.08 °C is also consistent with our simulation result of 36.87 °C. In his study, the infant is nursed in a single-walled incubator for period of 82 minutes, with skin servo control set on 36 °C instead of 36.5 °C. The $RH\%$ was $75.9\% \pm 1.6$, infant birth weight ranged between 750-1595 grams, gestational age 26-35 weeks and the age ranged from 6-49 days.

Another clinical result reported in [10], is slightly less than the simulation result of 36.87 °C. This suggests that the core temperature for an ill infant in the first day of life with a 900 grams birth weight and 28 weeks gestation age is 36.6 °C, when is nursed for duration of 34 hours in a humidified single-walled incubator ($RH\% \geq 70\%$) with skin servo control set on 36 °C.

There are also some other results that are comparable to the simulation results, but these are achieved in double-walled incubators with the skin temperature servo control set on 36.4 °C instead of 36.5 °C. The reported results are 36.6 ± 0.2 °C and 36.7 ± 0.3 °C [17]. The characteristics of the infant study are similar to those stated in section 4.3.1.2.

Figure 4-8 illustrates the variation in skin temperature over a period of two hours. The temperature rapidly drops slightly below 35.27 °C from the initial value 35.5 °C in less than 85 seconds, and then gradually rises to the set point of 36.5 °C in 57 minutes. Afterwards, the fluctuation remains constant at a range of 36.5 ± 0.01 °C.

Thus, this final temperature 36.5 °C is reached into the required level of thermo-neutral environment shown in Figure 1-2, in 57 minutes approximately.

This final reading represents the temperature of the skin where the thermistor probe is taped on infant skin. This is usually on the abdomen area, and does not indicate the infant mean skin temperature.

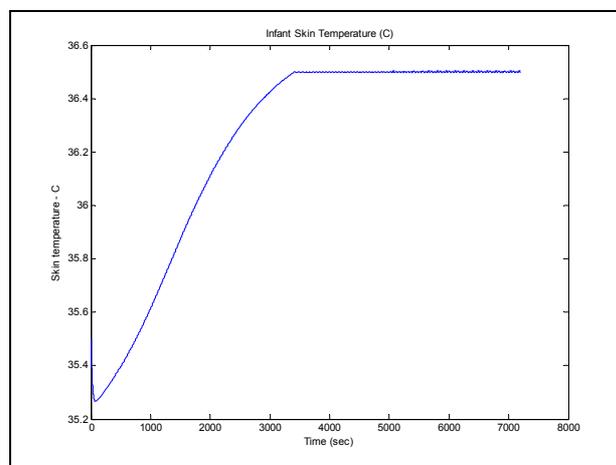


Figure 4-8 Infant skin temperature variation vs. time

Similarly, as for the core temperature described above, the final reading of the skin temperature is in agreement with the clinical empirical findings reported in [22-25, 27], as 36.4 ± 0.2 °C, 36.6 ± 0.2 , 36.3 ± 0.1 °C, 36.5 ± 0.1 °C, 36.4 ± 0.18 °C respectively.

The pattern of skin temperature fluctuations in single-walled incubator with $RH\% \geq 70\%$ reported in [8] and [10] is 36.04 ± 0.03 °C and 36 ± 0.3 °C respectively, when the skin servo control is set to 36 °C. This is comparable to the pattern of the simulation result of 36.5 ± 0.01 °C, although the setting temperature is 36.5 °C. Likewise, the fluctuations in skin temperature determined in double-walled incubator [17] is 36.3 ± 0.2 °C and 36.4 ± 0.4 °C which is also comparable to the simulation result despite the skin servo control being set to 36.4 °C.

Lastly, the margin between the final values of core and skin temperatures under skin mode is 0.37 °C below core temperature. This is in agreement with the range determined by Miller [11] which is 0.1 - 0.4 °C.

4.3.2.2 Incubator Air Temperature, T_a

Figure 4-9 represents the fluctuations in the incubator air temperature over two hours. The temperature rapidly increases to 40.53 °C in 33 minutes and then drops to below 39 °C. After the 1st hour, the temperature keeps dropping steadily to below 37.85 °C at the end of the simulation time. Nevertheless, the trend of the incubator air temperature indicates that it continues to drop after 90 minutes at a constant rate of 1.06×10^{-03} °C/min.

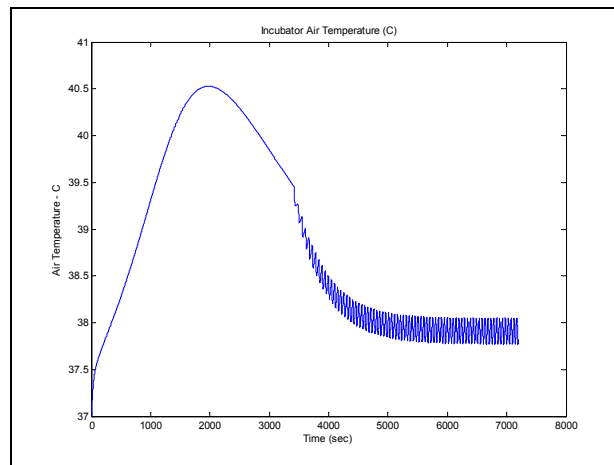


Figure 4-9 Incubator air temperature variation vs. time

The final value of 37.85 °C is significantly higher than the normal range of the incubator air temperature reported in most empirical clinical literatures [8, 10, 17, 19, 22-25, 27]. For single and double-walled incubator, this is between 30.2 – 37.4 °C, whether the temperature setting is 36 or 36.5 °C, with or without added humidity.

This difference between the simulation result and the clinical records can be attributed to the selected parameters of the PID, as they manipulate the performance of the whole system and consequently the outputs. For the sake of this project, the PID parameters were selected to provide the best outputs in the shortest time.

Based on the rate of temperature decreases given above, 1.06×10^{-03} °C/min however, it can be predicted that the incubator air temperature will be reduced to 37.34 °C after approximately eight hours. Thus, the incubator air temperature can be compromised

since the maximum limit given in the literatures, 37.4 °C, is achievable with a longer time than two hours.

In addition, the final value of 37.85 °C as well as the maximum value 40.53 °C is still relatively within the range of the incubator air temperature given by the manufacturer, which is between 20 - 40 °C. Thus, the overall performance of the Simulink model under skin mode is satisfactory.

4.3.3 Other Outcomes

It is worth noting that the coefficient of heat transfer for the infant (i.e. the cylinder), h_{scv} , is found to be 4.255 W/m².°C, which is consistent with the estimated values reported in [18, 46] which ranged from 4 - 5.4 W/m².°C.

Finally, other outcomes that are related to the air and skin modes, demonstrated in Appendix 1 and 2 respectively. These include the heat energy relationships, final temperatures of the other compartments, heater power I/O signals, PID I/O signals, and incubator air mass.

Chapter 5 Discussion

5.1 Introduction

This is the first detailed, comprehensive simulation model of infant-incubator-feedback system with a humidification process. The infant-incubator system incorporates the thermodynamics interactions between an infant and the environment provided by the incubator. The model considers the feedback systems used in most incubators, (air and skin servo controls) with a PID controller integrated in the circuitry.

Assumptions are made wherever needed in order to simplify the modelling processes for both the infant and the incubator. Furthermore, with the large number of parameters involved in the modelling procedures, not all of them are well documented and judgment is used to specify the parameters values not found in literatures (this includes physiological data related to infants e.g. blood flow rate parameter and inspired minute volume due to breathing).

The results of the simulation model using these parameters are validated against empirical clinical data available in the literature, in terms of the pattern of the fluctuations of the infant's compartments temperatures and incubator air temperature over 2 hours simulation. Both air and skin modes were tested and the results are in a good agreement with the published data.

5.2 Infant Modelling

The infant model is represented as one-lump with two compartments, core and skin. It can be modelled as four-lumps, (head, trunk, upper and lower limbs) as described in section 2.3.2. The geometry of the infant is also approximated to a cylinder in order to easily determine the overall heat transfer coefficient, h_{sev} .

The model includes the physics of heat exchange within the infant compartments (i.e. core and skin) and between the incubator compartments, in terms of conduction, convection, radiation and evaporation.

In contrast with other works, the metabolic heat production of the infant core in terms of W/m^2 is estimated at resting and not on basal metabolism as W/kg . This provides more

accuracy and reality to our model, due to the fact that the basal metabolic rate can be measured only after overnight fasting and this is ethically unacceptable for the neonate [32]. Furthermore, basal metabolic rate for a neonate at birth at resting is not well documented.

In this work, and since there is no standard available in literatures for infant length and weight versus birth weight or gestational age, the surface area of the infant is determined using a formula that depends only on the infant weight rather than weight and length. This estimation reduces the parameters required for the Simulink model to be used unconditionally without knowing a neonate's length.

5.3 Incubator Modelling

The incubator used in this work is a single-walled ATOM V-850 with humidification chamber manufactured in Japan and provided by Fisher and Paykel Healthcare Ltd.-Auckland. It has both air and skin feedback systems.

The incubator model developed in this work incorporated all compartments including the, incubator air space, mattress, incubator walls, air circulating fan, heating element and the water container with the aluminium-finned block inside it for humidification purposes. The model includes the heat transfer interactions between the infant and its surroundings environment (i.e. incubator inside), as well as the heat exchange relationships between the external walls of the incubator and the nursing room.

The mechanism of the feedback system developed for the Simulink model differs from those described in previous works, as the heater responds instantly to the variation magnitude in the controlled temperature (i.e. air or skin temperatures) changing its rating power between maximum and minimum limits over the simulation time. This process is implemented via PID controller. Whereas, in previous works, the heated air temperature that enters the hood is set to a constant value while the fan varies the amount of the air flow rate upon the variation in the controlled temperature by an on-off logic control system (i.e. zero to maximum).

5.4 Feedback System and Overall Stability Performance

Since the infant-incubator system is a closed-loop system, a PID controller element is needed to compensate the variation magnitude of the feedback signal. Using the

modified Ziegler-Nichols method, virtual parameters for the PID controller, for both air and skin modes, are chosen since the real values are unknown due to manufacturer confidentiality. In this work, the selected parameters are set to generate the optimum desired outputs that are so close to the empirical clinical outcomes in literatures.

Moreover, theoretical analysis of the overall system stability, which has not previously been investigated in other works, is verified using the SISOTOOL function available in MATLAB[®]/Simulink environment. The verification processes are carried out for both air and skin feedback systems, and their results are demonstrated in section 3.4.

5.5 Air Mode

Although, the infant core and skin temperatures on admission into incubator are assumed to be as severely low as 35.5 °C, the simulation results shown in section 4.3.1.2 proves that they both gain 0.52 °C and 0.17 °C, respectively over two hours.

Initially, the core temperature begins progressively rising above 35.5 °C till it reaches 36.02 °C, while the skin temperature drops to 35.21 °C well below 35.5 °C, but eventually rises to 35.67 °C. However, neither core or skin temperatures reaches 36.5-37.5 °C, which is the range required for a thermo-neutral environment in two hours in both simulation and clinical results.

These results are consistent with the clinical findings in literatures that are cited in section 4.3.1.2 (page 99). Firstly, the margin between the final values of core and skin temperatures is 0.35 °C below core temperature, and secondly the margin between the initial and final values of core temperature in two hours is 0.52 °C.

The pattern of the fluctuations in air temperature (i.e. the controlled temperature) is also comparable to the clinical literatures outcomes cited in section 4.3.1.1 (page 97).

Thus, it can be concluded that the performance of the Simulink model in two hours under air mode is satisfactory, since the trends of the generated figures are comparable to those in literatures.

5.6 Skin Mode

The simulation results shown in section 4.3.2.1 prove that the core and skin temperatures are increased from 35.5 °C (the admission temperature) to 36.87 °C and 36.5 °C in two hours respectively. Thus, the gain is 1.37 °C and 1 °C respectively.

The final temperatures of the core and the skin are strongly in agreement with the clinical data in literatures that are cited in section 4.3.2.1 (page 101). Also, a thermo-neutral environment is achieved in 2 hours with these two final values of temperatures, since the required range is between 36.5-37.5 °C. Furthermore, the margin between the final values of core and skin temperatures is 0.37 °C, which is well within the range determined by Miller [11] of 0.1-0.4 °C.

The pattern of the fluctuations in air temperature in figure Figure 4-9 is peculiar, as it ramps by 3.13 °C over the maximum limits, 37.4 °C, given in the literature, the temperature then drops to 37.85 °C as a final value. The reason behind this performance is strongly thought to be the parameters of the PID controller, as they are selected on virtual basis to acquire optimum outputs in less time. This behaviour of the air temperature can be tolerated however, as it does not exceed the operational limits required by the manufacturer of 20-42 °C and secondly, is based on the fluctuations rate estimated after 90 minutes as 1.06×10^{-03} °C/min. The predicted final air temperature would be 37.34 °C after eight hours which is slightly less than the upper limits in the literature 37.4 °C.

Nevertheless, the overall system performance under skin model is satisfactory since a thermo-neutral environment is achieved in two hours under the current circumstances and conditions of this model.

5.7 Model Limitations

Since the model is a feedback system, appropriate parameters for the PID controller are needed. The current parameters were chosen using modified Ziegler-Nichols Method, as the real values are not available and further investigation is required to tune the PID parameters for most common range of input temperatures (reference temperature), this should be between 30-39 °C for air servo-controller mode and 32-37 °C for skin servo-controller mode.

5.8 The Significance of the Model

The significance of this model can be outlined as follows:

- The model incorporates the infant, the incubator and the surrounding environment.
- Parameters that can be varied include the air and skin temperatures, and infant weight and size.

The model has the ability to:

- predict the final temperature of each compartment of the system.
- to switch from air servo control to skin servo control.
- to run with and without added humidity.
- to predict the energy exchange resulting from the interactions between the infant and the surroundings, through mechanisms such as convection, evaporation, radiation and conduction.
- Results of the simulation, including the temperature of an infant over time, are consistent with clinical empirical data using both air and skin servo controls.

5.9 Conclusions

A convectively-heated incubator with humidification has benefits and limitations when used to nurse preterm infants. The over all model presented in this work can be used for improving the performance of infant warming devices using comprehensive simulations.

References

1. Michael. H. LeBlanc, *Thermoregulation: Incubators, radiant warmers, artificial skins, and body hoods*. Clin Perinatol, 1991. **18**: p. 403-422.
2. Gerald B. Merenstein, D.F.K., George L. Brown, Leonard E. Weisman, *Radiant warmers vs incubators for neonatal care*. Am J Dis Child, 1979. **133**: p. 857-858.
3. Michael P. Meyer, M.J.P., Andrew Salmon, Chris Hutchinson, Alan de Kleck, *Comparison of Radiant Warmer and Incubators Care for Preterm Infants From Birth to 1800 Grams*. Pediatrics, August 2001. **108**: p. 395-401.
4. A J Lyon, M.E.P., P Badger, N McIntosh, *Temperature control in very low birth weight infants during the first five days of life*. Arch Dis Child, 1997. **76**: p. F47-F50.
5. Edward F. Bell and Margit-Andrea Glatzl-Hawlik, *Environmental Temperature Control*, in Polin RA, Fox WW, eds. *Fetal and Neonatal Physiology*. 1998, PA: WB Saunders: Philadelphia. p. 716-727.
6. William A. Silverman, J.W.F., Agnes P. Berger, *The influence of the thermal environment upon the survival of the newly born premature infant*. Pediatrics, 1958. **22**: p. 876-885.
7. Flenady VJ, W.P., *Radiant warmers vs incubators in newborn infants*. 2000(Issue 2).
8. Michael H. LeBlanc, *Relative efficacy of an incubator and an open radiant warmer in producing thermo neutrality for the small premature infant*. Pediatrics, 1982. **69**: p. 439-445.
9. P J J Sauer, H.J.D., and H K A Visser, *New standards for neutral thermal environment of healthy very low birth-weight infants in week one of life*. Arch Dis Child, 1984. **59**: p. 18-22.
10. Teertharaj K. Belgaumkar, K.E.S., *Effects of low humidity on small premature infants in servo control incubators*. Biol Neonate, 1975. **26**: p. 337-347.
11. D. L. Miller, T.K.O., JR., *Body temperature in the immediate neonatal period: The effect of reducing thermal losses*. Am J Obstet Gynecol, 1966. **94**: p. 964-969.
12. E. N. Hey and G. Katz, *The optimum thermal environment for naked babies*. Arch Dis Child, 1970. **45**: p. 328-334.
13. Sunita Vohra, G.F., Valerie Campbell, Michele Abbott, Robin Whyte, *Effect of polyethylene occlusive skin wrapping on heat loss in very low birth weight infants at delivery: A randomized trial*. Pediatrics, May 1999. **134**: p. 547-551.

14. Stephen Baumgart, *Reduction of oxygen consumption, insensible water loss, and radiant heat demand with the use of a plastic blanket for low-birth-weight infants under radiant warmers*. Pediatrics, 1984. **74**: p. 1022-1028.
15. Stephen Baumgart, W.D.E., William W. Fox, and Richard A. Polin, *Radiant warmer power and body size as determinants of insensible water loss in the critically ill neonate*. Pediatr Res, 1981. **15**: p. 1495-1499.
16. Stephen Baumgart, W.D.E., William W. Fox, and Richard A. Polin, *Effect of heat shielding on convective and evaporative heat losses and on radiant heat transfer in the premature infant*. J Pediatr, 1981. **99**: p. 948-956.
17. Phillippe Chessex, S.B., Jean Vaucher, *Environmental temperature control in very low birth weight infants (less than 1000 grams) cared for in double-walled incubators*. J Pediatr, 1988. **113**: p. 373-380.
18. Michael H. LeBlanc, *The Physics of Thermal Exchange between Infants and Their Environment*. AAMI Technology Assessment Report, Feb. 1987. **vol. 21**(No.1): p. pp11-15.
19. Edward F. Bell and Gladys R. Rios, *A Double-Walled Incubator Alters the Partition of Body Heat Loss of Premature Infants*. Pediatr. Res., 1983. **Vol. 17**: p. pp135-140.
20. J. C. Sinclair, *metabolic rate and temperature control in the newborn*, in *PERINATAL MEDICINE*. p. 558-575.
21. Fisher and Paykel Healthcare Ltd., *Training CD*. 2004/07, Fisher and Paykel Healthcare Ltd: Auckland.
22. Edward F. Bell, G.A.N., William J. Cashore, William Oh, *Combined effect of radiant warmer and phototherapy on insensible water loss in low-birth-weight infants*. J Pediatr, 1979. **94**: p. 810-813.
23. Edward F. Bell, M.R.W., William Oh, *Heat balance in premature infants: Comparative effects of convectively heated incubator and radiant warmer, with and without plastic heat shield*. J Pediatr, 1980. **96**: p. 460-465.
24. Robert A. Darnall, J., and Ronald L. Ariagno, *Minimal oxygen consumption in infants cared for under overhead radiant warmers compared with conventional incubators*. J Pediatr, 1978. **93**: p. 283-287.
25. Kieth H. Marks, R.C.G., John A. Rossi, and M. Jeffrey Maisels, *Oxygen consumption and insensible water loss in premature infants under radiant warmers*. Pediatrics, 1980. **66**: p. 228-232.
26. A.E. Wheldon and N. Rutter, *The heat balance of small babies nursed in incubators and under radiant warmers*. Early Human Development, 1982. **6**: p. 131-143.

27. Paul Y. K. Wu, J.E.H., *Insensible water loss in preterm infants: changes with postnatal development and non-ionizing radiant energy*. Pediatrics, 1974. **54**: p. 704-712.
28. Paul Y. K. Wu, J.E.H., Barry V. Kirkpatrick, Nathaniel B. White, Jr, M Phil, and Dolores A. Bryla, *Metabolic aspects of phototherapy*. Pediatrics, 1985. **75**: p. 427-433.
29. Barry Neil Simon, J., *Computer Simulation of Infant-Incubator System Dynamics*, in *Department of Biomedical Engineering*. December, 1991, The university of Akron: Akron, Ohio. p. 163.
30. R.D. Rojas, E.F.B., E.L. Dove, *A Mathematical model of premature baby thermoregulation and infant incubator dynamics*. International Conference on Simulation Modelling in Bioengineering, BIOSIM, 1996: p. p 23-38.
31. Jan A. J. Stolwijk, *Physiological and Behavioral Temperature Regulation*. Vol. chapter 48. 1970, springfield: Thomas. 703-721.
32. Fanaroff A, M.R., *Neonatal -Perinatal Medicine. Diseases of the Fetus and infant*. 5th Ed. ed. 1992: Mosby Year Book. pp 480.
33. James S. Ultman, *Computational Model for Insensible Water Loss from the New Born*. Pediatrics, 1987. **Vol 79**(#5): p. pp760-765.
34. Wilbert F. Stoecker/Jerold W. Jones, *Refrigeration & Air Conditioning*. Second Edition ed, Printed in Singapore: McGraw-Hill International Editions.
35. Yunus A. Cengel, *Heat Transfer: A practical Approach*. Second Edition ed: McGraw-Hill.
36. <http://www.newton.dep.anl.gov/askasci/gen99/gen99801.htm>. 2005.
37. Christopher Haslett, *Davidson's, Principles & Practice of Medicine*. 19th editions ed. 2002, printed in India: Churchil Livingstone. pp. 1219.
38. <http://www.aic.cuhk.edu.hk/web8/Paediatric%20anatomy%20&%20physiology.htm>. 2005.
39. BERND FISCHER, M.L., and ANDREAS MEISTER, *THE THERMOREGULATION OF INFANTS: MODELING AND NUMERICAL SIMULATION*. BIT, 2001. **41**(No.5): p. pp. 950-966.
40. K. W. Cross and D. Stratton, *Aural Temperature of the Newborn*. The Lancet, 1974. **304**(7890): p. 1179-1180.
41. V.M. Becerra, *Experiment 103: Process control simulation using SIMULINK*. 2000. p. 1-8.
42. <http://www.engin.umich.edu/group/ctm/PID/PID.html>. 2005. p. PID Tutorial.

43. W. Bolton, *Mechatronics : ELECTRICAL CONTROL SYSTEMS IN MECHANICAL AND ELECTRICAL ENGINEERING 2nd EDITION*. 2nd ED. ed. 1999: Addison Wesley Longman Limited 1999.
44. Ernest O. Doebelin, *System Dynamics : Modeling, Analysis, Simulation, Design*. 1998: New York : Marcel Dekker, c 1998.
45. Katsuhiko Ogata, *Modern Control Engineering*. Fourth Edition, International Edition ed. 2002: Prentice Hall, Inc. Upper Saddle River, New Jersey 07458, United States of America.
46. Alexander Sinclair, *Convection v. Radiant Heat Transfer: Engineering Perspective*. AAMI Technology Assessment Report, 1984: p. TAR #9-84.

Appendices

Appendix 1

1.1 Initial Conditions for the Infant-Incubator Simulink Model, M-File

```
%% Set up the constant parameters for the Infant-Incubator Simulink
Model
clear
% INFANT RELATED VARIABLES
m=0.900; % kg infant mass
Mrst=24.8; % W/m^2 Resting metabolic rate
age=1; % day postnatal age
GA=28; % weeks gestational age
ths=0.0005; % m skin thickness of the infant
%bf=0.00353; % sec^-1 blood flow rate parameter
IV=3.667; % mL/kg*sec Inspired minute volume

% INCUBATOR RELATED VARIABLES
Amat=0.61*0.345; % m2 Total Area of the Mattress
Awi=2*(0.403*0.42)+2*(0.853*0.42)+(0.853*0.403); % m2 Surface
area of the incubator walls
thw=0.006; % m thickness of the incubator wall
thm=0.02735; % m mattress thickness
Mm=0.2575; % kg mattress mass
qair=21/60; % l/sec volumetric air flow rate
qO2=0; % l/sec volumetric oxygen flow
rate
Vinc=0.403*0.42*0.835; % m^3 Incubator Volume
O2=0; % O2% Percentage of the Added
Oxygen
Aa11=5*2*(0.2*0.028); % m2 total surface area of the
exposed part of the finned-aluminium block
Aa12=5*2*(0.2*0.04)+4*0.02163*0.2; % m2 total surface area of the
submerged parts of the finned-aluminium block
Awa=(0.335*0.127-0.0035*0.2*5); % m2 total surface area of the
water surface in the water chamber
Mah=(0.028*0.335*0.127)*1.092; % kg mass of air inside the
water chamber
Mwa=(0.04*0.335*0.127)*0.001*10^(6); % kg mass of water inside the
water chamber
Mal=0.88183; % kg mass of the aluminium
block
Ru=8.31447; % KJ/Kmol universal gas constant

% VARIOUS THERMAL CONDUCTIVITIES and CONVECTIVE HEAT TRANSFER
COEFFICIENTS
Kc=0.51; % W/m.C thermal conductivity of the core
Kmat=0.04184; % W/m.C thermal conductivity of the mattress
Ka=0.02625; % W/m.C thermal conductivity of the
incubator air space @ 35 C

% VARIOUS DENSITIES
rhoc=1080; % kg/m3 core density
rhos=1000; % kg/m3 skin density
rhoa=1.145*10^-6; % kg/mL air density @ 35 C
rhow=1190.236; % kg/m3 wall density_Plexiglass
rhob=1.06E-3; % kg/mL blood density
rhowater=0.001; % kg/mL density of the water
% PRESSURE DATA
Pt=760; % ambient pressure @ 35 C, torr
```

```

% NATURAL CONVECTION PARAMETERS
Awh=0.403*0.853;           % m^2 surface area of the horizontal wall of
the incubator
g=9.81;                   % m/sec^2 gravitational acceleration
Beta=3.356*10^-3;        % 1/K volume expansion coefficient @ 30 C
Lc=Awh/(0.403+0.853);    % m characteristic length Lc of the
horizontal surface
mueao=1.872*10^-5;       % kg/m.sec dynamic viscosity @ 30 C
Cpao=1007;               % J/kg.C specific heat of the air @ 30 C
Kao=0.02588;            % W/kg.C thermal conductivity of the air @ 30
C
v=1.608*10^-5;          % m^2/sec kinematic viscosity of the air @ 30
C
Lc1=0.420;              % m characteristic length Lc1 of the vertical
surfaces
Awv=0.420*0.853;        % m^2 surface area of the vertical long side
of the incubator wall
Awv1=0.420*0.403;       % m^2 surface area of the vertical short side
of the incubator wall

% NATURAL CONVECTION FOR THE ALUMINIUM BLOCK
hal2=443.33;

% VARIOUS TEMPERATURES and HUMIDITY
%Tex=37                  % C exhaled air temperature
Te=25;                  % C environmental air temperature
RH1=1.00;               % relative humidity of the exhaled air
hfg=2419000;           % J/kg latent heat of water @ 35 C-Air Temp.
hfg1=2383000;          % J/kg latent heat of water @ 50 C-Air Temp.

% VARIOUS VARIABLES OF SPECIFIC HEAT TRANSFER
Cpa=1007;               % J/kg.C specific heat of the air @ 35 C
CpO2=925.2;            % J/kg.C specific heat of the added oxygen @
25 C
CpN2=1038.5;           % J/kg.C specific heat of the nitrogen @ 25
C
Cpc=3470;              % J/kg.C specific heat of the core
Cpsk=3766;             % J/kg.C specific heat of the skin
Cpm=1757;              % J/kg.C specific heat of the mattress
Cpb=3840;              % J/kg.C specific heat of the blood
Cpw=1297;              % J/kg.C specific heat of the
wall(plexiglass)
Cps=1900;              % J/kg.C specific heat of vapour @ 53.5 C
Cpwa=4180;             % J/kg.C specific heat of the water
Cpal=900;              % J/kg.C specific heat of the aluminium
block

% Nusselt Numbers for convective heat transfer coefficients
muea=1.895*10^-5;      % kg/m.sec Dynamic Viscosity of the air @ 35
C
mues=1.8996*10^-5;    % kg/m.sec Dynamic Viscosity of the skin @ 36
C
Va=0.1;                % m/sec air velocity
Diasph=0.08;           % m approximate infant diameter
Pr=(muea*Cpa)/Ka;      % Prandtl number @ 35 C
Re=rhoa*10^6*Va*Diasph/muea; % Reynolds number for infant
Nusph=2+(0.4*Re^(0.5)+0.06*Re^(2/3))*Pr^(0.4)*(muea/mues); %
Nusselt number for the infant
Ac=0.42*0.403;        % m^2 Incubator Area based on the direction
of the air flow

```

```

p=2(0.42+.403);           % m Incubator perimeter based on the
direction of the air flow
Dh=(4*Ac)/p;             % m Hydraulic diameter of the incubator
f=0.0119;                % friction factor for internal forced
convection
Re1=rhoa*10^6*Va*Dh/muea;           %
Reynolds number for incubator
Nu1=((f/8)*(Re1-1000)*Pr)/(1+12.7*(f/8)^(0.5)*(Pr^(2/3)-1)); %
Nusselt number for the incubator inside
rhoah=1.092;             % kg/m^3 air density @ 50 C
Lcwater=0.335;          % m characteristic length of water surface
mueah=1.963*10^-5;      % kg/m.sec Dynamic Viscosity of the air @ 50
C
ReL=(rhoah*Va*Lcwater)/mueah; % Reynolds Number for the air passes
over the water surface inside the water chamber
Cpah=Cpa;                % J/kg.C specific heat of the air @ 50
C
Kah=0.02735;            % W/m.C thermal conductivity of the air
@ 50 C
PrL=(mueah*Cpah)/Kah;   % Prandtl Number for the air @ 50 C
Nu2=0.664*ReL^(0.5)*PrL^(1/3); % Nusselt Number for the water surface
in the water chamber @ 50 C
Lcall=0.2;              % m characteristic length of the
finned-aluminium block
ReL1=(rhoah*Va*Lcall)/mueah; % Reynolds Number for the air passes
over the fin surfaces inside the water chamber
Nu3=0.664*ReL1^(0.5)*PrL^(1/3); % Nusselt Number for the finned-
aluminium block/THE EXPOSED PART @ 50 C

% RADIATION DEPENDENT FACTORS
sigma=5.67E-08;         % W/m2.K^4 stephan-boltzmann constant
epsilonskin=1.00;      % emissivity of the skin
epsilonwall=0.86;      % emissivity of the wall_Plexiglass

%% Initial conditions for the state variables
Tci = 35.5;             % deg C.
Tsi = 35.5;             % deg C.
Tai = 37;               % deg C.
Tmi = Tai;             % deg C.
Twi = 25.5;            % deg C.
TO2=25;                % deg C.
Tweti=45.5;            % deg C.
Twai=33;               % deg C.
Tali=34;               % deg C.

%% Now I am ready to run the simulink model
% sim('new');

```

1.2 State-Space Code for Skin Mode

```

clear all
%Run simulink Constants:
run Constants4oneLUMP

%Run simulink:
sim('Plant1_SKINmode');

%Linearize the simulink model
[A,B,C,D]=linmod('Plant1_SKINmode');

```

```
%State-Space model
PlantSKIN=ss(A,B,C,D);
```

```
sisotool(PlantSKIN)
```

```
%Now I am ready to test the stability of the model_SKIN MODE
```

1.3 State-Space Code for Air Mode

```
clear all
%Run simulink Constants:
run Constants4oneLUMP
```

```
%Run simulink:
sim('Plant2_AIRmode');
```

```
%Linearize the simulink model
[A,B,C,D]=linmod('Plant2_AIRmode');
```

```
%State-Space model
PlantAIR=ss(A,B,C,D);
```

```
sisotool(PlantAIR)
```

```
%Now I am ready to test the stability of the model_AIR MODE
```

Appendix 2

2.1 Air Mode Figures

-/+ sign means heat gain/ heat loss respectively.

2.1.1 Temperatures Figures

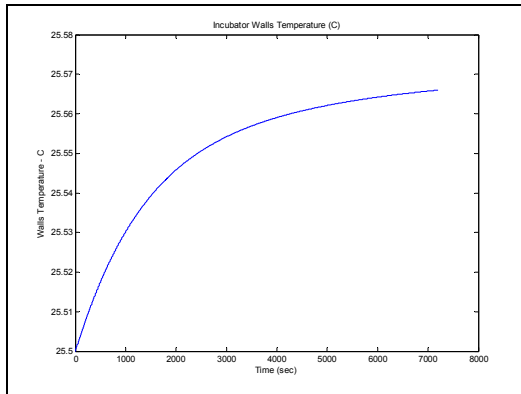


Figure 2-1 Wall temperature, T_w

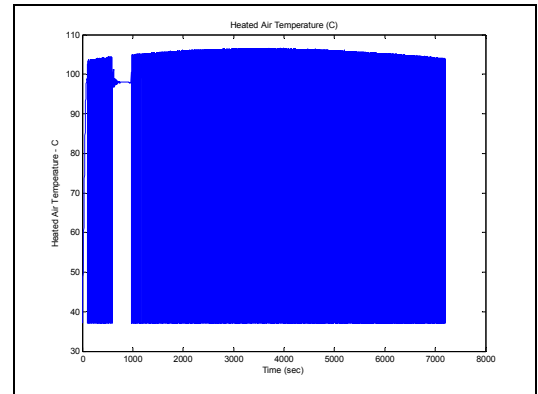


Figure 2-4 Heated air temperature, T_{ha}

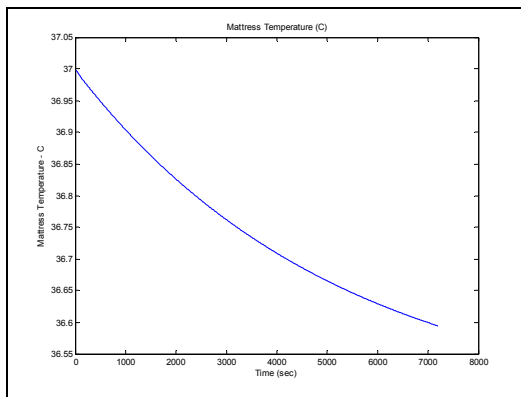


Figure 2-2 Mattress temperature, T_m

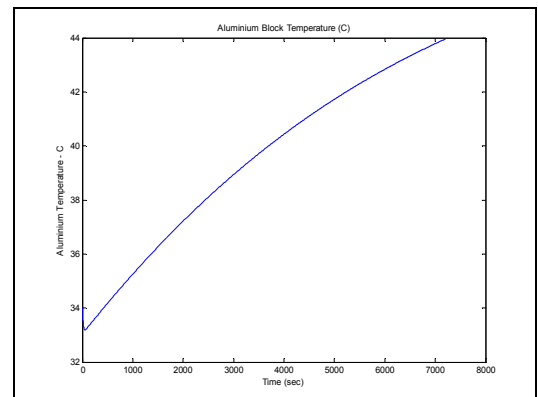


Figure 2-5 Aluminium block temperature, T_{al}

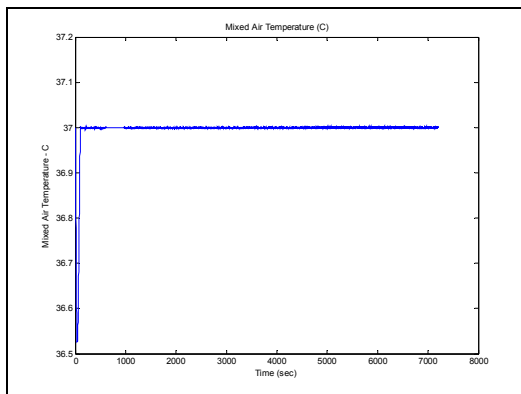


Figure 2-3 Mixed air temperature, T_{mx}

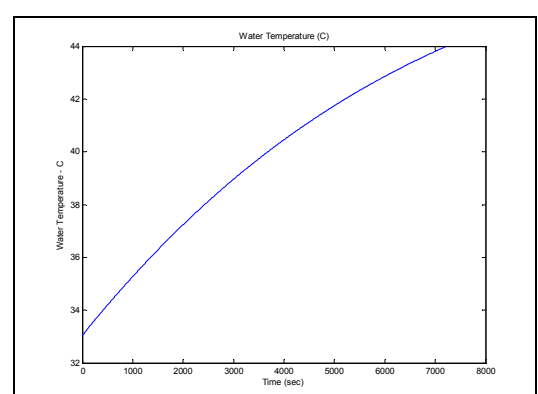


Figure 2-6 Water temperature, T_{wa}

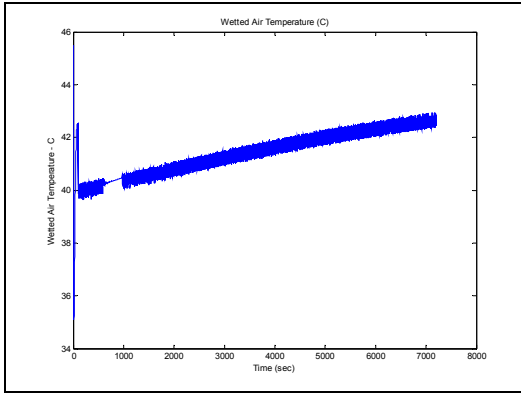


Figure 2-7 Wetted air temperature, T_{wet}

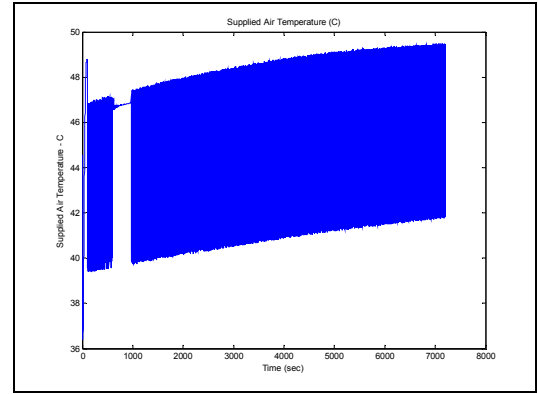


Figure 2-8 Supplied air temperature, T_{sply}

2.1.2 Heat Energy Relationships Figures

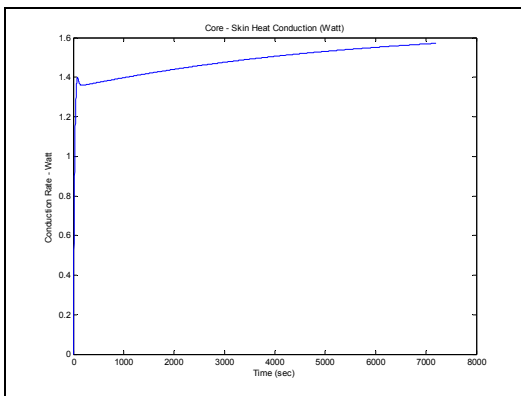


Figure 2-9 Core - skin conduction

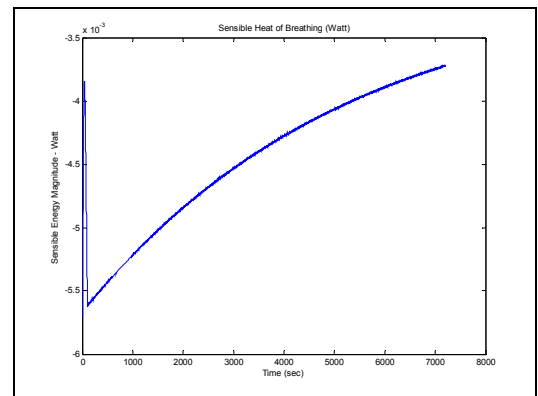


Figure 2-12 Breathing sensible heat

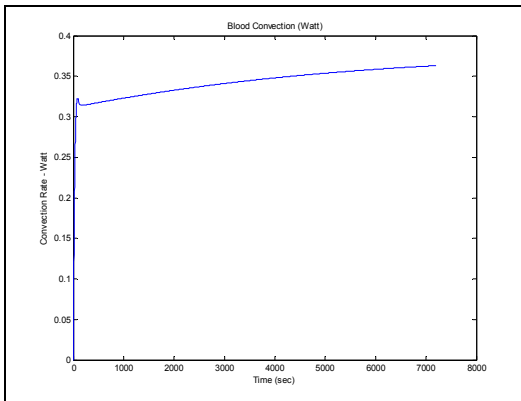


Figure 2-10 Blood convection relationship

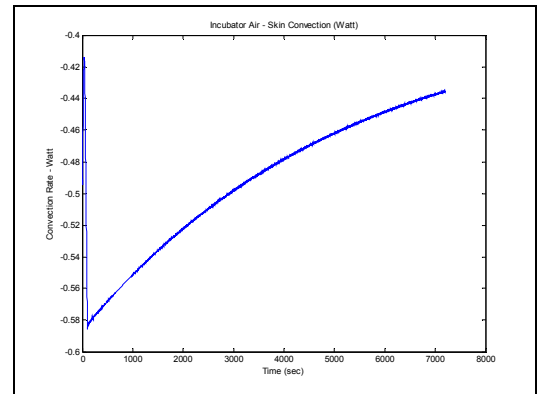


Figure 2-13 Skin - incubator air convection

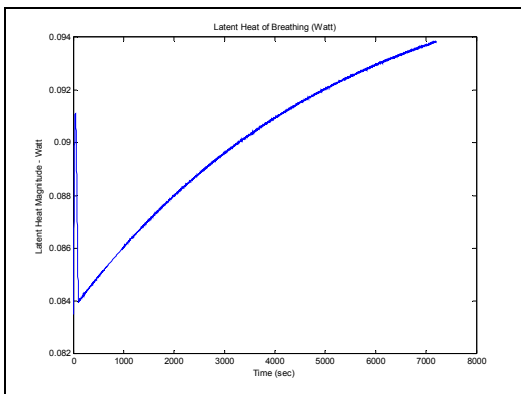


Figure 2-11 Breathing latent heat, Q_{lat}

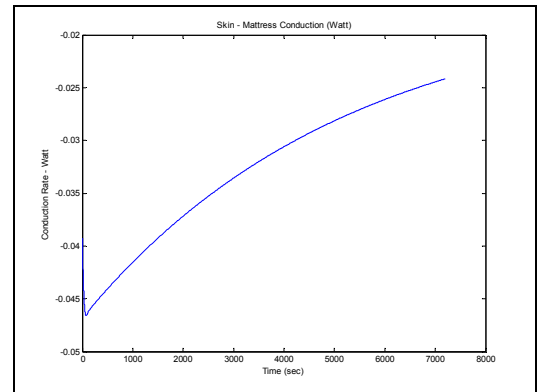


Figure 2-14 Skin - mattress conduction

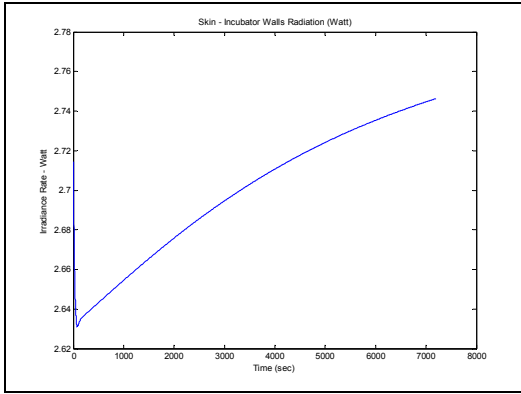


Figure 2-15 Skin - incubator walls radiation

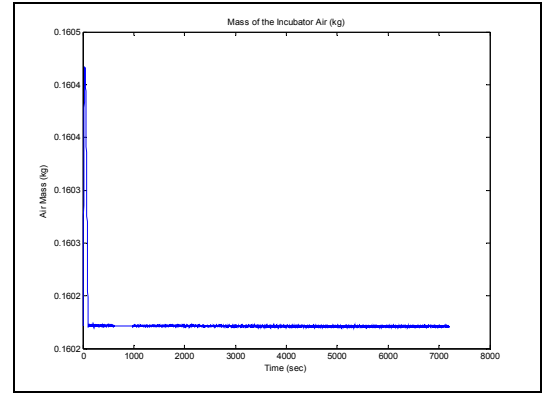


Figure 2-17 Incubator air mass Variation

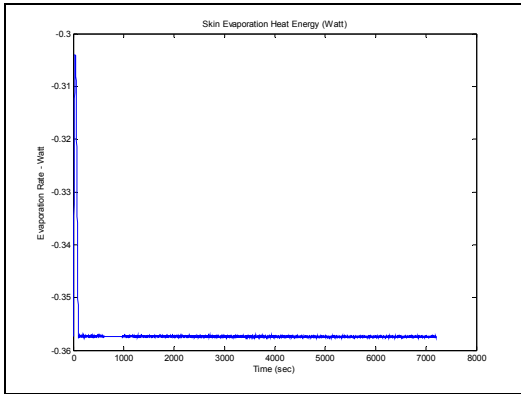


Figure 2-16 Skin evaporation heat energy

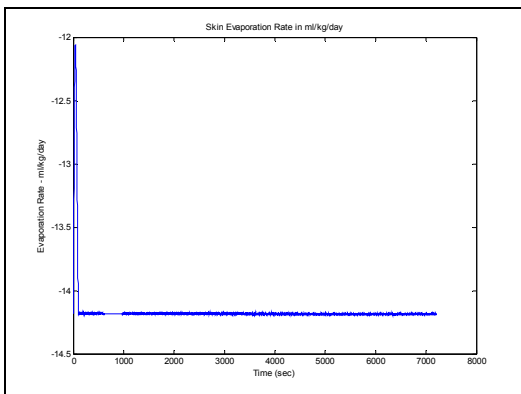


Figure 2-18 Skin evaporative rate in ml/ kg/day

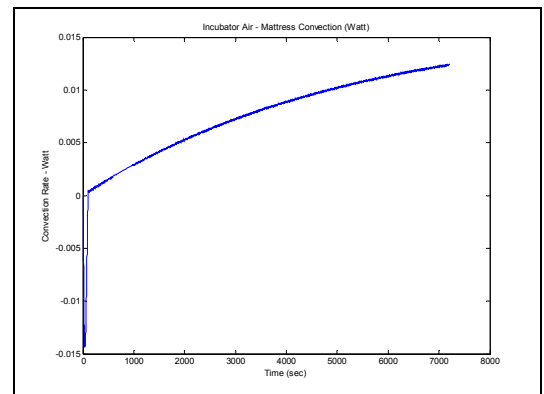


Figure 2-20 Incubator air - mattress convection relationship

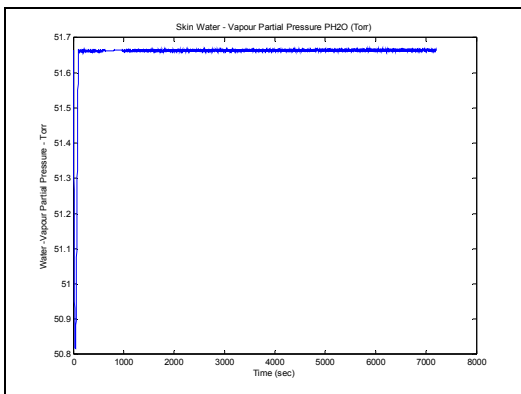


Figure 2-19 Skin water-vapour partial pressure, P_{H_2O} (torr)

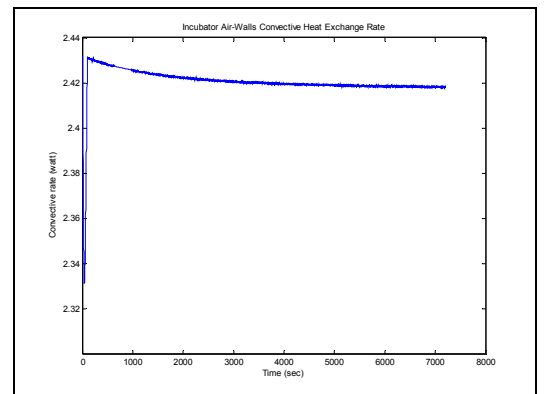


Figure 2-21 Incubator air - walls convection relationship

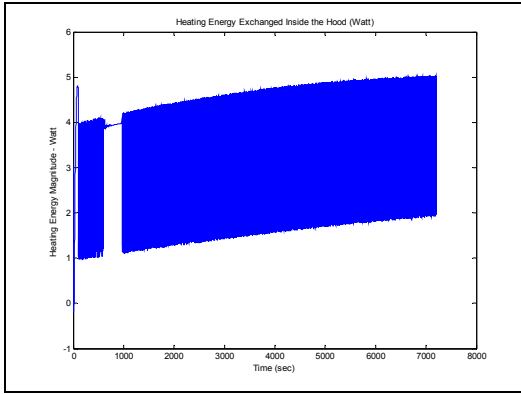


Figure 2-22 Heating energy exchanged inside incubator hood

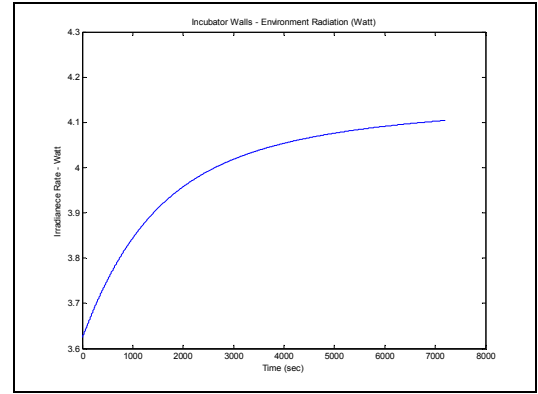


Figure 2-24 Incubator walls - environment radiation

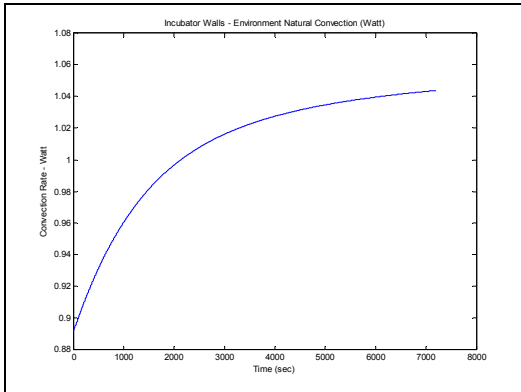


Figure 2-23 Incubator walls - environment natural convection

2.1.3 Feedback System Related Figures

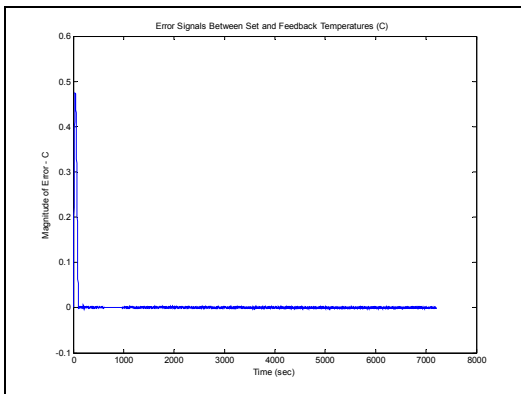


Figure 2-25 Error signals between set and feedback temperatures

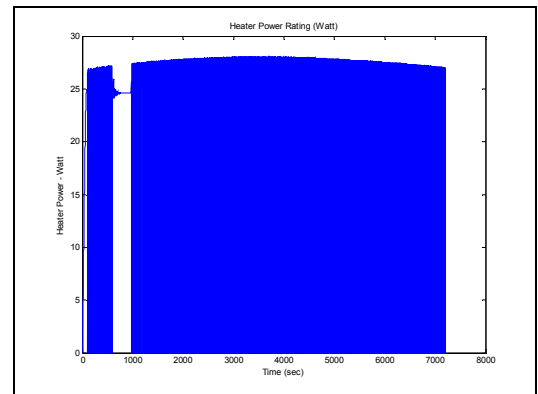


Figure 2-26 Heater power variation

Appendix 3

3.1 Skin Mode Figures

-/+ sign means heat gain/ heat loss respectively.

3.1.1 Temperatures Figures

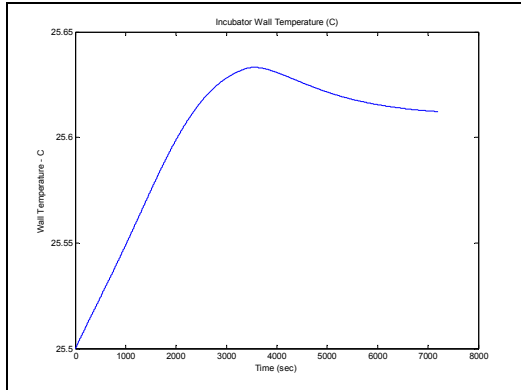


Figure 3-1 Incubator wall temperature, T_w

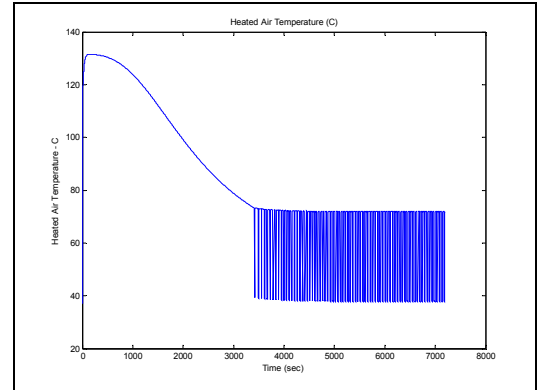


Figure 3-4 Heated air temperature, T_{ha}

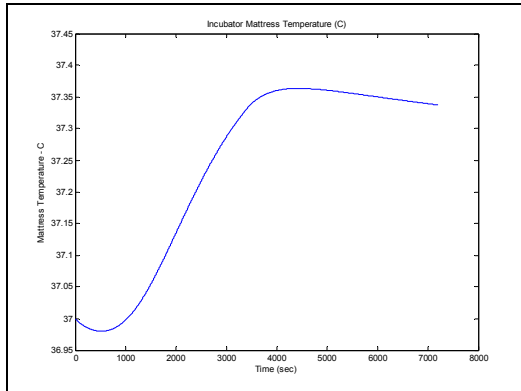


Figure 3-2 Mattress temperature, T_m

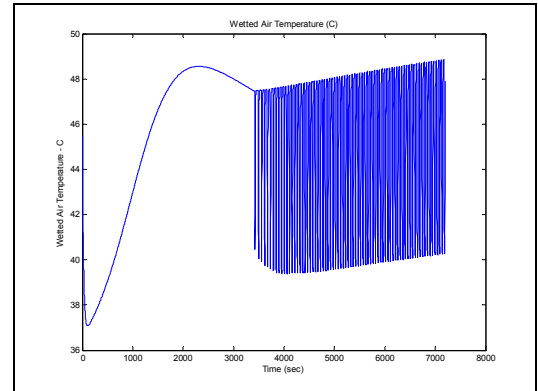


Figure 3-5 Wetted air temperature, T_{wet}

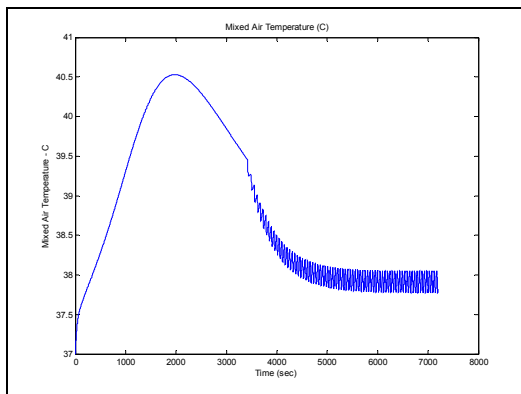


Figure 3-3 Mixed air temperature, T_{mx}

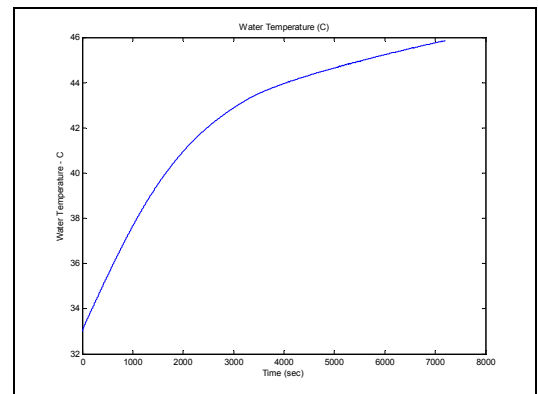


Figure 3-6 Water temperature, T_{wa}

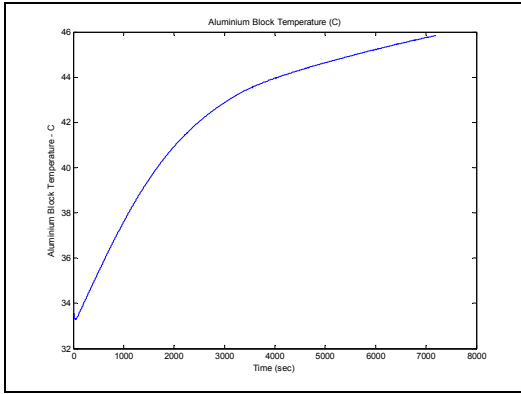


Figure 3-7 Aluminium block temperature, T_{al}

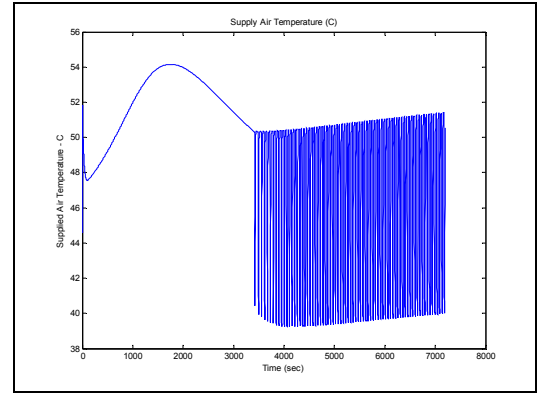


Figure 3-8 Supplied air temperature, T_{sply}

3.1.2 Heat Energy Relationships Figures

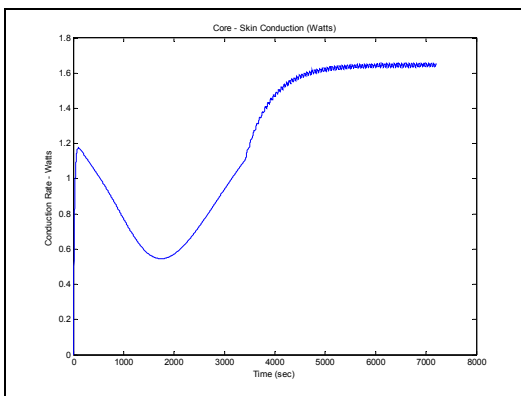


Figure 3-9 Core - skin conduction

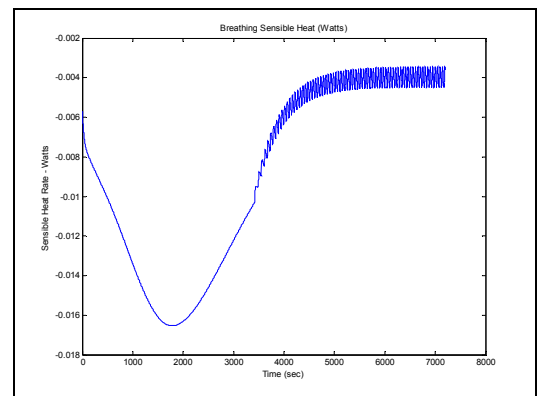


Figure 3-12 Breathing sensible heat

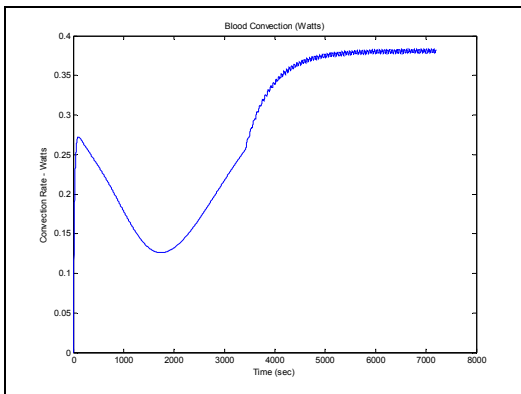


Figure 3-10 Blood convection

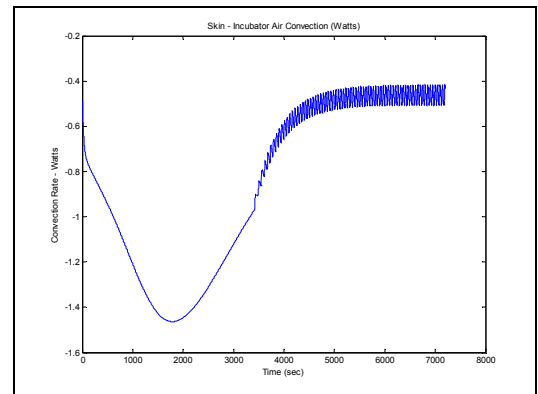


Figure 3-13 Skin - incubator air convection

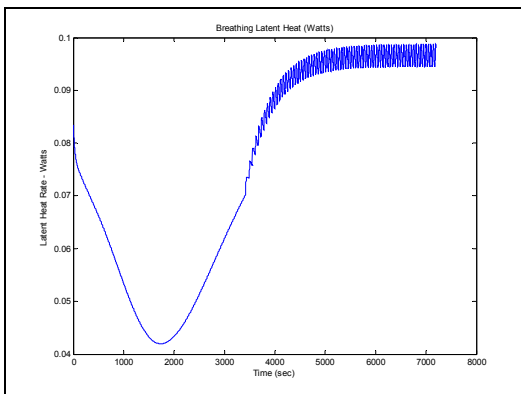


Figure 3-11 Breathing latent Heat

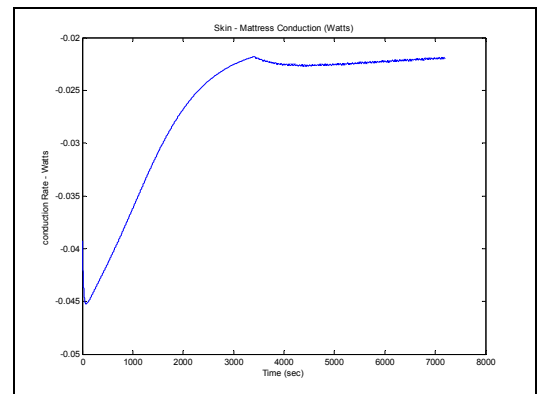


Figure 3-14 Skin - Mattress conduction

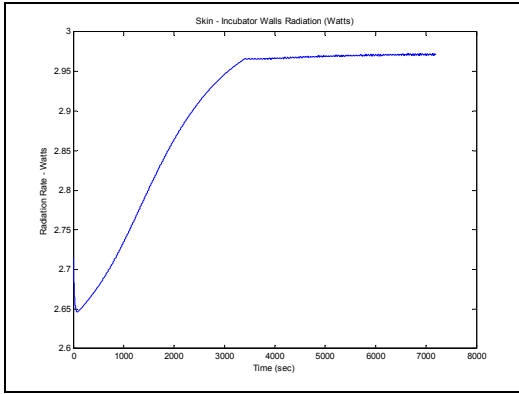


Figure 3-15 Skin - incubator walls radiation

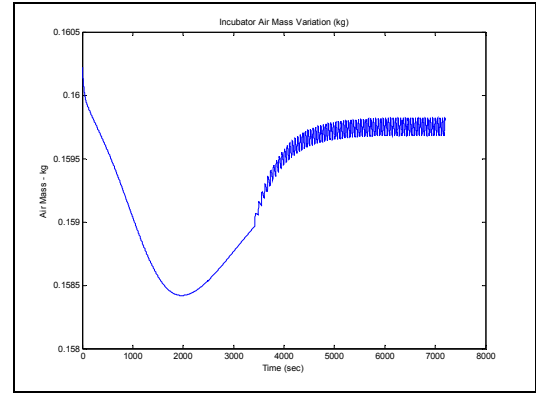


Figure 3-17 Incubator air mass Variation

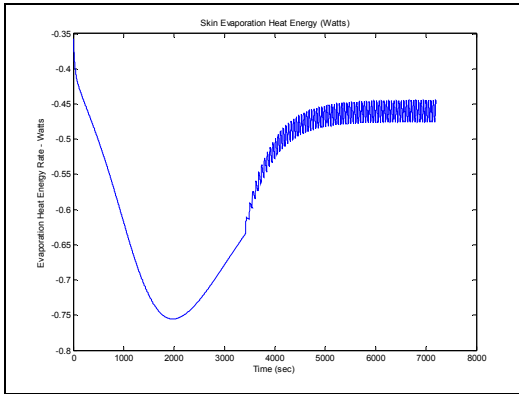


Figure 3-16 Skin evaporation heat energy

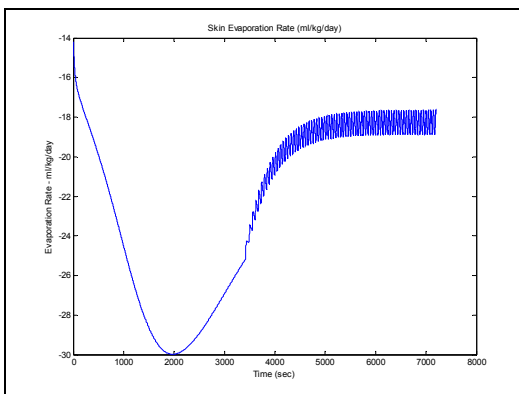


Figure 3-18 Skin evaporative rate in ml/ kg/day

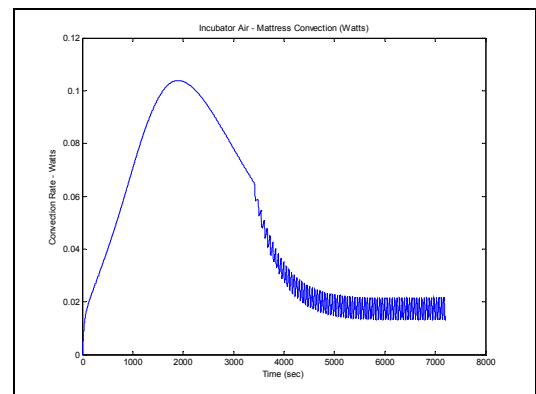


Figure 3-20 Incubator air - mattress convection relationship

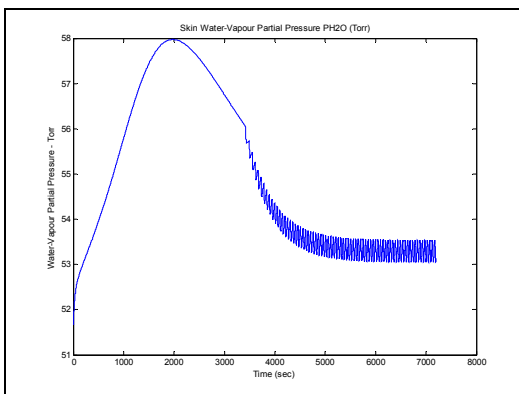


Figure 3-19 Skin water-vapour partial pressure, P_{H_2O} (torr)

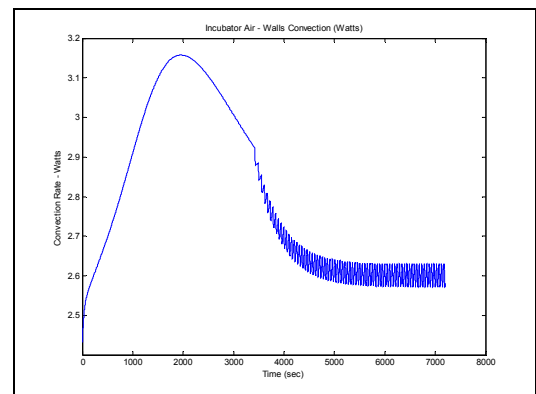


Figure 3-21 Incubator air - walls convection relationship

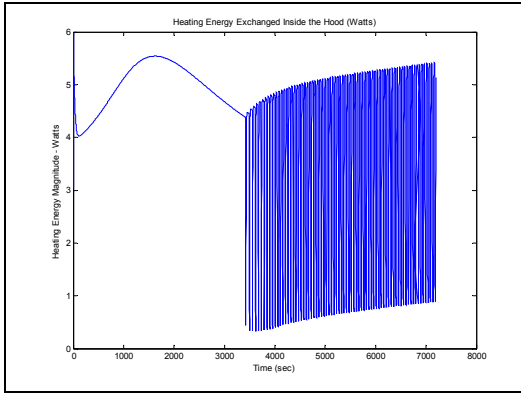


Figure 3-22 Heating energy exchanged inside incubator hood

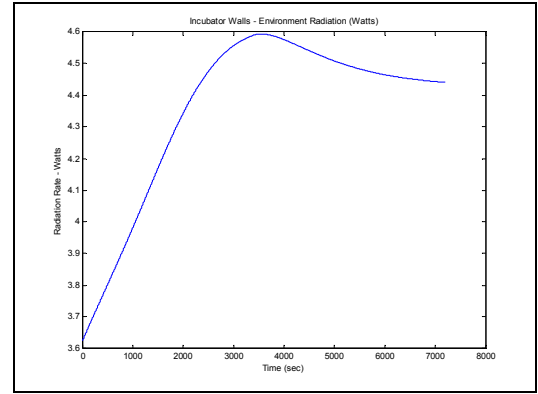


Figure 3-24 Incubator walls - environment radiation

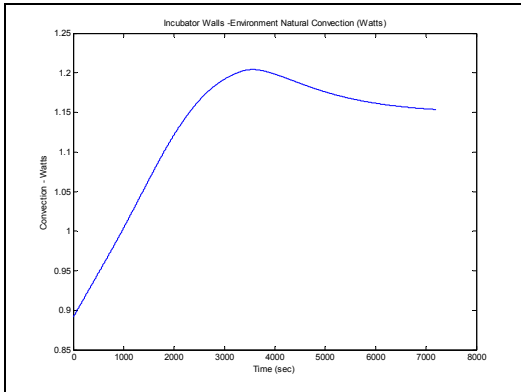


Figure 3-23 Incubator walls - environment natural convection

3.1.3 Feedback System Related Figures

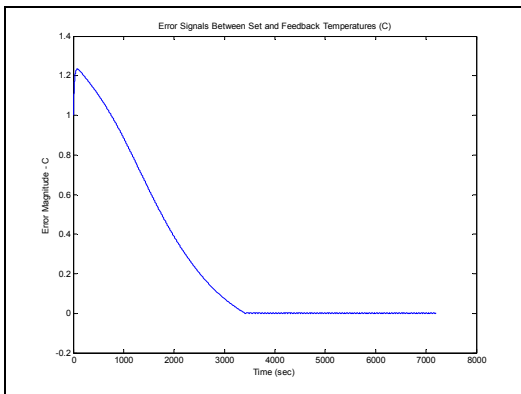


Figure 3-25 Error signals between set and feedback temperatures

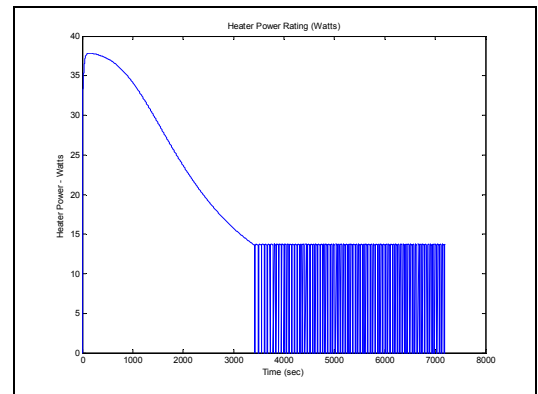


Figure 3-26 Heater power variation